Chapter 25
Handling Performance

25.1 Low Speed or Kinematic Steering

25.1.1 Two-Axle Vehicles Without Trailer

Low speed or kinematic steering is, as already stated, defined as the motion of a wheeled vehicle determined by pure rolling[1] of the wheels. The velocities of the centres of all the wheels lie in their midplane, that is the sideslip angles α_i are vanishingly small. In these conditions, the wheels cannot exert any cornering force to balance the centrifugal force due to the curvature of the path. Kinematic steering is possible only if the velocity is vanishingly small.

Kinematic steering of two-axle vehicles without trailer was dealt with in detail in Chap. 4 (Sect. 4.2). Here only the value of the *path curvature gain* needs be recalled,

$$\frac{1}{R\delta} = \frac{1}{l} \,. \tag{25.1}$$

Remark 25.1 The path curvature gain is a linearized value, holding only if the radius of curvature of the path R is much larger than the wheelbase. It is independent of the steering angle and of the curvature of the path.

Another important transfer function of the vehicle is ratio β/δ, usually referred to as *sideslip angle gain*. The sideslip angle of the vehicle, referred to the centre of mass, may be expressed as a function of the radius of the path R as

[1]The term 'pure rolling' is often used to indicate rolling without slip. 'Free rolling', as opposed to 'tractive rolling', is used to indicate rolling without exerting tangential (longitudinal or lateral) forces (K.L. Johnson, *Contact Mechanics*, Cambridge University Press, Cambridge, 1985). Here the two terms are considered as equivalent, because a tire must operate in slip (longitudinal or side slip) conditions to produce a tangential force.

G. Genta and L. Morello, *The Automotive Chassis*, Mechanical Engineering Series, https://doi.org/10.1007/978-3-030-35709-2_25

$$\beta = \arctan\left(\frac{b}{\sqrt{R^2 + b^2}}\right) . \tag{25.2}$$

By linearizing Eq. (25.2) and introducing the expression (25.1) linking R to δ, it follows:

$$\frac{\beta}{\delta} = \frac{b}{l} . \tag{25.3}$$

As seen in Chap. 6, the optimal condition for kinematic steering of a four-wheel steering vehicle (4WS) is equal and opposite steering angles of the two axles: the radius of the path is thus halved with respect to the same vehicle with a single steering axle.

Particularly in the case of long vehicles, the off-tracking distance, i.e., the difference of the radii of the trajectories of the front and the rear wheels, is an important parameter. If R_a is the radius of the path of the front wheels, the off-tracking distance is

$$R_a - R_1 = R_a \left\{1 - \cos\left[\arctan\left(\frac{l}{R_1}\right)\right]\right\} . \tag{25.4}$$

If the radius of the path is large when compared to the wheelbase, Eq. (25.4) reduces to

$$R_a - R_1 \approx R\left[1 - \cos\left(\frac{l}{R}\right)\right] \approx \frac{l^2}{2R} . \tag{25.5}$$

In the same way, it is possible to define a minimum steering radius between walls, that is the diameter of the largest circle described by any point of the vehicle at maximum steering. If the point following the curve with the largest radius is point A in Fig. 25.1 (note that the figure refers to a vehicle with three axles), the minimum steering radius is

$$D_v = 2\sqrt{(R_1 + y_A)^2 + x_A^2} . \tag{25.6}$$

25.1.2 Vehicles with More Than Two Axles Without Trailer

True kinematic steering of vehicles with more than two axles is possible only if the wheels of several axles (all except one) can steer, and if the steering angles comply with conditions similar to those seen in Chap. 6 for the steering axle of a two-axle vehicle. In order to avoid serious wear to the tires, it is possible to lift one axle from the ground in certain conditions: In some countries it is legal to design the suspensions in such a way that not all axles are on the ground when the vehicle is unloaded, while in others this is not allowed. Some axles can be lifted for low-speed manoeuvring while being in contact with the ground in normal driving.

Some axles may also be self-steering, i.e. the wheels are allowed to orient themselves to minimize sideslip. An axle of this type clearly cannot exert side forces

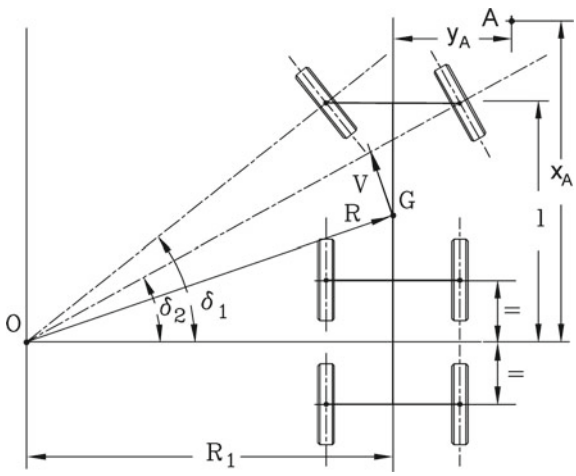

Fig. 25.1 Low speed steering of industrial vehicles; approximate kinematic condition for a truck with three axles

and reduce the overall cornering ability of the vehicle. Different laws hold in different countries, sometimes allowing the use of self-steering axles in normal driving and sometimes specifying that self-steering axles be blocked except in low speed manoeuvres. In the case of a three-axle vehicle with non-steering axles close to each other, an approximation such as the one shown in Fig. 25.1 can be used to study low speed steering.

25.1.3 Vehicles with Trailer

If the vehicle has a trailer with one or two axles, with the front axle on a dolly attached to the draw bar, kinematic steering is always possible if the tractor allows it.

Generally speaking, if the wheels of the trailer are fixed, the trailer follows a path which is internal to that of the tractor. In the case of the vehicle of Fig. 25.2a radius R_R is

$$R_R = \sqrt{R_1^2 + l_A^2 - l_R^2}\,. \tag{25.7}$$

If these equations can be linearized, the value of ratio θ/δ, i.e. the *trailer angle gain*, is

$$\frac{\theta}{\delta} = \frac{l_A + l_R}{l}\,, \tag{25.8}$$

where l_A is positive if point A is outside the wheelbase. Distance $l_A + l_R$ is the distance between the axle of the trailer and the rear axle of the tractor.

In the case of Fig. 25.2b, the radius of the path of the trailer can be obtained by considering the latter as two subsequent trailers of the type already considered.

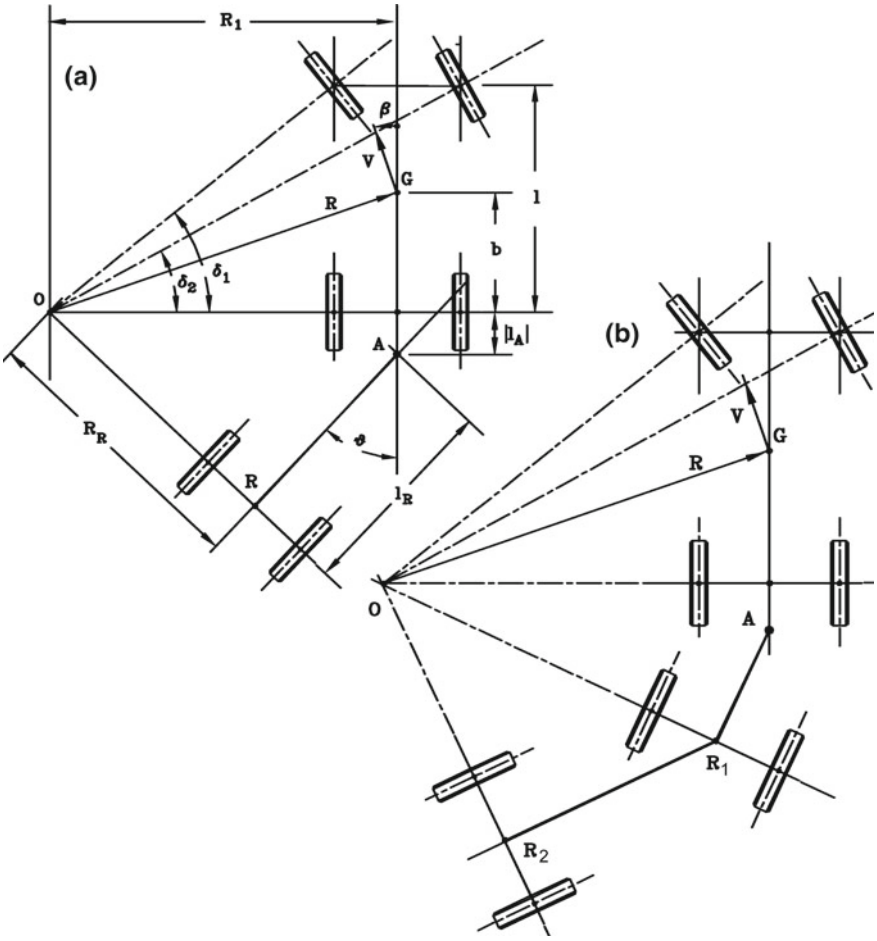

Fig. 25.2 Low speed steering of vehicles with trailer. **a** steering of a vehicle with a trailer with one axle or an articulated vehicle; **b** steering of a vehicle with a trailer with two axles

The radii of the trajectories of the centers of the axles of the two trailers are

$$\begin{aligned} R_{R_1} &= \sqrt{R_1^2 + l_A^2 - l_{R_1}^2}, \\ R_{R_2} &= \sqrt{R_{R_1}^2 - l_{R_2}^2} = \sqrt{R_1^2 + l_A^2 - l_{R_1}^2 - l_{R_2}^2}. \end{aligned} \tag{25.9}$$

The only way to prevent the trailer from following a path internal to that of the tractor is to provide its wheels with a steering mechanism (Fig. 25.3). The steering angle of the last axle must be opposite to the one of the tractor.

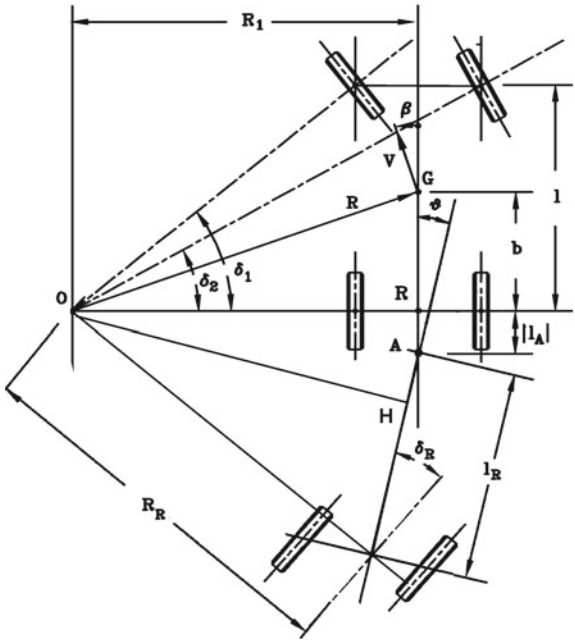

Fig. 25.3 Kinematic steering of a vehicle with a trailer with a steering angle

If the average steering angle of the wheels of the trailer is δ_R, the relationship linking the radii of the trajectories of points A and R is

$$R_A = \sqrt{R_R^2 + l_R^2 - 2 l_R R_R \sin(\delta_R)} \,. \tag{25.10}$$

The radius of the path of the trailer is then

$$R_R = \sqrt{R_1^2 + l_A^2 - l_R^2 + 2 l_R R_R \sin(\delta_R)} \,. \tag{25.11}$$

The difference between the radii of the trajectories of the trailer and the tractor can thus be reduced, allowing the space needed by the vehicle in a bend to be reduced. However, this method is not free from drawbacks, since the driver cannot visually control the rear part of the trailer that, at the beginning of the bend, seems to move outwards.

This last problem is sometimes solved by placing a second driver in the rear of the trailer to control the relevant steering mechanism, or better, by using an actuator controlled by a suitable control law from the steering control, to steer the trailer. The dynamic problems linked with the steering of trailers will be dealt with later.

The trailer angle gain is

$$\frac{\theta}{\delta} = \frac{l_A + l_R}{l} - \frac{\delta_R}{\delta} \,. \tag{25.12}$$

The value of the steering angle of the trailer allowing its axle to follow the same path as the rear axle of the tractor is

$$\sin(\delta_R) = \frac{1}{R_R}\frac{l_R^2 - l_A^2}{2l_R} . \tag{25.13}$$

If the radius of the path is much larger than the wheelbase, the radius of the path of the rear axle R_1 and of the center of mass R of the tractor are practically coincident and the linearized relationship linking the steering angles of the tractor and of the trailer is

$$\delta_R = \delta\frac{l_R^2 - l_A^2}{2ll_R} . \tag{25.14}$$

This relationship is actually between the moduli of the angles, since they must have opposite signs.

The trailer angle gain is then

$$\frac{\theta}{\delta} = \frac{(l_A + l_R)^2}{2ll_R} . \tag{25.15}$$

The mechanism controlling the steering of the trailer is usually not driven by the steering wheel but by the drawbar, because of which angle δ_R does not depend on δ but on θ. Assuming a linear relationship between the two angles

$$\delta_R = K_R\theta , \tag{25.16}$$

the trajectories of the trailer and of the tractor are the same if

$$K_R = \frac{l_R^2 - l_A^2}{(l_A + l_R)^2} . \tag{25.17}$$

Remark 25.2 The path of the trailer is circular only after a certain time: When the tractor starts to follow a circular path there is an initial transient in which the path of the trailer starts to bend, followed by the period of time needed to reach the steady state conditions.

The path of the trailer, or better of point R in Fig. 25.2a, can be computed as follows. In Fig. 25.4a the vehicle is sketched in its initial configuration with the trailer and tractor aligned; the generic configuration at time t is shown in Fig. 25.4b. In the second figure, the tractor is rotated by an angle α and the trailer is rotated by an angle β. Note that angle ϕ is positive if A lies between B and C.

The positions of the centre of rotation of the tractor O and of the trailer O_1 at time t and $t + dt$ are shown in Fig. 25.5. Distances $\overline{RR'}$, $\overline{AA'}$ and $\overline{RR''}$ are very small if compared with $\overline{AR}$ and $\overline{A'R'}$. Neglecting vanishingly small quantities, it follows that

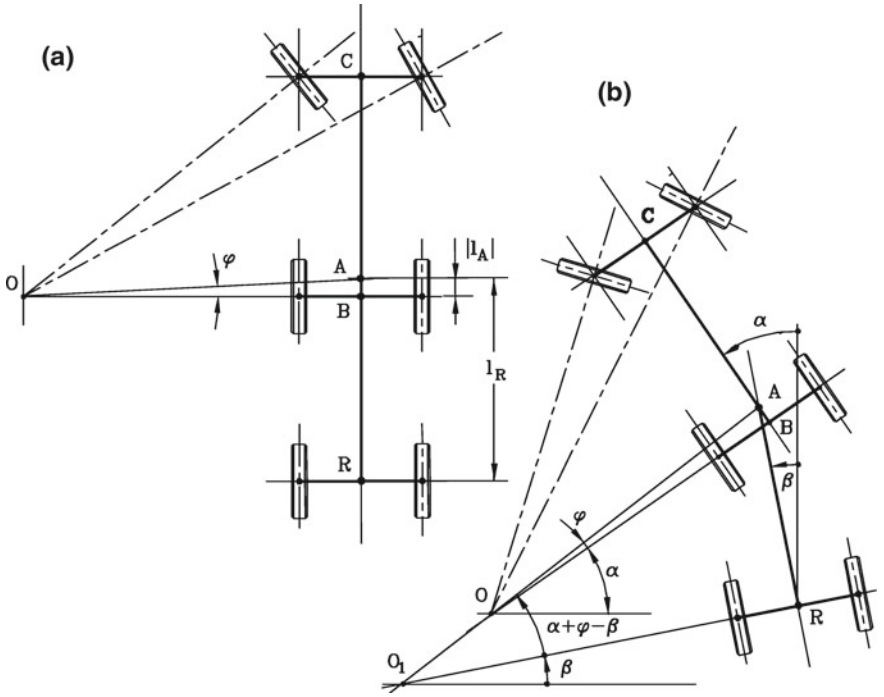

Fig. 25.4 Vehicle with two axles pulling a trailer with one axle. **a** Situation at time $t = 0$ with the vehicle in straight position; **b** Situation at time t

$$\begin{aligned} \overline{\mathrm{AA}'} &= R_A d\alpha \,, \\ \overline{\mathrm{A}'\mathrm{A}''} &= l_R d\beta = \overline{\mathrm{AA}'} \sin(\alpha + \phi - \beta) \,. \end{aligned} \tag{25.18}$$

Equations (25.18) yield

$$\frac{d\beta}{d\alpha} = \frac{R_A}{l_R} \sin(\alpha + \phi - \beta) \,. \tag{25.19}$$

Since $\alpha = \beta = 0$ at time $t = 0$, Eq. (25.19) can be easily integrated numerically. The radius of the path of the trailer R_R is

$$R_R = \frac{l_R}{\tan(\alpha + \phi - \beta)} \,. \tag{25.20}$$

A long trailer on a narrow bend requires a change of direction of more than 90° before steady-state conditions are reached and its path becomes almost circular.

The low-speed steering of a vehicle with a trailer with two axles like the one shown in Fig. 25.1b can be dealt with using the same equations seen above, applied to both the simple trailers modelling the actual two-axle trailer. The path of the first

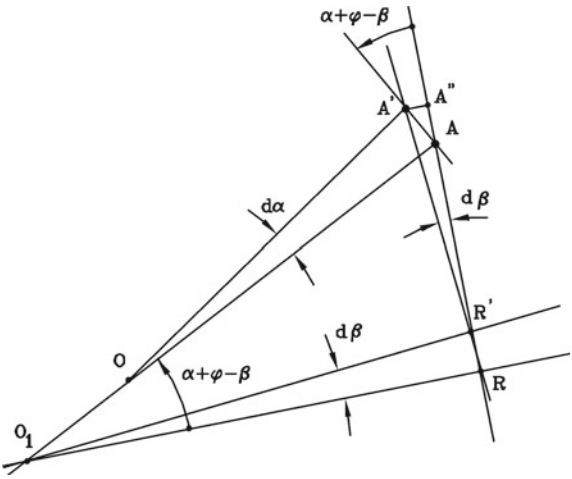

Fig. 25.5 Position of the vehicle of Fig. 25.4 at time t and $t + dt$

trailer (the dolly) is initially not circular, and this must be taken into account while integrating numerically Eq. (25.19).

Example 25.1 Study the conditions for kinematic steering of the articulated vehicle of Appendix E.10. Assume a value of the radius of the centre mass of the tractor of 10 m and compute the path of the trailer. Assume that the trailer has a single axle, coinciding with the third axle of the actual trailer.

The radius of the trajectories of the front and rear axles of the tractor is easily computed as 9.730 and 10.335 m; the off-tracking of the tractor is thus 605 mm. The approximated expression (25.5) for the off-tracking yields 607 mm, very close to the correct value even if the radius of the path is not actually very large compared to the wheelbase (10 m vs. 3.485 m).

The steering angles of the front wheels are 17.99° and 21.77°, with an average value of 19.71°. This value is also very close to the correct value of 19.88°, obtained without any linearization, and to the linearized value of 19.77°.

The steady state radius of the path of the trailer is 5.446 m, yielding a value of 4.889 m for the total off-tracking distance.

The path of the trailer has been computed by numerically integrating Eq. (25.19) for α included between 0 and 450°, with a step of 0.5°. The values of ϕ and R_A are, respectively, of 2.648° and 9.740 m. The path and the locus of points O′ are shown in Fig. 25.6. Note that after a rotation of 90° the radius of the path is still larger than that in steady-state conditions.

Example 25.2 Repeat the previous example, assuming that the trailer axle is steering with a mechanism realizing law (25.17).

The value of K is 1.118. The equation allowing the path of the trailer to be computed is the same as in the previous example, the only difference being that reference is made to point H in Fig. 25.3 instead of point R in Fig. 25.4.

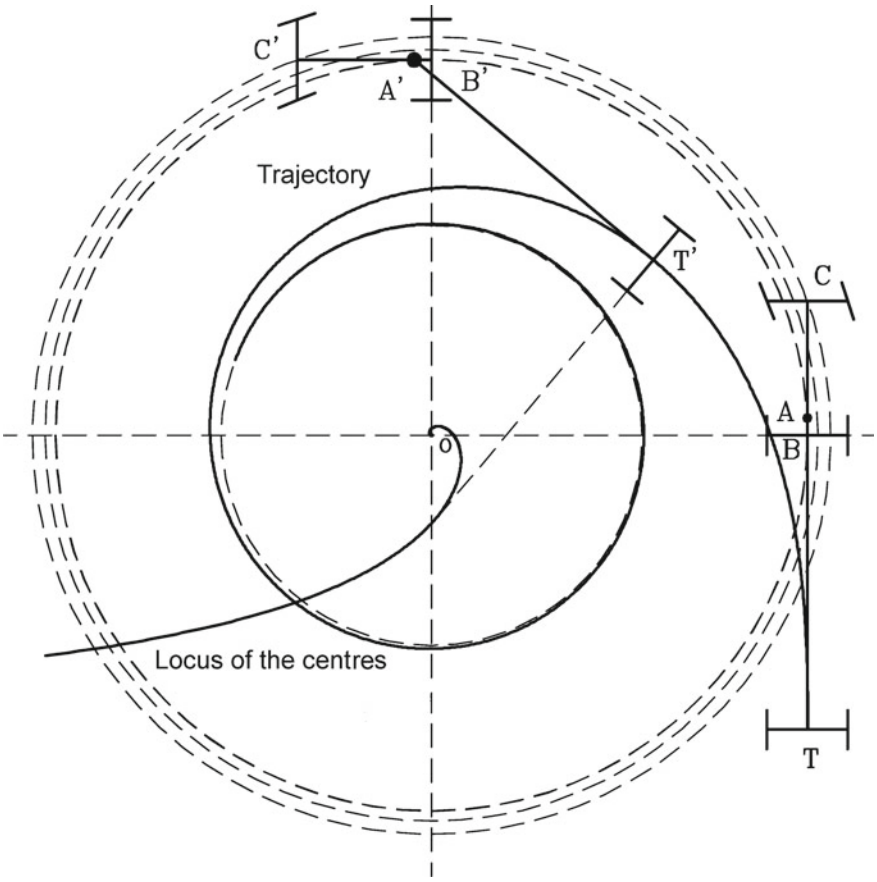

Fig. 25.6 Path and locus of the centres of curvature of the path of the trailer for an articulated vehicle. The positions of the vehicle before starting on the curved path and after a rotation of the tractor of 90° are reported

The radius of the steady-state path of the trailer is 9.942 m, very close to that of the trailer. The steering angle of the trailer is $\delta_R = 20.02°$ and the angle between the trailer and the tractor is $\theta = 19.76°$. The path of the trailer was computed by numerically integrating the relevant equation for values of α from 0 and 450°, with increments of 0.5°, as in the previous example. The path and the locus of points O′ are plotted in Fig. 25.7. Note that steady-state conditions are quickly reached and that at the beginning the trailer moves outwards.

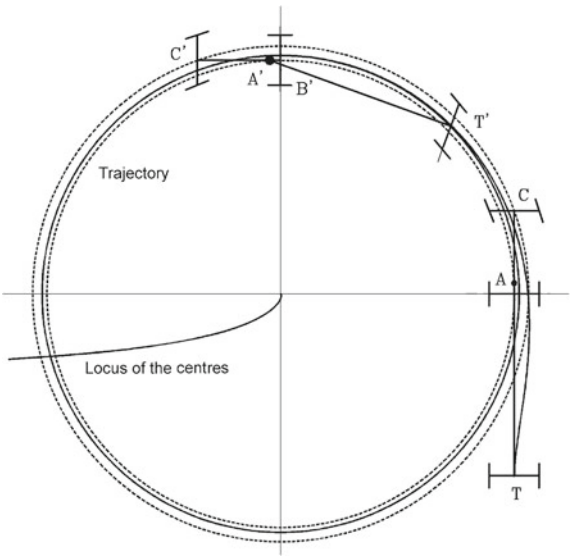

Fig. 25.7 Path and locus of the centers O′ of the path of the trailer with steering axle. The positions at the beginning of the maneouvre and after a 90° rotation are also reported

25.2 Ideal Steering

If the speed is not vanishingly small, the wheels must move with suitable sideslip angles to generate cornering forces. A simple evaluation of the steady-state steering of a vehicle in high-speed or dynamic[2] steering conditions may be performed as follows. Consider a rigid vehicle moving on level road with transversal slope angle α_t and neglect the aerodynamic side force. Define a η-axis parallel to the road surface, passing through the centre of mass of the vehicle and intersecting the vertical for the centre of the path, which in steady-state condition is circular (Fig. 25.8). Axis η does not coincide with the y axis, except at one particular speed.

25.2.1 Level Road

Assume that the road is flat and neglect aerodynamic forces. The equilibrium equation in η direction can be written by equating the centrifugal force mV^2/R to forces P_η due to the tires

$$\frac{mV^2}{R} = \sum_{\forall i} P_{\eta_i} \ . \tag{25.21}$$

[2]The term *dynamic steering* is used here to denote a condition in which the path is determined by the balance of forces acting on the vehicle, as opposed to *kinematic steering* in which the path is determined by the direction of the midplane of the wheels. Note that dynamic steering applies to both steady-state and unstationary turning.

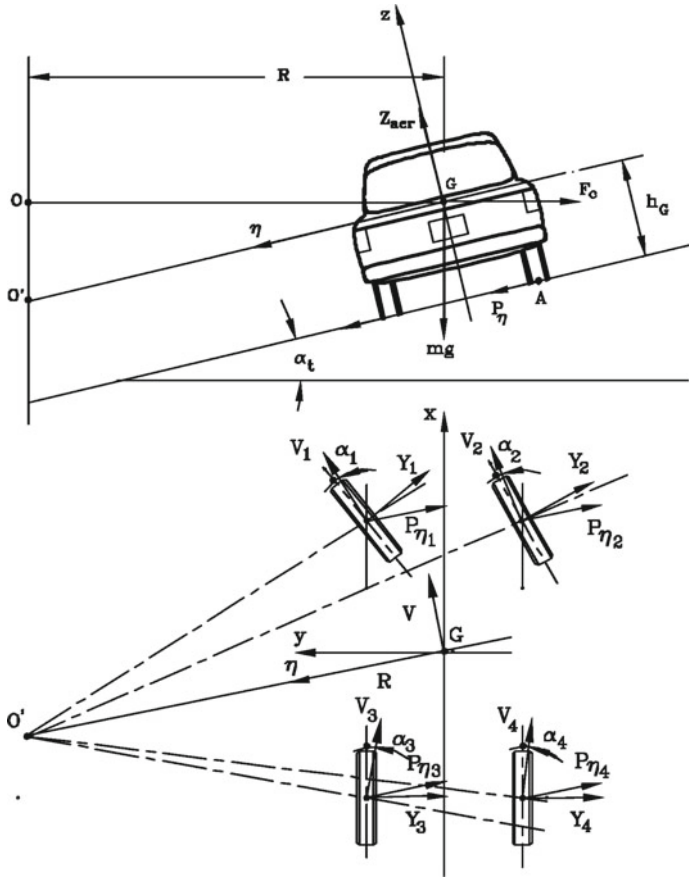

Fig. 25.8 Simplified model for dynamic steering

For a first approximation study, forces P_η may be conflated with the cornering forces F_y of the tires and all wheels may be assumed to work with the same side force coefficient μ_y. As the last assumption is similar to that seen for braking in ideal conditions, this approach will be referred to as *ideal steering*. These two assumptions lead to substituting the expression $\sum_{\forall i} P_{\eta_i}$ with $\mu_y F_z$.

Force

$$F_z = \sum F_{z_i}$$

exerted by the vehicle on the road is

$$F_z = mg \ . \tag{25.22}$$

By introducing Eq. (25.22) into Eq. (25.21) the ratio between the lateral acceleration and the gravitational acceleration g is

$$\frac{V^2}{Rg} = \mu_y \ . \tag{25.23}$$

By introducing the maximum value of the side force coefficient μ_{y_p} into Eq. (25.23), it is possible to obtain the maximum value of the lateral acceleration

$$\left(\frac{V^2}{R}\right)_{max} = g\mu_{y_p} \ . \tag{25.24}$$

The maximum speed at which a bend with radius R can be negotiated is

$$V_{max} = \sqrt{Rg}\sqrt{\mu_{y_p}} \ . \tag{25.25}$$

The limitation to the maximum lateral acceleration due to the cornering force the tires can exert is, however, not the only limitation, at least theoretically. Another can come from the danger of rollover occurring if the resultant of forces in the yz plane crosses the road surface outside point A (Fig. 25.8).

The moment of the forces applied to the vehicle in the ηz-plane about point A is

$$M_A = -\frac{t}{2}mg + h_G\frac{mV^2}{R} \ . \tag{25.26}$$

The limit condition for rollover can then be computed by equating moment M_A to zero,

$$\left(\frac{V^2}{R}\right)_{max} = g\frac{t}{2h_G} \ . \tag{25.27}$$

The rollover condition is identical to the sliding conditions, once ratio

$$\frac{t}{2h_G}$$

has been substituted for μ_{y_p}.

The maximum lateral acceleration is then

$$\left(\frac{V^2}{R}\right)_{max} = g \min\left\{\mu_{y_p}, \ \frac{t}{2h_G}\right\} \ . \tag{25.28}$$

Whether the limit condition first reached is that related to sliding, with subsequent spin out of the vehicle, or related to rolling over depends on the relative magnitude of μ_{y_p} and $\frac{t}{2h_G}$. If the former is smaller than the latter, as often occurs, the vehicle spins out. This condition can be written in the form

$$\mu_{y_p} < \frac{t}{2h_G} \ .$$

25.2.2 Effect of Aerodynamic Lift

If aerodynamic lift is accounted for, Eq. (25.22) becomes:

$$F_z = mg - \frac{1}{2}\rho V^2 S C_Z \ . \tag{25.29}$$

By introducing ratio

$$M = \frac{\rho S C_z}{2mg} \ ,$$

expressing the ratio between aerodynamic lift at unit speed and weight, it follows that

$$F_z = mg\left(1 - MV^2\right) \ . \tag{25.30}$$

Note that M is negative if the lift is directed downwards. To take aerodynamic lift into account it is sufficient to multiply the expressions seen in the previous section by $1 - MV^2$.

The maximum lateral acceleration is now

$$\left(\frac{V^2}{R}\right)_{max} = g\left(1 - MV^2\right) \min\left\{\mu_{y_p}, \ \frac{t}{2h_G}\right\} \ . \tag{25.31}$$

Term MV^2 is usually very small and often negligible, with the exception of racing cars. For instance, let $\rho = 1.22\,\text{kg/m}^3$ (value at sea level in standard atmosphere), $S = 1.7\ \text{m}^2$, $C_z = -0.5$ (an already high value) and $m = 1000$ kg. It follows that $M = -5.3 \times 10^{-5}\ \text{s}^2/\text{m}^2$ and thus, at 100 km/h, the value of the additional term is 0.05. To change things radically high speeds must be reached: at 300 km/h the additional term becomes $-MV^2 = 0.37$, i.e. the maximum lateral acceleration increases by 37%.

The negative value of C_z is very high in racing cars, and at high speed strong lateral accelerations are possible.

25.2.3 Transversal Slope of the Road

The equilibrium equation in η direction may be written by equating the components of weight mg and of the centrifugal force mV^2/R acting in that direction with forces P_η due to the tires

$$\frac{mV^2}{R}\cos(\alpha_t) - mg\sin(\alpha_t) = \sum_{\forall i} P_{\eta_i} \ . \tag{25.32}$$

By introducing the previously discussed assumptions characterizing ideal steering, substituting expression $\sum_{\forall i} P_{\eta_i}$ with $\mu_y F_z$, force $F_z = \sum F_{z_i}$ exerted by the vehicle on the road becomes

$$F_z = mg\cos(\alpha_t) + \frac{mV^2}{R}\sin(\alpha_t) - \frac{1}{2}\rho V^2 S C_Z \ . \tag{25.33}$$

By introducing Eq. (25.33) into Eq. (25.32), the latter yields the following value for the ratio between the lateral acceleration and the gravitational acceleration g,

$$\frac{V^2}{Rg} = \frac{\tan(\alpha_t) + \mu_y(1 - MV^2)}{1 - \mu_y \tan(\alpha_t)} \ . \tag{25.34}$$

Ratio M can be redefined as

$$M = \frac{\rho S C_z}{2mg\cos(\alpha_t)}$$

so that MV^2 is the ratio between the aerodynamic lift and the component of weight in a direction perpendicular to the road.

By introducing the maximum value of the side force coefficient μ_{y_p} into Eq. (25.34), the maximum value of the lateral acceleration is obtained,

$$\left(\frac{V^2}{R}\right)_{max} = g f_s \ , \tag{25.35}$$

where the so-called *sliding factor* f_s can be defined as[3]

$$f_s = \frac{\tan(\alpha_t) + \mu_{y_p}(1 - MV^2)}{1 - \mu_{y_p} \tan(\alpha_t)} \tag{25.36}$$

and is in general a function of the speed, if the aerodynamic lift is accounted for.

Note that on level road and with no aerodynamic lift the sliding factor reduces to μ_{y_p}.

The sliding factor is reported as a function of μ_{y_p} for different values of the transversal slope of the road in Fig. 25.9a and for different values of ratio MV^2 in Fig. 25.9b. Note that if the road is flat and the aerodynamic lift is neglected it reduces to the maximum value of the side force coefficient μ_{y_p}.

[3]The sliding factor is more commonly defined as the square root of the same quantity considered here. The present definition, which refers directly to the lateral acceleration instead of the speed at which a given turn may be negotiated, is here preferred as in particular conditions it reduces to the side force coefficient.

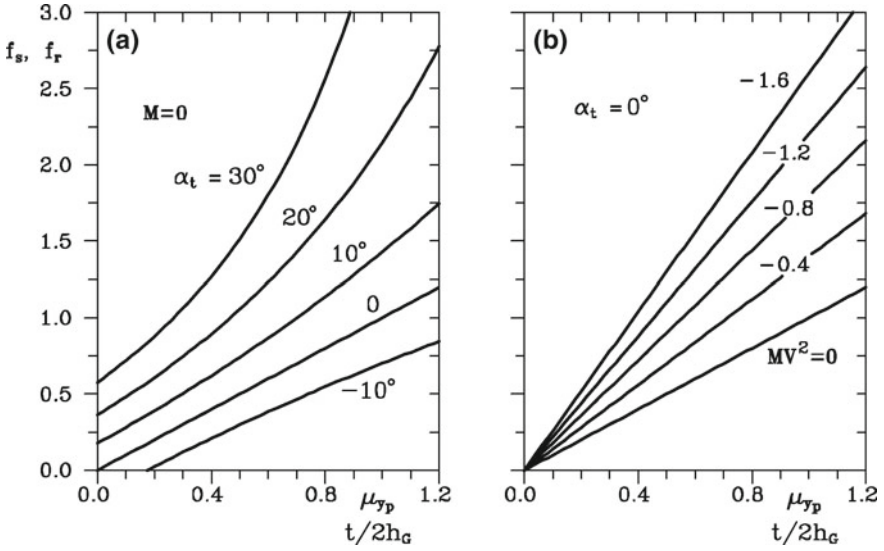

Fig. 25.9 Sliding and rollover factors as functions of μ_{y_p} and of $t/2h_G$ respectively for roads with different transversal slope (**a**) and for vehicles with different values of ratio MV^2 (**b**)

The maximum speed at which a bend with radius R can be negotiated is

$$V_{max} = \sqrt{Rg}\sqrt{\frac{\tan(\alpha_t) + \mu_{y_p}}{1 - \mu_{y_p}\left[\tan(\alpha_t) - RgM\right]}}\ , \tag{25.37}$$

i.e.,

$$V_{max} = \sqrt{Rg}\sqrt{f_s}\ . \tag{25.38}$$

The rollover condition can also be modified to take into account the transversal slope of the road and aerodynamic lift. The moment of all forces applied to the vehicle in the ηz plane about point A (Fig. 25.8) is

$$\begin{aligned} M_A = -\frac{t}{2}\left[mg\cos(\alpha_t) + \frac{mV^2}{R}\sin(\alpha_t) - \frac{1}{2}\rho V^2 S C_Z\right] + \\ + h_G\left[\frac{mV^2}{R}\cos(\alpha_t) - mg\sin(\alpha_t)\right]\ . \end{aligned} \tag{25.39}$$

The limit condition for rollover can be obtained by equating moment M_A to zero, obtaining

$$\left(\frac{V^2}{R}\right)_{max} = g f_r\ , \tag{25.40}$$

where the *rollover factor* can be defined as

$$f_r = \frac{\tan(\alpha_t) + \frac{t}{2h_G}(1 - MV^2)}{1 - \frac{t}{2h_G}\tan(\alpha_t)} \,. \tag{25.41}$$

The expression of the rollover factor is identical to that of the sliding factor, once ratio $t/2h_G$ has been substituted for μ_{y_p} (Fig. 25.9). It depends on speed because of the effects of aerodynamic lift.

The maximum lateral acceleration is then

$$\left(\frac{V^2}{R}\right)_{max} = g \min\{f_s, f_r\} \,. \tag{25.42}$$

Whether the limit condition first reached is that related to sliding, with subsequent spin out of the vehicle, or rolling over, depends on whether f_s is larger or smaller than f_r. If $f_s < f_r$, as often occurs, the vehicle spins out. This condition can be written in the form

$$\mu_{y_p} < \frac{t}{2h_G} \,,$$

and coincides with that seen on level road. Neither aerodynamic lift nor a transversal road slope have any influence on the possibility of rollover.

25.2.4 Considerations on Ideal Steering

The value of μ_{y_p} at which rollover may occur is as high as 1.2–1.7 for sports cars, 1.1–1.6 for saloon cars, 0.8–1.1 for pickup and passenger vans and 0.4–0.8 for heavy and medium trucks. Only in the latter case does rollover seem to be a possibility, at least if the lateral forces acting on the vehicle are restricted to the cornering forces of the tires.

The present model is only a rough approximation of the actual situation, as it is based on the assumption that the side force coefficients μ_y of all wheels are equal, implying that all wheels work with the same sideslip angle α. It also ignores the effect of the different directions of the cornering forces of the various wheels, which should be considered as perpendicular to the midplanes of the wheels and not directed along the η axis. The load transfer between the wheels of the same axle and the presence of the suspensions have also been neglected, two other assumptions contributing to the lack of precision of this model.

If the maximum speed at which a circular path can be negotiated is measured in a steering pad test and the value of the lateral force coefficient is computed through Eq. (25.25), a value of μ_{y_p}, well below that obtained from tests on the tires, is obtained.

Remark 25.3 The cornering force coefficient obtained in this way is that of the vehicle as a whole, and the difference between its value and that related to the tires gives a measure of how well the vehicle is able to exploit the cornering characteristics of its wheels.

The side force coefficient measured on the whole vehicle also depends on the radius of the path, with a notable decrease on narrow bends. The majority of industrial and passenger vehicles are able to use only a fraction, from 50 to 80%, of the potential cornering force of the tires, with higher values found only in sports cars. This reduction of the lateral forces makes the danger of rollover more remote.

Actually rolling over in a quasi-static condition is impossible for most vehicles, notwithstanding the fact that rollover actually occurs in many road accidents. Rollover can usually be ascribed to dynamic phenomena in nonstationary conditions or to lateral forces caused by side contacts, e.g. of the wheels with the curb of the road, that rule out the possibility of side slipping while causing far stronger lateral forces to be exerted on the wheels. The presence of the suspensions also contributes to this picture, making rollover a likely outcome of many accidents.

From the equations it is also clear that only the use of aerodynamic devices able to exert a strong negative lift allows high values of lateral acceleration, well above 1 g in the case of racers, to be reached (Fig. 25.10).

25.2.5 *Vehicles with Two Wheels*

The cornering dynamics of a vehicle with two wheels are radically different from those of four-wheeled vehicles (Fig. 25.11). If the gyroscopic moments of the wheels are neglected, the equation expressing rolling equilibrium can be used to compute the roll angle the vehicle must maintain in order not to capsize, since a two-wheeled vehicle is a system underconstrained in roll.

The limitation on lateral acceleration and speed on a curved path is solely the result of lateral sliding, with a further geometric limitation on the maximum roll angle that can be reached before the vehicle or the driver touches the road on one side. Equation (25.24) yielding the maximum lateral acceleration still holds, the difference being that the global side force coefficient is usually higher.

The roll angle is easily computed,

$$\phi = \arctan\left(\frac{V^2}{Rg}\right) , \tag{25.43}$$

and the geometrical limitation

$$\phi \leq \pi/2 + \alpha_t - \gamma$$

Figure 25.11 usually does not induce further limitations.

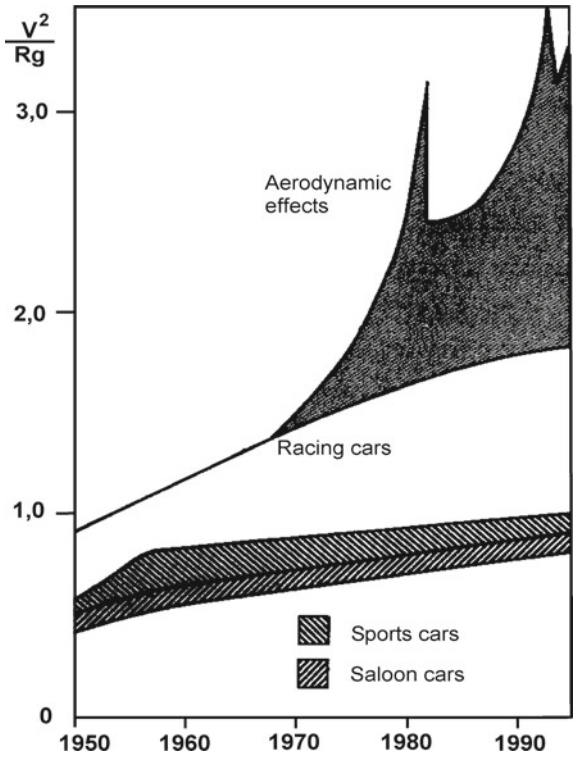

Fig. 25.10 Evolution in time of the maximum lateral acceleration for saloon cars, sports cars and racers. Note that for the latter the change of racing rules caused sharp changes in the maximum lateral acceleration

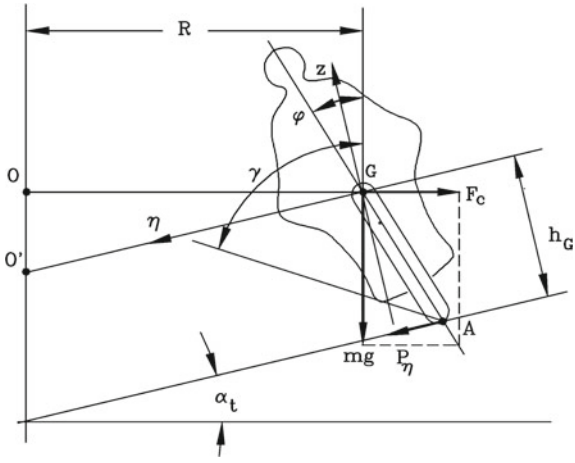

Fig. 25.11 High-speed steering of a two-wheeled vehicle. Point G is the centre of mass of the vehicle-driver system and can be displaced from the plane of symmetry of the former if the latter is displaced to one side, as usually occurs in bends

Remark 25.4 Since motorcycles roll into the curve, the lateral forces due to camber add to those due to sideslip, instead of subtracting as in the case of motor vehicles that roll towards the outside of the curve.

Further terms must be introduced into the relevant equations if gyroscopic moments of the wheels are considered . When the vehicle runs on a circular path with radius R, the gyroscopic moment, due to the ith wheel with radius R_i and moment of inertia J_{p_i} about its spin axis, is equal to

$$\frac{J_{p_i} V^2 \cos(\phi)}{R R_i} .$$

The equation expressing the equilibrium for rolling motions is then

$$mgh_G \sin(\phi) - \frac{V^2}{R} \cos(\phi) \left[mh_G + \sum_{\forall i} \left(\frac{J_{p_i}}{R_i} \right) \right] = 0 . \tag{25.44}$$

The roll angle is

$$\phi = \arctan \left\{ \frac{V^2}{Rg} \left[1 + \frac{1}{mh_G} \sum_{\forall i} \left(\frac{J_{p_i}}{R_i} \right) \right] \right\} . \tag{25.45}$$

The added term in Eq. (25.45) is positive and thus the roll angle needed to manage a certain bend at a certain speed is increased by gyroscopic moments.

Remark 25.5 Generally speaking, the effect of the gyroscopic moment of the wheels on the dynamic behavior of the whole vehicle is small even in the case of vehicles with two wheels. Gyroscopic moments are usually important only in the dynamics of the steering device.

25.3 High Speed Cornering: Simplified Approach

To go beyond the extremely simplified model of ideal steering, the distribution of cornering forces between the axles, the sideslip angle of the vehicle on the path and the sideslip angles of the wheels must be taken into account.

Assume that the vehicle is moving at constant speed on a circular path and that the road is level. Moreover, assume that the radius of the path R is much larger than the wheelbase l and, as a consequence, all sideslip angles are small. The small size of all angles allows the "monotrack" or "bicycle" model to be used.

Neglecting aerodynamic forces and aligning torques, the forces acting in the xy plane at the tire-road interface in a monotrack vehicle are shown in Fig. 25.12.

The equilibrium equation in the direction of the y axis is similar to Eq. (25.21), except for the presence of the sideslip and steering angles

$$\frac{mV^2}{R} \cos(\beta) = \sum_{\forall i} F_{x_i} \sin(\delta_i) + \sum_{\forall i} F_{y_i} \cos(\delta_i) . \tag{25.46}$$

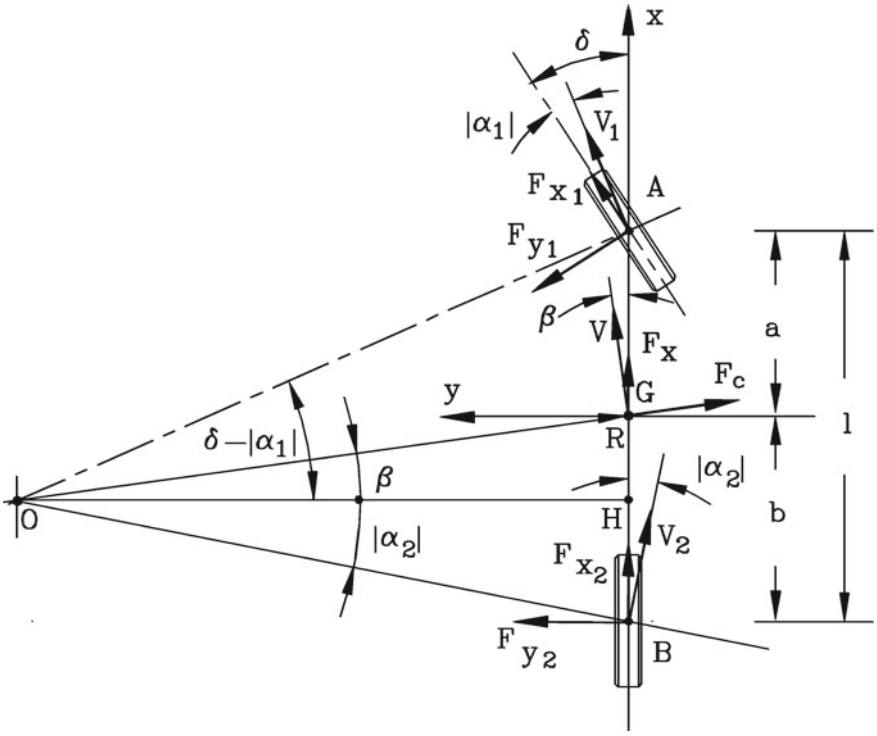

Fig. 25.12 Simplified model (monotrack vehicle) for studying the handling of a two-axle vehicle

The equilibrium to rotations about point G can be expressed as

$$\sum_{\forall i} F_{x_i} \sin(\delta_i) x_i + \sum_{\forall i} F_{y_i} \cos(\delta_i) x_i = 0 \,. \tag{25.47}$$

Since angles β and δ_i are assumed to be small, the terms containing the longitudinal forces of the tires can be neglected and the equilibrium equations reduce to

$$\begin{cases} \sum_{\forall i} F_{y_i} = \frac{mV^2}{R} \\ \sum_{\forall i} F_{y_i} x_i = 0 \,. \end{cases} \tag{25.48}$$

For a two-axle vehicle, they can be immediately solved, yielding

$$F_{y_1} = \frac{mV^2}{R} \frac{b}{l} \,, \quad F_{y_2} = \frac{mV^2}{R} \frac{a}{l} \,. \tag{25.49}$$

Assuming that the cornering forces of the axles are proportional to the sideslip angles through their cornering stiffness, it follows that

$$\alpha_1 = -\frac{mV^2}{R}\frac{b}{lC_1}\,, \quad \alpha_2 = -\frac{mV^2}{R}\frac{a}{lC_2}\,, \tag{25.50}$$

where C_i is the cornering stiffness of the ith axle, and is equal to the cornering stiffness of the wheels multiplied by the number of wheels of the axle.

A relationship between the sideslip and steering angles can be found with simple geometrical considerations from Fig. 25.12,

$$\delta - \alpha_1 + \alpha_2 = \frac{l}{R}\,. \tag{25.51}$$

Introducing the expressions of the sideslip angles into Eq. (25.51), it follows that

$$\delta = \frac{l}{R} + \frac{mV^2}{Rl}\left(\frac{b}{C_1} - \frac{a}{C_2}\right)\,, \tag{25.52}$$

or, in terms of path curvature gain,

$$\frac{1}{R\delta} = \frac{1}{l}\frac{1}{1 + K_{us}\frac{V^2}{gl}}\,, \tag{25.53}$$

where

$$K_{us} = \frac{mg}{l^2}\left(\frac{b}{C_1} - \frac{a}{C_2}\right) \tag{25.54}$$

is the so-called *understeer coefficient* or *understeer gradient* of the vehicle. The understeer coefficient is a non-dimensional quantity, and is often expressed in radians.

As already stated, in kinematic conditions

$$\left(\frac{1}{R\delta}\right)_{\text{kin}} = \frac{1}{l}\,. \tag{25.55}$$

The expression $1 + K_{us}V^2/gl$ can be considered as a correction factor giving the response of the vehicle in dynamic conditions as opposed to kinematic conditions.

From Eq. (25.52) it follows that

$$\delta - \delta_{\text{kin}} = \frac{V^2}{Rg}K_{us}\,, \tag{25.56}$$

i.e.,

$$K_{us} = \frac{g}{a_y}\left(\delta - \delta_{\text{kin}}\right)\,. \tag{25.57}$$

The understeer factor can thus be interpreted as the difference between the steering angles in kinematic and dynamic conditions divided by the centrifugal acceleration expressed as a multiple of the gravitational acceleration.

Sometimes, instead of the understeer coefficient, a *stability factor*

$$K = \frac{m}{l^2}\left(\frac{b}{C_1} - \frac{a}{C_2}\right) \tag{25.58}$$

is defined.

As a first approximation, K and K^* may be considered as constant for a given vehicle and load condition. As will be seen below, however, in many cases their dependence on speed cannot be neglected for more precise assessments.

It is possible to define a *lateral acceleration* gain as the ratio between the lateral acceleration and the steering input:

$$\frac{V^2}{R\delta} = \frac{V^2}{l}\frac{1}{1 + K_{us}\frac{V^2}{gl}} . \tag{25.59}$$

The sideslip angle can be obtained through simple geometrical considerations, yielding

$$\beta = \frac{b}{R} - \alpha_2. \tag{25.60}$$

A *sideslip angle gain*, expressing the ratio between the sideslip angle and the steering angle can be defined as well. Its value is

$$\frac{\beta}{\delta} = \frac{b}{l}\left(1 - \frac{maV^2}{blC_2}\right)\frac{1}{1 + K_{us}\frac{V^2}{gl}} . \tag{25.61}$$

25.4 Definition of Understeer and Oversteer

If $K_{us} = 0$ the value of $1/R\delta$ is constant and equal to the value characterizing kinematic steering; i.e. the response of the vehicle to a steering input is, at any speed, equal to that in kinematic conditions. This does not mean, however, that the vehicle is in kinematic conditions, since the value of the sideslip angle β is not equal to its kinematic value and the values of the sideslip angles of the wheels are not equal to zero.

A vehicle behaving in this way is said to be *neutral-steer* (Fig. 25.13a).

If $K_{us} > 0$ the value of $1/R\delta$ decreases with increasing speed. The response of the vehicle is then smaller than in kinematic conditions and, to maintain a constant radius of the path, the steering angle must be increased as speed increases.

A vehicle behaving in this way is said to be *understeer*.

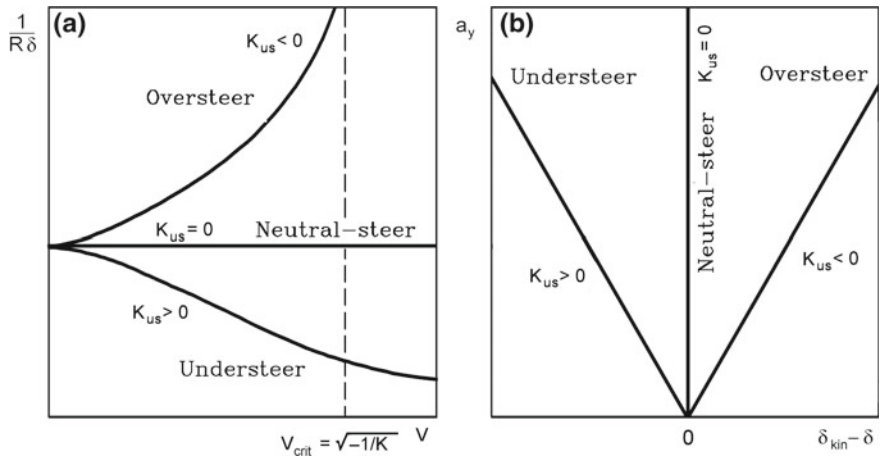

Fig. 25.13 Steady state response to a steering input. Plot of the path curvature gain as a function of speed (**a**) and handling diagram (**b**) for an oversteer, an understeer and a neutral steer vehicle. The understeer factor is assumed to be independent of speed

A quantitative measure of the understeering of a vehicle is given by the *characteristic speed*, defined as the speed at which the steering angle needed to negotiate a turn is equal to twice the Ackerman angle, i.e. the path curvature gain is equal to $1/2l$.

Using the simplified approach outlined above, the characteristic speed is

$$V_{car} = \sqrt{\frac{gl}{K_{us}}} = \sqrt{\frac{1}{K}} \,. \tag{25.62}$$

If $K_{us} < 0$ the value of $1/R\delta$ increases with increasing speed until, for a speed

$$V_{crit} = \sqrt{-\frac{gl}{K_{us}}} = \sqrt{-\frac{1}{K}} \tag{25.63}$$

the response tends to infinity, i.e., the system develops an unstable behavior.

A vehicle behaving in this way is said to be *oversteer*, and the speed given by Eq. (25.63) is called the *critical speed*. The critical speed of any oversteer vehicle must be well above the maximum speed it can reach, at least in normal road conditions.

Instead of plotting the path curvature gain as a function of the speed, it is possible to plot the *handling diagram*, i.e., the plot of the lateral acceleration a_y as a function of $\delta_{\text{kin}} - \delta$ (Fig. 25.13b). If the vehicle is neutral steer, the plot is a vertical straight line, if it is oversteer it is a straight line sloping to the right, while in case of an understeer vehicle it slopes to the left.

The value of β, or better, of β/δ, decreases with the speed from the kinematic value up to the speed

$$(V)_{\beta=0} = \sqrt{\frac{blC_2}{am}} \tag{25.64}$$

at which it vanishes. At higher speed it becomes negative, tending to infinity when approaching the critical speed for oversteer vehicles and tending to

$$\frac{aC_1}{aC_1 - bC_2}$$

when the speed tends to infinity in the case of understeering vehicles.

The sideslip angles of the front and rear wheels are equal in neutral-steer vehicles. In oversteer vehicles, the rear wheels have a larger sideslip angle (in absolute value, since the sideslip angles are negative when the radius of the path is positive), while the opposite holds in understeer vehicles. It follows that oversteer vehicles can be

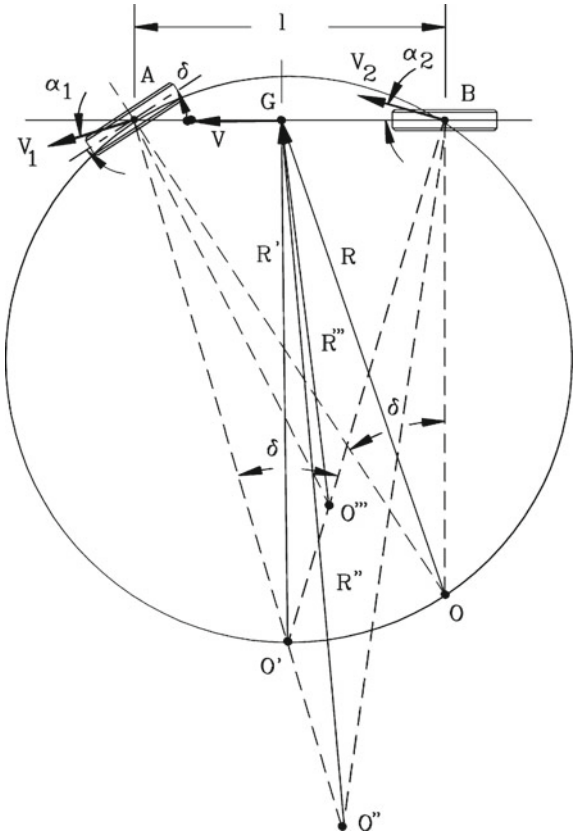

Fig. 25.14 Geometrical definition of the behavior of a vehicle with a single steering axle

expected to reach limit conditions at the rear wheels and understeer vehicles at the front wheels, even if the present model cannot be applied when the sideslip angles increase, approaching limit conditions.

A graphical interpretation of this result, for a vehicle with a single steering axle, is shown in Fig. 25.14. The vehicle is modelled as a steering front axle and a fixed rear axle. Kinematic steering applies if the speed tends to zero: the sideslip angles vanish and the center of path is point O. It follows immediately that

$$\frac{l}{R} = \tan(\delta) \approx \delta \, .$$

With increasing speed the wheels work with increasing sideslip angles α_1 and α_2. If $\alpha_1 = \alpha_2$ angle BO′A is still equal to δ (its value is $|\alpha_2| + \delta - |\alpha_1|$) and thus O′ lies on a circle through points A, B and O.

Since $l \ll R'$, O′ is in a position almost opposite to A and B and then $R' \approx R$. The radius of the path is still equal to that characterizing kinematic steering, and the vehicle is neutral steer.

If $|\alpha_1| > |\alpha_2|$ the center of the path moves to O″ and radius R'' is larger than R. The vehicle is then understeer. If, on the other hand, $|\alpha_1| < |\alpha_2|$, the center of the path is O‴, radius R''' is smaller than R' and the vehicle is oversteer.

25.5 High Speed Cornering

25.5.1 Equations of Motion

The study of handling seen in the previous sections was based on the assumption of steady-state operation. Moreover, only the cornering forces acting on the tires were considered.

A simple mathematical model for the handling behavior of a rigid vehicle that overcomes the above limitations can, however, be built.

To keep the model as simple as possible, the following assumptions may be made

1. The sideslip angle of the vehicle β and of the wheels α are small. The yaw angular velocity $\dot{\psi}$ can also be considered a small quantity.
2. The vehicle can be assumed to be a rigid body moving on a flat surface, i.e., roll and pitch angles are neglected as well as the vertical displacements due to suspensions.

If a motor vehicle is considered as a rigid body moving on a surface, a model with three degrees of freedom is needed for the study of its motion. If the road is considered as a flat surface, the motion is planar. By using the inertial reference

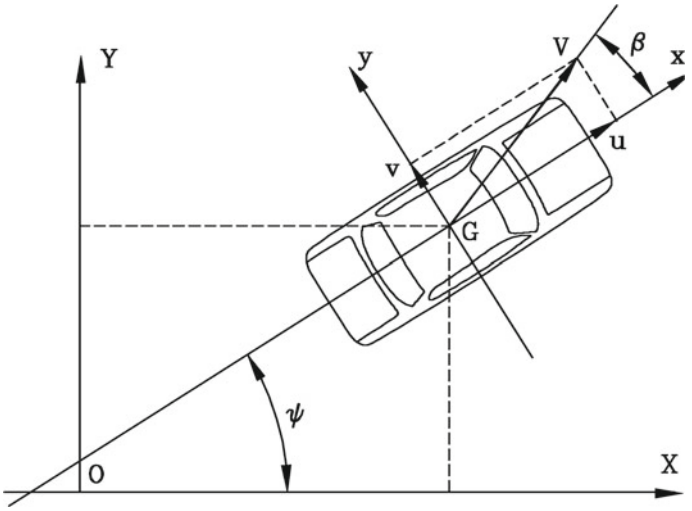

Fig. 25.15 Reference frame for the study of the motion of a rigid vehicle. The vehicle has three degrees of freedom, and the coordinates X and Y of the centre of mass G and the yaw angle ψ can be used as generalized coordinates

frame[4] XY shown in Fig. 25.15, it is possible to use the coordinates X and Y of the centre of mass G of the vehicle and the yaw angle ψ between the x and X axes as generalized coordinates.

The equations of motion of the vehicle are

$$\begin{cases} m\ddot{X} = F_X \\ m\ddot{Y} = F_Y \\ J_z\ddot{\psi} = M_z \end{cases}, \tag{25.65}$$

where F_X, F_Y and M_z are the total forces acting in the X and Y directions and the total yawing moment. For the latter, subscript z has been used instead of Z since the directions of the two axes coincide.

Equations (25.65) are very simple but include the forces acting on the vehicle in the direction of the axes of the inertial frame. They are clearly linked with the forces acting in the directions of axes x and y of the vehicle by the obvious relationship

$$\begin{Bmatrix} F_X \\ F_Y \end{Bmatrix} = \begin{bmatrix} \cos(\psi) & -\sin(\psi) \\ \sin(\psi) & \cos(\psi) \end{bmatrix} \begin{Bmatrix} F_x \\ F_y \end{Bmatrix} . \tag{25.66}$$

[4] As already stated, such a reference frame is not, strictly speaking, inertial, since it is fixed to the road surface and hence follows the motion of Earth. It is, however, inertial "enough" for the problems here studied, and this issue will not be dealt with any further.

If the model is used to perform a numerical integration in time, they can be used directly without any difficulty.

However, if the model has to be used to obtain linearized equations in order to gain a general insight into the behavior of the vehicle, it is better to write the equations of motion with reference to the non-inertial xy frame, to avoid dealing with the trigonometric functions of angle ψ, which in general is not a small angle, and would make linearizations impossible.

To write the equations of motion with reference to the body-fixed frame xyz, it is expedient to use the components u and v of the speed in the directions of the x and y axes and the yaw angular velocity

$$r = \dot{\psi} \, .$$

There are many ways to obtain the mathematical model, but perhaps the simplest is to remember that the derivative with respect to time of a generic vector $\vec{A}$, expressed in the body-fixed frame, but performed in the inertial frame

$$\left. \frac{d\vec{A}}{dt} \right|_i \, ,$$

can be expressed starting from the derivative performed in the body fixed frame

$$\left. \frac{d\vec{A}}{dt} \right|_m$$

as

$$\left. \frac{d\vec{A}}{dt} \right|_i = \left. \frac{d\vec{A}}{dt} \right|_m + \vec{\Omega} \wedge \vec{A} \, , \tag{25.67}$$

where $\vec{\Omega}$ is the absolute angular velocity of the body-fixed frame.

In the present case, the velocity and the angular velocity vectors, in the body-fixed frame, are

$$\vec{V} = \left\{ \begin{array}{c} u \\ v \\ 0 \end{array} \right\} \, , \quad \vec{\Omega} = \left\{ \begin{array}{c} 0 \\ 0 \\ r \end{array} \right\} \, . \tag{25.68}$$

The derivative of the velocity of the vehicle is then

$$\left. \frac{d\vec{V}}{dt} \right|_i = \left. \frac{d\vec{V}}{dt} \right|_m + \vec{\Omega} \wedge \vec{V} = \left\{ \begin{array}{c} \dot{u} - rv \\ \dot{v} + ru \\ 0 \end{array} \right\} \, . \tag{25.69}$$

The equations of motion of the vehicle, expressed with reference to the xyz frame, are

$$\begin{cases} m(\dot{u} - rv) = F_x \\ m(\dot{v} + ru) = F_y \\ J_z \dot{r} = M_z \ . \end{cases} \tag{25.70}$$

As an alternative, a procedure based on Lagrange equations can be followed. Although apparently more complicated, it will be shown here, since it is consistent with what will be done later for more complex models. In the present case other approaches are more straightforward.

The kinetic energy of the vehicle is

$$\mathcal{T} = \frac{1}{2} m \left(u^2 + v^2\right) + \frac{1}{2} J_z r^2 \ . \tag{25.71}$$

The rotational kinetic energy of the wheels has been neglected: No gyroscopic effect of the wheels will be obtained in this way.

Velocities u, v and r are linked to the derivatives of the generalized coordinates $\dot{X}$, $\dot{Y}$ and $\dot{\psi}$ by the relationship:

$$\begin{Bmatrix} u \\ v \\ r \end{Bmatrix} = \begin{bmatrix} \cos(\psi) & \sin(\psi) & 0 \\ -\sin(\psi) & \cos(\psi) & 0 \\ 0 & 0 & 1 \end{bmatrix} \begin{Bmatrix} \dot{X} \\ \dot{Y} \\ \dot{\psi} \end{Bmatrix} \ , \tag{25.72}$$

i.e.,

$$\mathbf{w} = \mathbf{A}^T \dot{\mathbf{q}} \ , \tag{25.73}$$

where

$$\mathbf{w} = \begin{bmatrix} u & v & r \end{bmatrix}^T$$

is the vector containing the generalized velocities, and

$$\dot{\mathbf{q}} = \begin{bmatrix} \dot{X} & \dot{Y} & \dot{\psi} \end{bmatrix}^T$$

is the vector containing the derivatives of the generalized coordinates.

Since matrix $\mathbf{A}$ is a rotation matrix,

$$\mathbf{A}^T = \mathbf{A}^{-1} \tag{25.74}$$

and the inverse transformation is

$$\dot{\mathbf{q}} = \mathbf{A}\mathbf{w} \ . \tag{25.75}$$

The equations of motion are

$$\frac{d}{dt}\left(\frac{\partial \mathcal{T}}{\partial \dot{q}_i}\right) - \frac{\partial \mathcal{T}}{\partial q_i} = Q_i \ , \tag{25.76}$$

where coordinates q_i are X, Y and ψ and forces Q_i are the corresponding generalized forces F_X, F_Y and M_z.

The derivatives needed to write the equations of motion are

$$\begin{cases} \dfrac{\partial \mathcal{T}}{\partial \dot{X}} = \dfrac{\partial \mathcal{T}}{\partial u}\dfrac{\partial u}{\partial \dot{X}} + \dfrac{\partial \mathcal{T}}{\partial v}\dfrac{\partial v}{\partial \dot{X}} + \dfrac{\partial \mathcal{T}}{\partial r}\dfrac{\partial r}{\partial \dot{X}} \\ \dfrac{\partial \mathcal{T}}{\partial \dot{Y}} = \dfrac{\partial \mathcal{T}}{\partial u}\dfrac{\partial u}{\partial \dot{Y}} + \dfrac{\partial \mathcal{T}}{\partial v}\dfrac{\partial v}{\partial \dot{Y}} + \dfrac{\partial \mathcal{T}}{\partial r}\dfrac{\partial r}{\partial \dot{Y}} \\ \dfrac{\partial \mathcal{T}}{\partial \dot{\psi}} = \dfrac{\partial \mathcal{T}}{\partial u}\dfrac{\partial u}{\partial \dot{\psi}} + \dfrac{\partial \mathcal{T}}{\partial v}\dfrac{\partial v}{\partial \dot{\psi}} + \dfrac{\partial \mathcal{T}}{\partial r}\dfrac{\partial r}{\partial \dot{\psi}} \end{cases}, \tag{25.77}$$

i.e.,

$$\left\{\frac{\partial \mathcal{T}}{\partial \dot{q}}\right\} = \mathbf{A}\left\{\frac{\partial \mathcal{T}}{\partial w}\right\}, \tag{25.78}$$

where

$$\left\{\frac{\partial \mathcal{T}}{\partial \dot{q}}\right\} = \left[\begin{array}{ccc} \dfrac{\partial \mathcal{T}}{\partial \dot{X}} & \dfrac{\partial \mathcal{T}}{\partial \dot{Y}} & \dfrac{\partial \mathcal{T}}{\partial \dot{\psi}} \end{array}\right]^T$$

is the vector containing the derivatives with respect to the derivatives of the generalized coordinates, while

$$\left\{\frac{\partial \mathcal{T}}{\partial w}\right\} = \left[\begin{array}{ccc} \dfrac{\partial \mathcal{T}}{\partial u} & \dfrac{\partial \mathcal{T}}{\partial v} & \dfrac{\partial \mathcal{T}}{\partial w} \end{array}\right]^T$$

is the vector containing the derivatives with respect to the generalized velocities.

By differentiating with respect to time, it follows that

$$\frac{\partial}{\partial t}\left(\left\{\frac{\partial \mathcal{T}}{\partial \dot{q}}\right\}\right) = \mathbf{A}\frac{\partial}{\partial t}\left(\left\{\frac{\partial \mathcal{T}}{\partial w}\right\}\right) + \dot{\mathbf{A}}\left\{\frac{\partial \mathcal{T}}{\partial w}\right\}, \tag{25.79}$$

where

$$\dot{\mathbf{A}} = \dot{\psi}\begin{bmatrix} -\sin(\psi) & -\cos(\psi) & 0 \\ \cos(\psi) & -\sin(\psi) & 0 \\ 0 & 0 & 0 \end{bmatrix}. \tag{25.80}$$

The computation of the derivatives with respect to the generalized coordinates $\left\{\frac{\partial \mathcal{T}}{\partial q}\right\}$ [5] is more complex. The generic derivative $\frac{\partial \mathcal{T}}{\partial q_k}$ is

$$\frac{\partial \mathcal{T}^*}{\partial q_k} = \frac{\partial \mathcal{T}}{\partial q_k} + \sum_{i=1}^{n}\frac{\partial \mathcal{T}}{\partial w_i}\frac{\partial w_i}{\partial q_k} = \frac{\partial \mathcal{T}}{\partial q_k} + \sum_{i=1}^{n}\frac{\partial \mathcal{T}}{\partial w_i}\sum_{j=1}^{n}\frac{\partial A_{ij}}{\partial q_k}\dot{q}_j, \tag{25.81}$$

[5] For details on this part of the analysis, see L. Meirovitch, *Methods of Analytical Dynamics*, Mc Graw-Hill, New York, 1970.

where $\mathcal{T}^*$ is the kinetic energy expressed as a function of the generalized coordinates and their derivatives (the expression to be introduced into Lagrange equations in their original form), while $\mathcal{T}$ is expressed as a function of the generalized coordinates and the velocities in the body-fixed frame. It is possible to show that

$$\frac{\partial \mathcal{T}^*}{\partial q_k} = \frac{\partial \mathcal{T}}{\partial q_k} + \mathbf{w}^T \mathbf{A}^T \frac{\partial \mathbf{A}}{\partial q_k} \left\{ \frac{\partial \mathcal{T}}{\partial w} \right\} . \tag{25.82}$$

Note that product

$$\mathbf{w}^T \mathbf{A}^T \frac{\partial \mathbf{A}}{\partial q_k}$$

is a row matrix of order n (3 in the present case) that, multiplied by the column $\left\{ \frac{\partial \mathcal{T}}{\partial w} \right\}$, yields the required number.

To use a more synthetic notation, those row matrices can be superimposed, yielding a square matrix

$$\left[\mathbf{w}^T \mathbf{A}^T \frac{\partial \mathbf{A}}{\partial q_k} \right] ,$$

and thus

$$\left\{ \frac{\partial \mathcal{T}^*}{\partial q_k} \right\} = \left\{ \frac{\partial \mathcal{T}}{\partial q_k} \right\} + \left[\mathbf{w}^T \mathbf{A}^T \frac{\partial \mathbf{A}}{\partial q_k} \right] \left\{ \frac{\partial \mathcal{T}}{\partial w} \right\} . \tag{25.83}$$

The equation of motion is thus

$$\mathbf{A} \frac{\partial}{\partial t} \left(\left\{ \frac{\partial \mathcal{T}}{\partial w} \right\} \right) + \dot{\mathbf{A}} \left\{ \frac{\partial \mathcal{T}}{\partial w} \right\} - \left\{ \frac{\partial \mathcal{T}}{\partial q_k} \right\} - \left[\mathbf{w}^T \mathbf{A}^T \frac{\partial \mathbf{A}}{\partial q_k} \right] \left\{ \frac{\partial \mathcal{T}}{\partial w} \right\} = \begin{Bmatrix} F_X \\ F_Y \\ M_z \end{Bmatrix} . \tag{25.84}$$

By premultiplying all terms of matrix $\mathbf{A}^T = \mathbf{A}^{-1}$, it follows that

$$\frac{\partial}{\partial t} \left(\left\{ \frac{\partial \mathcal{T}}{\partial w} \right\} \right) + \mathbf{A}^{\mathbf{T}} \left(\dot{\mathbf{A}} - \left[\mathbf{w}^T \mathbf{A}^T \frac{\partial \mathbf{A}}{\partial q_k} \right] \right) \left\{ \frac{\partial \mathcal{T}}{\partial w} \right\} + \tag{25.85}$$

$$- \mathbf{A}^T \left\{ \frac{\partial \mathcal{T}}{\partial q_k} \right\} = \mathbf{A}^T \begin{Bmatrix} F_X \\ F_Y \\ M_z \end{Bmatrix} .$$

By performing the derivatives of the kinetic energy and all products, the equation becomes

$$\begin{Bmatrix} m\dot{u} \\ m\dot{v} \\ J_z r \end{Bmatrix} + \begin{bmatrix} 0 & -r & 0 \\ r & 0 & 0 \\ 0 & 0 & 0 \end{bmatrix} \begin{Bmatrix} mu \\ mv \\ J_z \psi \end{Bmatrix} = \begin{Bmatrix} F_x \\ F_y \\ M_z \end{Bmatrix} , \tag{25.86}$$

where forces F_x and F_y refer to the body-fixed frame. The final expression of the equations of motion is then

$$\begin{cases} m(\dot{u} - rv) = F_x \\ m(\dot{v} + ru) = F_y \\ J_z\dot{r} = M_z \ , \end{cases} \tag{25.87}$$

which obviously coincides with that obtained previously.

Velocities u and v are not derivatives of true coordinates, but nevertheless they can be used to write the equations of motion. They are actually derivatives of pseudo-coordinates, and the procedure here followed can also be used in cases where the kinematic equation (25.72) is more complicated, and where, in particular, the equation contains a matrix $\mathbf{A}^T$ that does not satisfy the relationship

$$\mathbf{A}^T = \mathbf{A}^{-1} \ .$$

Equations (25.87) are nonlinear in the velocities u, v and r but, since the sideslip angle β is small and its trigonometric functions can be linearized, the linearization of the equations is possible. The components of velocity V can be written as

$$\begin{cases} u = V\cos(\beta) \approx V \\ v = V\sin(\beta) \approx V\beta \ . \end{cases} \tag{25.88}$$

Product $\dot{\psi}v$ can be considered the product of two small quantities and it is thus of the same order as the first term ignored in the series for the cosine. It is therefore cancelled.

The speed V can be considered a known function of time, which amounts to studying the motion with a given law $V(t)$ (in many cases at constant speed) and assuming as an unknown the driving or the braking force needed to follow such a law. The unknown for the degree of freedom related to translation along the x-axis in this case is the force F_{x_d} exerted by the driving wheels. When braking, force F_{x_d} is the total braking force exerted by all wheels.

Equations (25.87) reduces to the linear form in F_x, v and r:

$$\begin{cases} m\dot{V} = F_x \\ m\,(\dot{v} + rV) = F_y \\ J_z\dot{r} = M_z \end{cases} . \tag{25.89}$$

If the interaction between longitudinal and transversal forces due to the tires is neglected or accounted for in an approximate way, the first equation of motion, which has already been studied in the section dealing with the longitudinal performance of the vehicle, uncouples from the other two.

This amounts to saying that the lateral behavior is uncoupled from the longitudinal behavior and can be studied using just two variables, either velocities v and r:

$$\begin{cases} m\,(\dot{v} + rV) = F_y \\ J_z\dot{r} = M_z \end{cases} , \tag{25.90}$$

or β and r if the equations are written in the equivalent form

$$\begin{cases} mV\left(\dot{\beta}+r\right)+m\beta\dot{V}=F_y \\ J_z\dot{r}=M_z \end{cases} . \tag{25.91}$$

25.5.2 Sideslip Angles of the Wheels

The sideslip angles of the wheels may be expressed easily in terms of the generalized velocities. With reference to Fig. 25.16, the velocity of the centre P_i of the contact area of the ith wheel, located in a point whose coordinates are x_i and y_i in the reference frame of the vehicle, is

$$\vec{V}_{P_i}=\vec{V}_G+\dot{\psi}\Lambda\overline{(\mathrm{P}_i-\mathrm{G})}=\begin{Bmatrix} u-\dot{\psi}y_i \\ v+\dot{\psi}x_i \end{Bmatrix} . \tag{25.92}$$

Angle β_i between the direction of the velocity of point P_i and x-axis is

$$\beta_i=\arctan\left(\frac{v_i}{u_i}\right)=\arctan\left(\frac{v+\dot{\psi}x_i}{u-\dot{\psi}y_i}\right) . \tag{25.93}$$

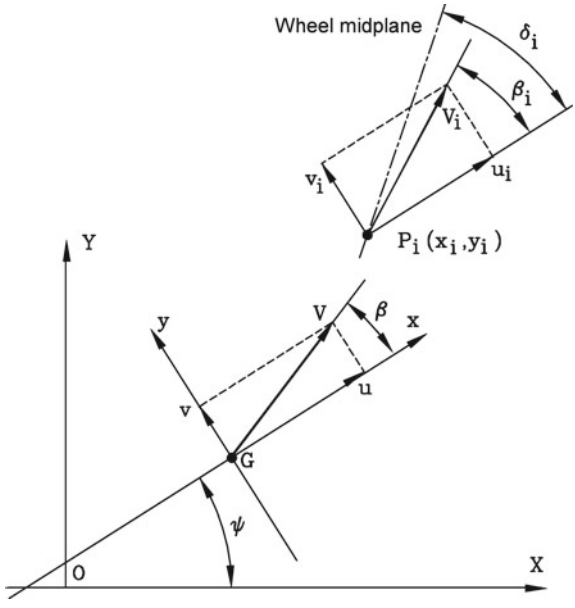

Fig. 25.16 Position and velocity of the centre P_i of the contact area of the i-th wheel

If the ith wheel has a steering angle δ_i, its sideslip angle is

$$\alpha_i = \beta_i - \delta_i = \arctan\left(\frac{v + \dot{\psi} x_i}{u - \dot{\psi} y_i}\right) - \delta_i \ . \tag{25.94}$$

Equation (25.94) can be easily linearized. By noting that $y_i \dot{\psi}$ is far smaller than the speed V, it follows that

$$\alpha_i = \beta_i - \delta_i \approx \frac{v + r x_i}{V} - \delta_i = \beta + \frac{x_i}{V} r - \delta_i \ . \tag{25.95}$$

Coordinate y_i of the centre of the contact area of the wheel does not appear in the expression for the sideslip angle α_i. If the differences between the steering angles δ_i of the wheels of the same axle are neglected, the values of their sideslip angles are then equal. This allows one to work in terms of axles instead of single wheels and to substitute a model of the type of Fig. 4.1b to that of Fig. 4.1a. This approach is very common and is often referred to as the monotrack vehicle or bicycle model.

The explicit expressions of the sideslip angles of the front and rear axles of a vehicle with two axles are then

$$\begin{cases} \alpha_1 = \beta + \dfrac{a}{V} r - \delta_1 \\ \alpha_2 = \beta - \dfrac{b}{V} r - \delta_2 \end{cases} . \tag{25.96}$$

In the majority of cases only the front axle can steer and $\delta_2 = 0$.

Remark 25.6 The assumption of a rigid vehicle prevents one from considering roll steering.

25.5.3 Forces Acting on the Vehicle

Normal forces acting on the vehicle in symmetrical conditions were obtained in Chap. 23. When lateral accelerations are present, the vehicle is not in symmetrical conditions and the forces on the ground are not equally subdivided between the two wheels of each axle. However, the assumption of a small sideslip angle β and the subsequent linearization and uncoupling between lateral and longitudinal behavior allow one to use the same values of the forces on the ground previously seen. Moreover, to investigate how forces are subdivided between the wheels of the same axle has little meaning in a monotrack vehicle.

The forces acting in the xy plane at the tire-road interface in a monotrack vehicle are shown in Fig. 25.12.

Since the lateral behavior is uncoupled from the longitudinal one, only the resultants of the side force F_y and of the yaw moment M_z need to be computed:

$$F_y = \sum_{\forall i} F_{x_i} \sin(\delta_i) + \sum_{\forall i} F_{y_i} \cos(\delta_i) + \frac{1}{2}\rho V_r^2 S C_y + F_{y_e} \ , \tag{25.97}$$

where the external force F_{y_e} may be $mg\sin(\alpha_t)$ in the case of a road with transversal slope α_t, and

$$M_z = \sum_{\forall i} F_{x_i} \sin(\delta_i) x_i + \sum_{\forall i} F_{y_i} \cos(\delta_i) x_i + \sum_{\forall i} M_{z_i} + \frac{1}{2}\rho V_r^2 S C_{M_z} + M_{z_e} \ , \tag{25.98}$$

where x_i and y_i are the coordinates of the center of the contact zone, M_{z_i} represents the aligning moments of the wheels and M_{z_e} is a yawing moment applied to the vehicle. Subscript i indicates the axle, and thus if the vehicle has two axles $i = 1, 2$. If the rear axle does not steer, $\delta_2 = 0$.

Cornering Forces

Owing to linearization, equation (25.97) reduces to

$$F_y = \sum_{\forall i} F_{x_i} \delta_i + \sum_{\forall i} F_{y_i} + \frac{1}{2}\rho V_r^2 S C_y + F_{y_e} \ , \tag{25.99}$$

where products $F_{x_i} \delta_i$ can usually be neglected, since they are far smaller than the other forces included in the equation.

Since the model has been linearized, cornering forces can be expressed as the product of the cornering stiffness by the sideslip angle

$$F_{y_i} = -C_i \alpha_i = -C_i \left(\beta + \frac{x_i}{V} r - \delta_i\right) \ . \tag{25.100}$$

Equation (25.100) is written in terms of axles. The cornering stiffness is then that of the axle and not of the single wheel. In this way no allowance is taken for the camber force as, owing to the assumption of a rigid vehicle, no roll is considered and the wheels of a given axle have opposite camber. The camber forces then cancel each other.

Nor is allowance made for toe-in and transversal load transfer. If the dependence of the cornering stiffness were linear with the load F_z, this would be correct since the increase of cornering stiffness of the more loaded wheel would exactly compensate for the decrease of the other wheel. As this is not exactly the case, the load transfer causes a decrease of the cornering stiffness of each axle, but this effect is usually considered negligible, at least for lateral accelerations lower than 0.5 g.[6] Toe-in

[6] L. Segel, *Theoretical Prediction and Experimental Substantiation of the Response of the Automobile to Steering Control*, Cornell Aer. Lab., Buffalo, N.Y.

causes an increase of the cornering stiffness of the axle if it is positive, a decrease if it is negative.

By linearizing also the value of the aerodynamic coefficient C_y

$$C_y = (C_y)_{,\beta}\beta$$

and assuming that the steering angles of the various axles can be expressed as

$$\delta_i = K_i'\delta, \tag{25.101}$$

the expression of the total lateral force (25.99) can be reduced to the linear equation

$$F_y = Y_\beta\beta + Y_r r + Y_\delta\delta + F_{y_e}, \tag{25.102}$$

where

$$\begin{cases} Y_\beta = -\sum_{\forall i} C_i + \frac{1}{2}\rho V_r^2 S(C_y)_{,\beta} \\ Y_r = -\frac{1}{V}\sum_{\forall i} x_i C_i \\ Y_\delta = \sum_{\forall i} K_i'\left(C_i + F_{x_i}\right) \end{cases} . \tag{25.103}$$

Equation (25.102) can be considered as a Taylor series for the force $F_y(\beta, r, \delta)$ about the condition $\beta = r = \delta = 0$, truncated after the linear terms. Coefficients Y_β, Y_r and Y_δ are the derivatives of the force with respect to the three variables β, r and δ and may be obtained in any way, even experimentally, if possible.

In the case of vehicles with only one steering axle, all K_i' vanish except $K_1' = 1$, while in other cases they can be functions of many parameters. If the variables of motion β or r enter such equations the model is no longer linear.

The first Eq. (25.98) has been obtained conflating the sideslip angle of the vehicle β with the aerodynamic sideslip angle β_a, as occurs when no side wind is present, and in the third equation the terms in $F_{x_{i_t}}$ are usually neglected.

Yawing Moments

Equation (25.98) can be linearized yielding

$$M_z = \sum_{\forall i} F_{x_i}\delta_i x_i + \sum_{\forall i} F_{y_i} x_i + \sum_{\forall i} M_{z_i} + \frac{1}{2}\rho V_r^2 S C_{M_z} + M_{z_e} . \tag{25.104}$$

The aligning torque can be expressed as a linear function of the sideslip angle,

$$M_z = (M_z)_{,\alpha}\alpha , \tag{25.105}$$

holding only in a range of α smaller than that for which the side force can be linearized.

The same considerations seen for the cornering force hold here; moreover, the aligning torque is far less important and the errors in its evaluation affect the global behavior of the vehicle far less than errors in the cornering force. In the following equations the values of $(M_z)_{,\alpha}$ are referred to the whole axle.

Acting similarly to that seen for the cornering forces, the linearized expression for the yawing moments is

$$M_z = N_\beta \beta + N_r r + N_\delta \delta + M_{z_e} \ , \tag{25.106}$$

where

$$\begin{cases} N_\beta = \displaystyle\sum_{\forall i} \left[-x_i C_i + (M_{z_i})_{,\alpha} \right] + \frac{1}{2} \rho V_r^2 S (C_{M_z})_{,\beta} \\ N_r = \displaystyle\frac{1}{V} \sum_{\forall i} \left[-x_i^2 C_i + (M_{z_i})_{,\alpha} x_i \right] \\ N_\delta = \displaystyle\sum_{\forall i} K_i' \left[C_i x_i - (M_{z_i})_{,\alpha} + F_{x_i} x_i \right] \ . \end{cases} \tag{25.107}$$

In this case the terms in $F_{x_{i_t}}$ are usually neglected.

25.5.4 Derivatives of Stability

As already stated, the terms Y_β, Y_r, Y_δ, N_β, N_r and N_δ are nothing but the derivatives $\partial F_y / \partial \beta$, $\partial F_y / \partial r$, etc. They are usually referred to as derivatives of stability. N_r is sometimes referred to as yaw damping, as it is a factor that, multiplied by an angular velocity, yields a moment, like a damping coefficient.

In a simplified study of the handling of road vehicles, aerodynamic forces are usually neglected, as is the interaction between the longitudinal and transversal forces of the tires. In these conditions, Y_β, Y_δ, N_β and N_δ are constant while Y_r and N_r are proportional to $1/V$. Note that they are strongly influenced by the load and road conditions through the cornering stiffness of the tires.

If aerodynamic forces are considered, the airspeed V_r is often substituted by the groundspeed V. These forces introduce a strong dependence with V^2 in Y_β and N_β and with V in N_r.

Example 25.3 Compute the derivatives of stability at 100 km/h of the vehicle of Appendix E.2, using the simplified and the complete formulations. Plot the derivatives of stability as functions of the speed for the same vehicle. In the whole computation neglect the longitudinal forces on the tires.

The normal forces on the ground are first computed. At 100 km/h, at constant velocity on level road, they are 4.804 and 3.536 kN for the front and rear axles respectively.

From these values the cornering and aligning stiffness can be computed as $C_1 = 67{,}369$ N/rad, $C_2 = 63{,}411$ N/rad, $(M_{z_1})_{,\alpha} = 2{,}010$ Nm/rad and $(M_{z_2})_{,\alpha} = 1{,}366$ Nm/rad.

These values refer to the axles; the normal load on each wheel must be first computed and introduced into the "magic formula"; the results are then multiplied by the number of wheels on the axles.

By taking into account only the cornering forces of the tires, the following values of the derivatives of stability at 100 km/h are obtained:

Y_β (N/rad)	Y_r (Ns/rad)	Y_δ (N/rad)	N_β (Nm/rad)	Y_r (Nms/rad)	Y_δ (Nm/rad)
−130,570	824.62	67,374	22,906	−5,622	58,615

If the complete expressions, including aligning torques, aerodynamic forces and load shift between the wheels of the same axle are used, the values of the derivatives of stability at 100 km/h are:

Y_β (N/rad)	Y_r (Ns/rad)	Y_δ (N/rad)	N_β (Nm/rad)	Y_r (Nms/rad)	Y_δ (Nm/rad)
−132,340	824.62	67,374	26,488	−5,630	55,962

The derivatives of stability are plotted as functions of the speed in Fig. 25.17. The values obtained from the complete expressions are reported as full lines while the dashed lines are the constant values (proportional to $1/V$ for Y_r and N_r) obtained when considering the cornering forces only, computed at 100 km/h.

Note that N_β is the only derivative of stability strongly affected by load shift, aligning torques and the other effects. Here an apparently strange result is obtained: From the formula a decrease in N_β seems to occur with increasing speed, as the aerodynamic term is negative, while the plot shows an increase.

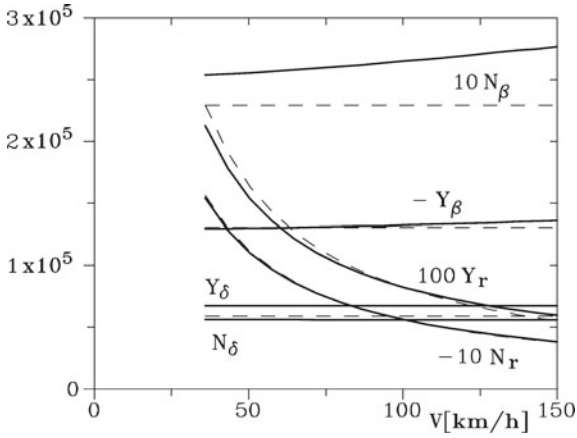

Fig. 25.17 Derivatives of stability as functions of the speed. Full lines: Values obtained from the complete expressions; dashed lines: Constant values (proportional to $1/V$ for Y_r and N_r) obtained considering the cornering forces only, computed at 100 km/h

The latter is due to the longitudinal load shift which, while causing an increase of the load on the rear axle, produces an increase of N_β that is larger than the decrease due to the aerodynamic moment M_z.

25.5.5 Final Expression of the Equations of Motion

The final expression of the linearized equations of motion for the handling model is thus

$$\begin{cases} mV\left(\dot{\beta}+r\right)+m\dot{V}\beta = Y_\beta\beta + Y_r r + Y_\delta\delta + F_{y_e} \\ J_z\dot{r} = N_\beta\beta + N_r r + N_\delta\delta + M_{z_e}\ . \end{cases} \tag{25.108}$$

These are two first order differential equations for the two unknown β and r.

These equations are apparently first order equations: the variables β and r are actually an angular velocity (r) or a quantity linked with a velocity (β was introduced instead of velocity v); their derivatives are thus accelerations. The missing term is therefore not the second derivative (acceleration), but the displacement.

Alternatively, a set of two first order differential equations in v and r could be written.

The steering angle δ can be considered as an input to the system, together with the external force and moment F_{y_e} and M_{z_e}. This approach is usually referred to as the "locked controls" behavior.

Alternatively, it is possible to study the "free controls" behavior, in which the steering angle δ is one of the variables of the motion and a further equation expressing the dynamics of the steering system is added.

In the first case, β and r can be considered as state variables and Eq. (25.108) can be written directly as a state equation

$$\dot{\mathbf{z}} = \mathbf{A}\mathbf{z} + \mathbf{B}_c\mathbf{u}_c + \mathbf{B}_e\mathbf{u}_e\ , \tag{25.109}$$

where the state and input vectors $\mathbf{z}$, $\mathbf{u}_c$ and $\mathbf{u}_e$ are

$$\mathbf{z} = \begin{Bmatrix} \beta \\ r \end{Bmatrix}\ , \qquad \mathbf{u}_c = \delta\ , \qquad \mathbf{u}_e = \begin{Bmatrix} F_{y_e} \\ M_{z_e} \end{Bmatrix}\ ,$$

the dynamic matrix is

$$\mathbf{A} = \begin{bmatrix} \dfrac{Y_\beta}{mV} - \dfrac{\dot{V}}{V} & \dfrac{Y_r}{mV} - 1 \\ \dfrac{N_\beta}{J_z} & \dfrac{N_r}{J_z} \end{bmatrix}$$

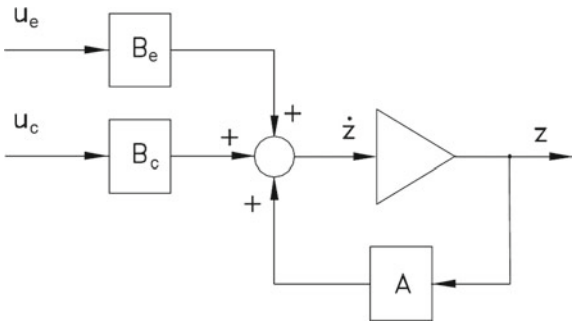

Fig. 25.18 Block diagram for the rigid vehicle handling model

and the input gain matrices are

$$\mathbf{B}_c = \begin{bmatrix} \dfrac{Y_\delta}{mV} \\ \\ \dfrac{N_\delta}{J_z} \end{bmatrix}, \quad \mathbf{B}_e = \begin{bmatrix} \dfrac{1}{mV} & 0 \\ \\ 0 & \dfrac{1}{J_z} \end{bmatrix}.$$

The block diagram corresponding to the state equation is shown in Fig. 25.18.

The study of the system is straightforward: The eigenvalues of the dynamic matrix allow one to see immediately whether the behavior is stable or not, and the study of the solution to given constant inputs yields the steady state response to a steering input or to external forces and moments.

There is, however, an interesting analogy. If the speed is kept constant in such a way that the derivatives of stability are constant in time, there is no difficulty in obtaining r from the first Eq. (25.108) and substituting it into the second, which becomes a second order differential equation in β. Similarly, solving the second in β and substituting it in the first one, an equation in r is obtained. The result is

$$P\ddot{\beta} + Q\dot{\beta} + U\beta = S'\delta + T'\dot{\delta} - N_r F_{y_e} + J_z \dot{F}_{y_e} - (mV - Y_r) M_{z_e} \tag{25.110}$$

or

$$P\ddot{r} + Q\dot{r} + Ur = S''\delta + T''\dot{\delta} + N_\beta F_{y_e} - Y_\beta M_{z_e} + mV\dot{M}_{z_e}\,, \tag{25.111}$$

where

$$\begin{cases} P = J_z mV \\ Q = -J_z Y_b - mV N_r \\ U = N_\beta (mV - Y_r) + N_r Y_\beta \end{cases} \qquad \begin{cases} S' = -N_\delta (mV - Y_r) - N_r Y_\delta \\ S'' = Y_\delta N_\beta - N_\delta Y_\beta \\ T' = J_z Y_\delta \\ T'' = mV N_\delta\,. \end{cases}$$

If the simplified expressions of the derivatives of stability are used, the expressions for P, Q, etc., for a vehicle with two axles reduce to

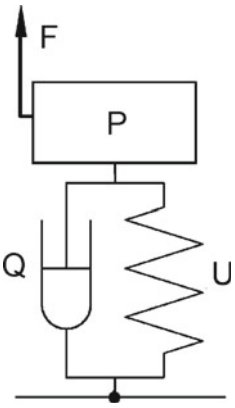

Fig. 25.19 Formal analogy of the motor vehicle with a mass-spring-damper system (mass P, stiffness U, damper Q). Force F includes the different forcing functions

$$\begin{cases} P = J_z m V \\ Q = J_z(C_1 + C_2) + m(a^2 C_1 + b^2 C_2) \\ U = mV(-aC_1 + bC_2) + C_1 C_2 \dfrac{l^2}{V} \end{cases} \qquad \begin{cases} S' = C_1 \left(-amV + C_2 \dfrac{bl}{V} \right) \\ S'' = lC_1 C_2 \\ T' = J_z C_1 \\ T'' = mVaC_1 \, . \end{cases}$$

Each of Eqs. (25.110) and (25.111) is sufficient for the study of the dynamic behavior of the vehicle.

The equations are formally identical to the equation of motion of a spring-mass-damper system (Fig. 25.19).

The linearized behavior of a rigid motor vehicle at constant speed is thus identical to that of a mass P suspended from a spring with stiffness U and a damper with damping coefficient Q, excited by the different forcing functions stated above (the command δ and the external disturbances).

Remark 25.7 The analogy here suggested is only a formal one: as already stated, the state variables β and r are dimensionally an angular velocity (r) or are related to velocities (β has been introduced to express the lateral velocity v) and not displacements, and thus P, Q and U are dimensionally far from being a mass, a damping coefficient and a stiffness.

25.6 Steady-State Lateral Behavior

In steady state driving the radius of the path is constant, i.e. the path is circular. The relationship linking the angular velocity r to the radius R of the path is thus

$$r = \frac{V}{R} \, . \tag{25.112}$$

Computing the steady state response to a steering angle δ is the same as computing the equilibrium position of the equivalent mass-spring-damper system under the effect of a constant force $S'\delta$ or $S''\delta$, since in steady-state motion $\dot{\delta} = 0$

$$\begin{cases} \beta = \dfrac{S'}{U}\delta = \dfrac{-N_\delta\,(mV - Y_r) - N_r Y_\delta}{N_\beta\,(mV - Y_r) + N_r Y_\beta}\delta \\ r = \dfrac{S''}{U}\delta = \dfrac{Y_\delta N_\beta - N_\delta Y_\beta}{N_\beta\,(mV - Y_r) + N_r Y_\beta}\delta\,. \end{cases} \tag{25.113}$$

The transfer functions of the vehicle are thus the

- *path curvature gain*

$$\frac{1}{R\delta} = \frac{Y_\delta N_\beta - N_\delta Y_\beta}{V\left[N_\beta\,(mV - Y_r) + N_r Y_\beta\right]}\,, \tag{25.114}$$

expressing the ratio between the curvature of the path and the steering input; the

- *lateral acceleration gain*

$$\frac{V^2}{R\delta} = \frac{V\left[Y_\delta N_\beta - N_\delta Y_\beta\right]}{N_\beta\,(mV - Y_r) + N_r Y_\beta}\,, \tag{25.115}$$

expressing the ratio between the lateral acceleration and the steering input: the

- *sideslip angle gain*

$$\frac{\beta}{\delta} = \frac{-N_\delta\,(mV - Y_r) - N_r Y_\delta}{N_\beta\,(mV - Y_r) + N_r Y_\beta}\,, \tag{25.116}$$

expressing the ratio between the sideslip angle and the steering angle; and the

- *yaw velocity gain*

$$\frac{r}{\delta} = \frac{Y_\delta N_\beta - N_\delta Y_\beta}{N_\beta\,(mV - Y_r) + N_r Y_\beta}\,, \tag{25.117}$$

expressing the ratio between the yaw velocity and the steering angle.

If a simplified expression of the derivatives of stability, including only the cornering forces of the tires, is introduced in the above expressions, the same values of the gains reported in equations from (25.53) to (25.61) are obtained.

When the dependence of the derivatives of stability on the speed is accounted for, the law $1/R\delta$ as a function of V is no more monotonic as those shown in Fig. 25.13a and the behavior may change from understeer to oversteer (or viceversa).

The aerodynamic yawing moment produces a strong effect. If $\partial C_{M_z}/\partial\beta$ is negative (the side force F_y acts forward of the centre of mass), the effect is increasing oversteer or decreasing understeer, at increasing speed. If a critical speed exists, such an aerodynamic effect lowers it and has an overall destabilizing effect, increasing with the absolute value of $(C_{M_z})_{,\beta}$. The opposite occurs if $(C_{M_z})_{,\beta}$ is positive.

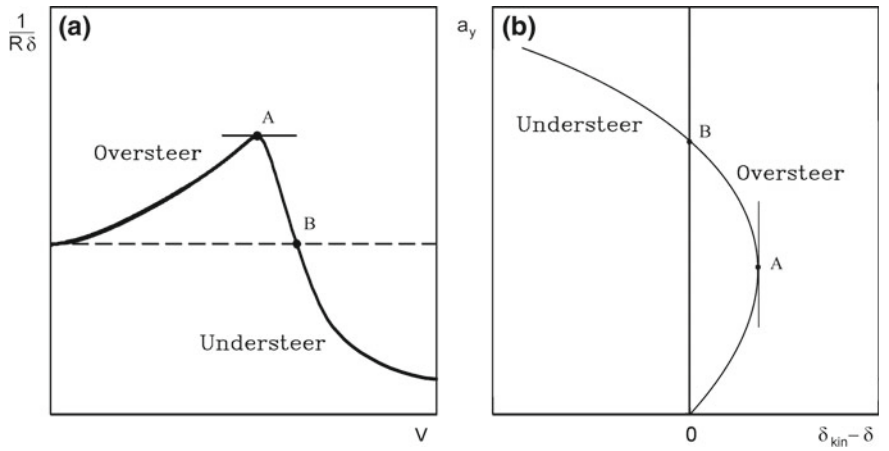

Fig. 25.20 Steady-state response to a steering input. Plot of the path curvature gain as a function of speed (**a**) and handling diagram (**b**) for a vehicle that at low speed is oversteer and then becomes understeer at high speed

The longitudinal load shift produces another important effect. If the load on the rear axle increases more, or decreases less, than that on the front axle, the understeer increases with increasing speed.

The case of a vehicle that is oversteer at low speed and understeer at high speed, as can be caused by a positive value of $(C_{M_z})_{,\beta}$, is shown in Fig. 25.20. Following the definition seen above, the speed at which neutral-steer is obtained is identified by point B.

If the simplified expressions for the derivatives of stability are not used, a new definition of a neutral-steer, and hence under- and oversteer, vehicle may be introduced. Instead of referring to the condition

$$\frac{1}{R\delta} = \frac{1}{l} ,$$

neutral-steering can be defined by the relationship

$$\frac{d}{dV}\left(\frac{1}{R\delta}\right) = 0 . \tag{25.118}$$

On the plot of Fig. 25.20 the speed at which neutral-steering is obtained is point A, where the curve reaches its maximum.

Remark 25.8 In case the derivatives of stability are constant (Y_r and N_r are proportional to $1/V$) the first definition, which can be said to be *absolute* and the second, which can be said to be *incremental*, coincide.

Remark 25.9 The incremental definition corresponds to the sensations of the driver, who perceives the vehicle as oversteering if an increase of speed is accompanied by a decrease in radius of the path and vice versa. The driver clearly has no way of sensing the kinematic value of the radius of the path and hence the absolute definition has little meaning for him. From the viewpoint of the equations of motion, on the other hand, the absolute definition is more significant.

The generalized definition (25.57) of the understeer factor

$$K_{us} = \frac{g}{a_y} (\delta - \delta_{\text{kin}}) \ ,$$

and the corresponding definition of the stability factor holds in the present case as well. They are essentially the difference between the steering angle needed to keep the vehicle on a given trajectory in dynamic conditions and that corresponding to kinematic steering, multiplied by a suitable factor proportional to $1/V^2$.

Generally speaking, they depend on the speed and on other conditions, such as acceleration.

Also for the understeer factor it is, however, possible to introduce an incremental definition

$$\frac{1}{K_{us}} = \frac{1}{g} \frac{da_y}{d(\delta - \delta_{\text{kin}})} \ . \tag{25.119}$$

In this case the point in which the understeer factor vanishes and the vehicle is neutral steer is point A in Fig. 25.20b instead of being point B.

25.7 Neutral-Steer Point and Static Margin

The neutral-steer point of the vehicle is usually defined as the point on the plane of symmetry to which is applied the resultant of the cornering forces due to the tires as a consequence of a sideslip angle β, obviously with $\delta = 0$ and $r = 0$. The cornering forces under these conditions, computed through the linearized model, are simply $-C_1\beta$ and $-C_2\beta$ and the x coordinate of the neutral point is

$$x_N = \frac{aC_1 - bC_2}{C_1 + C_2} \ . \tag{25.120}$$

A better definition of neutral-steer point may, however, be introduced. If all forces and moments due to a sideslip angle β, with $\delta = 0$ and $r = 0$ are considered, the resultant force and moment are simply $Y_\beta\beta$ and $N_\beta\beta$ respectively.[7] The x coordinate of the neutral-steer point, defined as the point of application of the resultant of all lateral forces is thus

[7] Y_β may be considered as a sort of cornering stiffness of the vehicle.

Table 25.1 Directional behavior of the vehicle

Behavior	K	K_{us}	$\mathcal{M}_s$	x_N	$\lvert\alpha_1\rvert - \lvert\alpha_2\rvert$	N_β
Understeer	>0	>0	<0	<0	>0	>0
Neutral steer	0	0	0	0	0	0
Oversteer	<0	<0	>0	>0	<0	<0

$$x_N = \frac{N_\beta}{Y_\beta} \, . \tag{25.121}$$

The static margin $\mathcal{M}_s$ is the ratio between the x coordinate of the neutral point and the wheelbase

$$\mathcal{M}_s = \frac{x_N}{l} \, . \tag{25.122}$$

An external force applied to the neutral-steer point does not cause any steady-state yaw velocity, as will be seen when dealing with the response to external forces and moments. Owing to the mathematical model used in the present chapter, the height of the neutral-steer point cannot be defined.

Note that to obtain a neutral-steer response, the neutral-steer point must coincide with the centre of mass, i.e.

$$x_N = 0 \, , \, \mathcal{M}_s = 0 \, , \, N_\beta = 0 \, .$$

If they are positive the vehicle is oversteer[8] (centre of gravity behind the neutral point); the opposite applies to understeer vehicles.

The signs of parameters K, K^*, $\mathcal{M}_s$, x_N, $\lvert\alpha_1\rvert - \lvert\alpha_2\rvert$ and N_β corresponding to oversteer, understeer or neutral-steer behavior are reported in Table 25.1.

Since $N_\beta = 0$ in case of neutral-steer, the second equation of motion (25.108) uncouples from the first and simplifies as

$$J_z \dot{r} = N_r r + N_\delta \delta + M_{z_e} \, . \tag{25.123}$$

The behavior of a neutral-steer motor vehicle is thus that of a first order system rather than a second order system.

Example 25.4 Study the directional behavior of the vehicle of Appendix E.2, using the simplified and the complete formulations.

The value of N_β is positive and hence the vehicle is understeer. Using the values of the derivatives of stability computed from the cornering stiffness at 100 km/h, the values of the coordinate of the neutral-steer point and of the static margin are

[8] Sometimes the position of the neutral-steer point and the static margin are defined with different sign conventions: Instead of referring to the position of the neutral-steer point with respect to the centre of mass, the position of the latter with respect to the former is given. In this case the signs of x_N and $\mathcal{M}_s$ are changed and an understeer vehicle has a positive static margin.

$x_N = -175$ mm, $\mathcal{M}_s = -0.081$, while the values obtained, always at 100 km/h, using a complete expression of the derivatives of stability are $x_N = -200$ mm, $\mathcal{M}_s = -0.093$.

The path curvature gain, the lateral acceleration gain, the sideslip angle gain and the yaw velocity gain are plotted as functions of the speed in Fig. 25.21. The values obtained from the complete expressions of the derivatives of stability are shown as full lines, while the dashed lines refer to the simplified expressions for the derivatives of stability (constant or proportional to $1/V$ for Y_r and N_r) obtained by considering only the cornering forces computed at 100 km/h. The dotted lines refer to a neutral-steer vehicle.

The vehicle has a strong understeer behavior, even more so if the complete expression of the derivatives of stability is considered. However, the simplified approach allows one to obtain a fair approximation of the directional behavior of the vehicle.

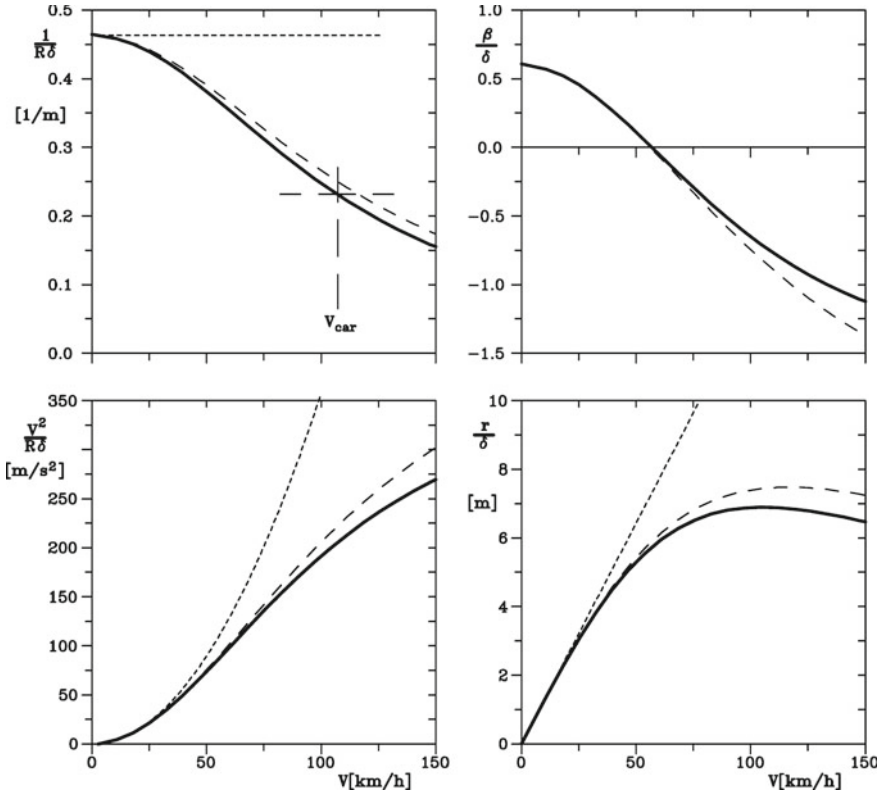

Fig. 25.21 Example 25.4: path curvature gain, lateral acceleration gain, sideslip angle gain and yaw velocity gain as functions of the speed. Full lines: Values obtained from the complete expressions of the derivatives of stability; dashed lines: Simplified approach (constant derivatives of stability, Y_r and N_r proportional to $1/V$, obtained considering only the cornering forces computed at 100 km/h); dotted lines: Neutral-steer vehicle

25.8 Response to External Forces and Moments

From the equivalent mass-spring-damper model the steady state response to an external force F_{y_e} or an external moment M_{z_e} is immediately obtained. The relevant gains are

$$\begin{cases} \dfrac{1}{RF_{y_e}} = \dfrac{N_\beta}{VU} \\ \dfrac{V^2}{RF_{y_e}} = \dfrac{VN_\beta}{U} \\ \dfrac{\beta}{F_{y_e}} = \dfrac{-N_r}{U} \end{cases} \qquad \begin{cases} \dfrac{1}{RM_{z_e}} = \dfrac{-Y_\beta}{VU} \\ \dfrac{V^2}{RM_{z_e}} = \dfrac{-VY_\beta}{U} \\ \dfrac{\beta}{M_{z_e}} = \dfrac{-mV + Y_r}{U} \end{cases} . \tag{25.124}$$

If the vehicle is neutral-steer, $N_\beta = 0$ and consequently

$$\frac{1}{RF_{y_e}} = 0 .$$

In neutral steer vehicles, then, the path remains straight under the effect of an external force (Fig. 25.22Ia). This may be easily understood considering that the neutral-steer point lies in the centre of mass, i.e. in the point of application of the external force.

Actually, this condition can be used to define the neutral-steer point as the point in which the application of an external force does not cause a yaw rotation of the vehicle. If the presence of the suspension is accounted for, it is possible to define, instead of a neutral-steer point, a neutral-steer line as the locus of the points in the xz plane in which an external force applied in the y direction does not cause any yaw rotation.

The path is, however, changed from the one preceding the application of force F_{y_e}: The deviation is equal to angle β, i.e. to $-F_{y_e}/Y_\beta$. The lateral velocity of the vehicle is simply

$$v = V\beta = -V\frac{F_{y_e}}{Y_\beta} .$$

Remark 25.10 It is very important that Y_β be as large as possible in order to avoid large lateral velocities, particularly in the case of fast vehicles.

If the vehicle is understeer, the neutral-steer point is behind the centre of mass and the path bends as in Fig. 25.22Ib. The opposite effect can be found in the case of oversteer vehicles. Note that the trajectories so computed are steady-state trajectories, and when the force is applied an unstationary motion occurs (dashed lines in the figure). This first part of the path cannot be computed with the above mentioned equations.

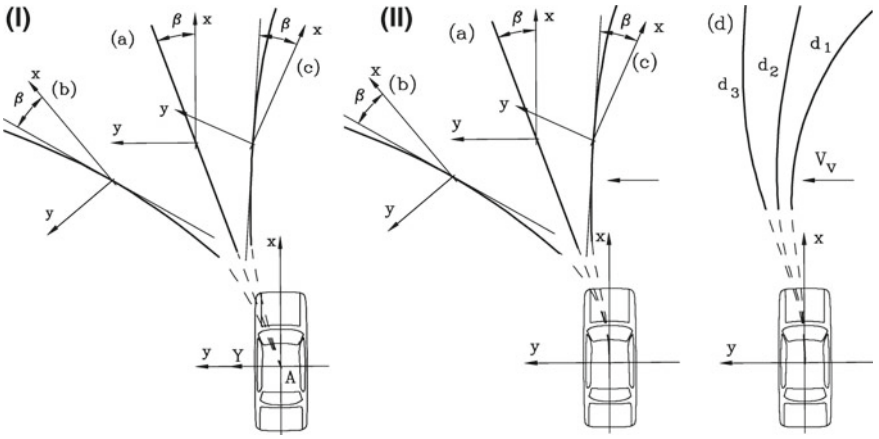

Fig. 25.22 I. Response to a force F_{y_e} applied to the centre of mass; (a) neutral-steer, (b) understeer and (c) oversteer vehicle. II. Response to a lateral wind; point of application of the side force in the neutral-steer point (a), forward (b) and after the neutral-steer point (c) and (d)

All the gains expressed by Eq. (25.124) tend to infinity when approaching the critical speed if the vehicle is oversteer, while they decrease with the speed in case of understeer vehicles.

The effect of a crosswind may be considered as the combined effect of a force and a moment. If the relative velocity is changed by angle ψ_w with respect to the velocity in still air, the force and the moment acting on the vehicle due to crosswind are

$$F_{y_w} = (F_{y_{aer}})_{,\beta}\psi_w \ , \qquad M_{z_w} = (M_{z_{aer}})_{,\beta}\psi_w \ . \tag{25.125}$$

Note that this approach, essentially a linearization of aerodynamic forces, holds only for small values of ψ_w, or, better, for values causing angle $\beta + \psi_w$ to remain within the range where the side force and the yawing moment can be linearized. This occurs either for feeble crosswinds or for head- or tailwinds. If the wind velocity is not small, the aerodynamic terms of the derivatives of stability must be computed using V_r instead of V.

The response in terms of curvature of the path, computed as the sum of the response to a force and to a moment, is

$$\frac{1}{R} = \frac{F_{y_w} N_\beta - M_{z_w} Y_\beta}{V\left[N_\beta\left(mV - Y_r\right) N_r Y_\beta\right]} = \frac{F_{y_w} Y_\beta}{VU}\left(\frac{N_\beta}{Y_\beta} - \frac{M_{z_w}}{F_{y_w}}\right) \ . \tag{25.126}$$

Ratio M_{z_w}/F_{y_w} is nothing but the distance of the point of application of the aerodynamic side force from the centre of mass. If it is equal to N_β/Y_β, the aerodynamic force is applied to the neutral steer point and a straight path occurs. The deviation angle is

$$\beta = \frac{M_{z_w}}{Y_\beta} = -\frac{F_{y_w} x_N}{N_\beta} \ . \tag{25.127}$$

In general, the value of β is

$$\beta = \frac{F_{y_w}}{U}\left[-\frac{M_{z_w}}{F_{y_w}}(mV - Y_r) - N_r\right] \ . \tag{25.128}$$

The trajectories are shown in Fig. 25.22II.

Usually the point of application of the aerodynamic force is in front of both the centre of mass and the neutral-steer point. In this case the path bends downwind (curve b).

The path bends upwind (curves c and d) on the other hand, if the point of application of aerodynamic forces is behind the neutral-steer point . If this effect is not too strong (curve d_3), it is beneficial since very little correction is needed, but if the result resembles that of curve d_1, a large correction may be required in a direction opposite to the instinctive reaction of the driver.

Remark 25.11 It must be noted again that the present steady-state model has limited application in the case of wind gusts, which involve primarily unsteady phenomena.

The application of a side force to the centre of mass is easy: It is sufficient to use a road with a transversal slope fashioned in a proper way. Wind gusts may be simulated using jet engines and suitable ducts to distribute the gust with the required profile.

25.9 Slip Steering

As stated in Chap. 20, the trajectory of a vehicle on pneumatic tires may be controlled by applying differential longitudinal forces to the tires on the right and left side instead of steering some of the wheels. This method of driving a vehicle is usually referred to as slip steering: While it is the usual strategy for controlling tracked vehicles, it is used as a primary strategy for wheeled vehicles only on some light construction machines. In the automotive field, however, it is increasingly used as an additional control in connection with VDC (Vehicle Dynamics Control) systems (see Chap. 27).

Consider the mathematical model of the vehicle expressed by Eqs. (25.108), and add a control yawing torque M_{z_c} to the second equation

$$\begin{cases} mV\left(\dot{\beta} + r\right) + m\dot{V}\beta = Y_\beta \beta + Y_r r + Y_\delta \delta + F_{y_e} \\ J_z \dot{r} = N_\beta \beta + N_r r + N_\delta \delta + M_{z_e} + M_{z_c} \ . \end{cases} \tag{25.129}$$

If the two wheels of the ith axle, whose track is t_i, produce a longitudinal force

$$F_{x_{iL,R,}} = \frac{F_{x_i}}{2} \pm \Delta F_{x_i} \ , \tag{25.130}$$

where subscripts L and R designate the left and right wheel, the control torque is

$$M_{z_c} = \sum_{\forall i} \Delta F_{x_i} t_i \ . \tag{25.131}$$

If the longitudinal slip σ of the tires is small enough, the longitudinal force is proportional to the slip through the slip stiffness C_σ (see Sect. 2.6). Assuming that the differential longitudinal slip $\Delta\sigma$ is the same on all axles, the yawing moment can thus be expressed as

$$M_{z_c} = N_\sigma \Delta\sigma \ , \tag{25.132}$$

where

$$N_\sigma = \sum_{\forall i} C_{\sigma_i} t_i \ . \tag{25.133}$$

The equation of motion is still Eq. (25.109)

$$\dot{\mathbf{z}} = \mathbf{A}\mathbf{z} + \mathbf{B}_c\mathbf{u}_c + \mathbf{B}_e\mathbf{u}_e \ ,$$

but now

$$\mathbf{u}_c = \left\{ \begin{array}{c} \delta \\ \Delta\sigma \end{array} \right\} \ , \ \mathbf{B}_c = \left[\begin{array}{cc} \dfrac{Y_\delta}{mV} & 0 \\ \dfrac{N_\delta}{J_z} & \dfrac{N_\sigma}{J_z} \end{array} \right] \ .$$

In steady-state conditions, it is possible to define a path curvature gain for slip steering

$$\frac{1}{R\Delta\sigma} = \frac{-N_\sigma Y_\beta}{V\left[N_\beta\left(mV - Y_r\right) + N_r Y_\beta\right]} \ , \tag{25.134}$$

expressing the ratio between the curvature of the path and the differential longitudinal slip. If the simplified expressions for the derivatives of stability are accepted, it follows that

$$\frac{1}{R\Delta\sigma} = \frac{C_1 + C_2}{C_1 C_2 l^2} \frac{\sum_{\forall i} C_{\sigma_i} t_i}{1 + K_{us}\frac{V^2}{gl}} \ . \tag{25.135}$$

Remark 25.12 This approach to slip steering assumes that the differential longitudinal slip is imposed. Different equations would be obtained for cases in which the differential velocity of the wheels is imposed.

Remark 25.13 The formulae above are based on the assumption that the radius of the trajectory is much larger than the wheelbase: They do not hold when slip steering is used for very sharp turns, or even for turning on the spot.

Remark 25.14 Even when the speed tends to zero no kinematic conditions exist: By definition slip steering implies that the wheels operate with both longitudinal and side slip.

25.10 Influence of Longitudinal Forces on Handling

A vehicle's directional behavior is strongly influenced by the presence of longitudinal forces between tires and road. Any longitudinal force causes a reduction of cornering stiffness: If applied to the front axle, it reduces the value of C_1 and consequently makes the vehicle more understeer or less oversteer. The opposite effect is caused by a longitudinal force applied to the rear axle.

In the linearized model this can be easily accounted for by using the elliptical approximation which, if a complete linearization of the behavior of the tires is assumed, can be applied directly to each axle

$$C_i = C_{0_i}\sqrt{1-\left(\frac{F_{x_i}}{\mu_p F_{z_i}}\right)^2}\,. \tag{25.136}$$

Note that the forces and the cornering stiffness refer to the whole axle.

The driving force needed to maintain a constant speed increases with the latter and, as a consequence, the cornering stiffness of the tires of the driving axle decreases. The effect is felt particularly if road conditions are poor, since in Eq. (25.136) the ratio between the actual and the maximum value of the driving force is present.

The variation of static margin for a front-wheel and a rear-wheel drive saloon car with the speed due to the effect of the driving forces is shown in Fig. 25.23. It is clear that the effect is minor in the whole practical speed range of the car if the road conditions are good while, if μ_p is low, the change in handling of the car due to traction is quite strong.

In the case of rear-wheel drive vehicles, driving forces increase oversteer or decrease understeer. The critical speed, if it exists, decreases or a critical speed may appear. In bad road conditions, a rear-wheel drive vehicle may have a very low critical speed and the driver may be required to limit the speed for stability reasons, to avoid spinout. Starting and accelerating the vehicle may be difficult and the driver has to exert great care in operating the accelerator control; antispin or TCS devices are very useful in these conditions.

Front-wheel drive vehicles, on the other hand, have a tendency toward understeering and become more stable with increasing speed or decreasing μ_p and an increasingly large steering angle is needed to maintain the vehicle on a given path.

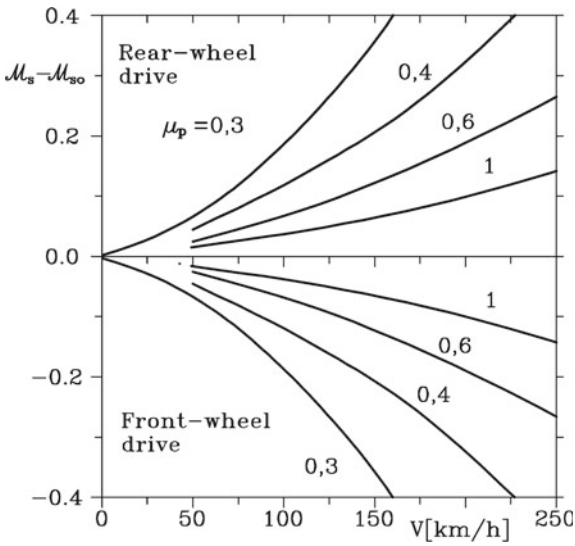

Fig. 25.23 Variation of the stability margin due to the longitudinal forces on the tires in the cases of front- and rear-wheel drive saloon cars. Various values of μ_p; a completely linearized model has been used

The limit condition is that of an infinitely stable vehicle, i.e., a vehicle that can only move on a straight line.

In vehicles with more than one driving axle, and when braking, handling depends upon how the longitudinal forces are distributed between the axles. If the front axle is working with a larger longitudinal force coefficient μ_x than the rear axle, which does not necessarily imply that force F_x is larger but that the ratio F_x/F_z of the front wheels is larger than that of the rear wheels, the vehicle becomes more understeering and is, in a sense, more stable. When the limit conditions are reached and the front wheels slip (lock in braking or spin in traction) the vehicle cannot be steered and follows a straight path.

A larger ratio F_x/F_z at the rear wheels makes the vehicle more oversteer and readily introduces a critical speed. When reaching limit conditions a spinout occurs, unless the driver promptly reduces the longitudinal forces and countersteers, a manoeuvre that can be expected only from very proficient drivers. To avoid this situation the braking system must be such that the working point on the F_{x_1}, F_{x_2} plane is not found above the curve for ideal braking. Antispin and antilock devices are very important from this viewpoint.

When all values of μ_x are equal, the behavior should theoretically not be affected by the longitudinal forces; however, when limit conditions occur, the vehicle can spin out or go straight depending on small changes in many parameters, such as the conditions of the individual wheels and brakes, the load transfer, etc.

Example 25.5 Study the directional behavior of the vehicle of Appendix E.2, taking into account the reduction of the cornering stiffness of the driving wheels caused by the longitudinal forces needed to move at constant speed. Repeat the computation for two values of μ_p, namely 1 and 0.2.

The study is performed by computing, at each speed, the values of the longitudinal and normal component of the tire forces, using the "magic formula" for the cornering stiffness and then reducing it through the elliptic expression (25.136).

The results, in terms of path curvature gain, lateral acceleration gain, sideslip angle gain and yaw velocity gain, are plotted as functions of the speed in Fig. 25.24 for both values of the maximum longitudinal force coefficient. The dashed lines refer to the simplified expressions for the derivatives of stability (constant or proportional to $1/V$ for Y_r and N_r) obtained considering only the cornering forces computed at 100 km/h; the dotted lines refer to a neutral-steer vehicle.

By comparing Fig. 25.24 with Fig. 25.21, it is clear that the effect of the driving force is almost negligible throughout the entire speed range if the road conditions are good ($\mu_p = 1$): The lines of the two figures are almost completely superimposed.

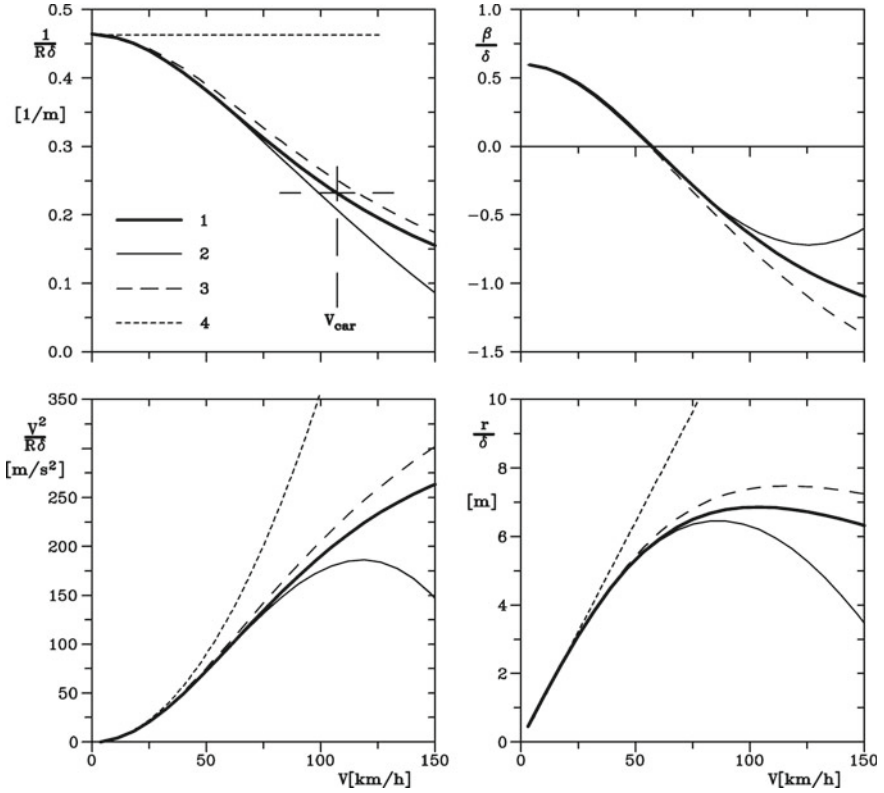

Fig. 25.24 Example 25.5: path curvature gain, lateral acceleration gain, sideslip angle gain and yaw velocity gain as functions of the speed. Values obtained from the complete expressions of the derivatives of stability, with the effect of the driving forces accounted for; (1) $\mu_t = 1$; (2) $\mu_t = 0.2$; (3) Simplified approach (constant derivatives of stability, Y_r and N_r proportional to $1/V$, obtained considering only the cornering forces computed at 100 km/h, assuming no longitudinal force effects); (4) Neutral-steer vehicle

However, if μ_p is lowered to 0.2, the understeer behavior becomes much more marked, particularly at high speed.

25.11 Transversal Load Shift

No allowance has yet been taken for the transversal load shift. If the dependence on the load of the cornering stiffness of a single wheel is of the type shown in Fig. 25.25, this does not introduce errors if the load transfer ΔF_z is small, lower than $(\Delta F_z)_{lim}$ in the figure (condition a).

But if the load shift is larger, as in the case of ΔF_{zb}, the increase in stiffness of the more loaded wheel cannot compensate for the decrease in the other wheel and the cornering stiffness of the axle is reduced. This effect introduces a nonlinearity in the behavior of the vehicle.

The simultaneous presence of longitudinal forces and load transfer makes things more complicated. Even if the cornering stiffness is still in the linear part of the plot of Fig. 25.25, i.e., the load transfer is smaller than $(\Delta F_z)_{lim}$, the combined effect yields a nonlinear behavior. Assuming that the longitudinal force splits equally on its two wheels, the cornering stiffness of the axle, computed using the elliptical approximation, is

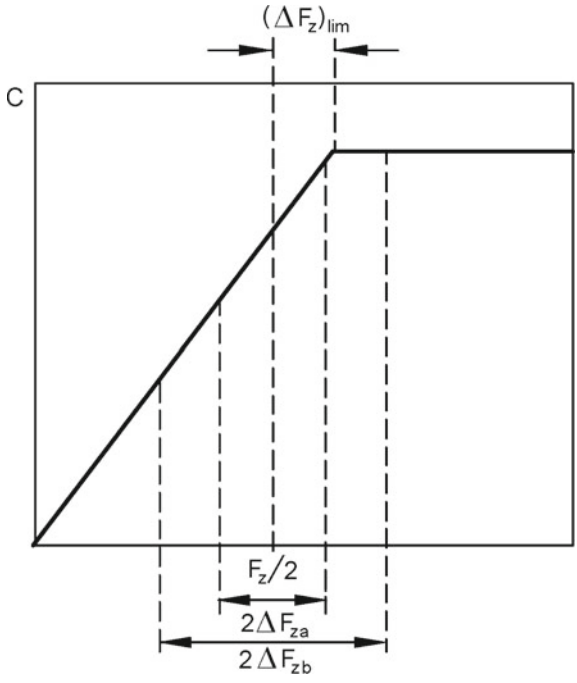

Fig. 25.25 Effect of load transfer on the cornering stiffness

$$C = \frac{1}{2}\left(C_0 + \Delta F_z \frac{\partial C}{\partial F_z}\right)\sqrt{1 - \left[\frac{F_x}{\mu_p(F_z + 2\Delta F_z)}\right]^2} + \\ + \frac{1}{2}\left(C_0 - \Delta F_z \frac{\partial C}{\partial F_z}\right)\sqrt{1 - \left[\frac{F_x}{\mu_p(F_z - 2\Delta F_z)}\right]^2}, \tag{25.137}$$

where forces F_x and F_z refer to the whole axle.

Owing to the presence of the square root, the decrease in cornering stiffness of the less loaded wheel is greater, particularly if μ_x is low, than the increase at the other wheel.

Load transfer on the driving axle thus increases the effect of longitudinal forces; this combined action can be reduced by introducing an anti-roll bar on the other axle. Operating in this way, the increased load transfer on the non-driving axle also reduces its cornering stiffness, reducing the overall effect of longitudinal forces on handling.

Anti-roll bars affect the distribution of transversal load shift between the axles, increasing the load shift on the relevant one while decreasing that on the other axles. They can be used to correct the behavior of the vehicle, particularly in conditions approaching the limit lateral acceleration, as their effect on the cornering stiffness increases when the latter increases.

Remark 25.15 A large rear-wheel drive saloon car can benefit from the application of an anti-roll bar at the front axle to correct the strong oversteering tendency when the rear wheels approach their traction limit, while a small front wheel car can use an anti-roll bar at the rear axle to reduce its understeering behavior.

It is impossible to state the effect of anti-roll bars on the gains defined in the previous sections since they introduce a strong nonlinearity into the mathematical model of the vehicle and the very definition of the gains is based on a complete linearization. It is only possible to study a number of specific cases where the lateral acceleration is defined, and to compute the response of the vehicle in such conditions.

25.12 Toe-In

Consider an axle (e.g., the front axle), in which the midplanes of the wheels are not exactly parallel and assume that the x-axes of the reference frames of the wheels converge in a point lying forward with respect to the axle.[9]

Let α_c be the angle each wheel makes with the symmetry plane of the vehicle, positive when the toe-in is positive. With reference to Fig. 4.1, the steering angle of

[9]Toe-in is usually defined as the difference between the distance of the front part and the rear part of the wheels of an axle, measured at the height of the hub, when the steering is in its central position. It is positive when the midplanes converge forward.

the wheel on the right side of the vehicle is increased by an angle equal to α_c, while the steering angle of the wheel on the left side is decreased by the same quantity.

If the usual linearization assumptions are accepted, the sideslip angles of the two wheels of the axle are then

$$\begin{cases} \alpha_{i_r} = \beta + \dfrac{x_i}{V} r - \delta_i - \alpha_c = \alpha_i - \alpha_c \\ \\ \alpha_{i_l} = \beta + \dfrac{x_i}{V} r - \delta_i + \alpha_c = \alpha_i + \alpha_c \ , \end{cases} \tag{25.138}$$

where subscripts r and l refer to the right and left wheels respectively and i refers to the ith axle.

Consider a vehicle negotiating a bend to the left; the sideslip angle α_i is negative while the side force is positive. The transversal load shift causes an increase of the load on the wheels on the right, the sideslip angle α_i is negative and the side force is positive.

If C is the total stiffness of the axle, the cornering force the axle exerts is

$$F_y = -\frac{1}{2}\left[(\alpha_i - \alpha_c) \left(C + \Delta F_z \frac{\partial C}{\partial F_z} \right) + (\alpha_i + \alpha_c) \left(C - \Delta F_z \frac{\partial C}{\partial F_z} \right) \right], \tag{25.139}$$

i.e.,

$$F_y = C|\alpha_i| + \alpha_c \Delta F_z \frac{\partial C}{\partial F_z} \ . \tag{25.140}$$

If transversal load shift is not taken into account, and the two wheels have the same cornering stiffness, toe-in has no effect within the validity of the linearized model. The situation is different if load shift is included into the model: then toe-in causes an increase of the cornering force due to the axle. This has the effect of increasing the cornering stiffness of the axle, depending on the load shift. Toe-in at the front wheels or toe-out of the rear ones thus has an oversteer effect.

The effect of toe-in is complicated since α_c depends on the steering angle due to steering error, on suspension geometry and on the relative roll stiffness of the suspensions that affect the total shift of the various axles.

25.13 Effect of the Elasto-Kinematic Behavior of Suspensions and of the Compliance of the Chassis

In the present chapter the vehicle is modelled as a rigid body moving on a plane. Suspensions, apart from causing inertial effects that cannot be studied using the present model, also change all working angles of the tires and thus affect the forces acting on the vehicle. The effects introduced by the elasto-kinematic characteristics of suspensions may be of two different types: some of these effects may be studied

using linearized models, at least for small motion about a nominal configuration, while others must be studied by considering their nonlinear effects, even for small displacements

An example of the first type is roll steer. The characteristics $\delta(\phi)$ can be linearized, and a steering angle

$$(\delta)_{,\phi}\,\phi$$

can easily be added to the steering angle of the various wheels, or the various axles in monotrack models.

When, on the contrary, the compliance of the suspensions is accounted for, the characteristic angles of the wheels depend in a nonlinear way on the variables of motion and the resulting effects are nonlinear. No general results can thus be obtained and numerical simulation must be used.

Even if it is possible to remain within linearity limits, the mathematical models seen in this chapter are too simplified to depict how the elasto-kinematic characteristics of the suspensions affect the behavior of the vehicle. Some more complex models taking suspensions into account will be seen in Part V.

Similar considerations also hold for the compliance of the chassis or the body. In this case, the displacements due to compliance are usually considered small and the models describing their flexibility are linearized. However, although linear, these models are complex owing to the large number of deformation degrees of freedom involved, together with the rigid body degrees of freedom typical of the rigid-body models. Some models of this kind will be studied in Part V.

In general, we can say that the compliance of the chassis in its plane has little influence on the handling of the vehicle. On the other handy, its torsional deformations can strongly affect handling and lateral behavior.

25.14 Stability of the Vehicle

It is customary to define a static and a dynamic stability. A system is statically stable in a given equilibrium condition if, when its state is perturbed, it tends to return to the previous situation. If the motion following this tendency towards the previous state of equilibrium succeeds, at least asymptotically, at restoring it, then the system is dynamically stable. This motion can tend to the equilibrium condition monotonically or through a damped oscillation. If, on the contrary, the equilibrium conditions are not reached, usually because a divergent oscillation takes place, the system is dynamically unstable. If an undamped oscillation occurs, as in the case of an undamped spring-mass system, the dynamic stability is neutral.

Remark 25.16 If the system is linear, such definitions hold in the entire range in which the state variables are defined. If, on the contrary, the system is nonlinear, this definition holds “in the small”, i.e. for small variations of the state variables about

the values corresponding to an equilibrium point in the state space. The linearized model here studied is then a linearization suitable for the stability "in the small".

The definition of stability above refers to the state of the system; in the case of the handling model with two degrees of freedom the state variables are β and r (or v and r). A motor vehicle is thus stable if, when in motion with given values β_0 and r_0 of β and r, after a small external perturbation, it follows that

$$\beta(t) \to \beta_0 \ , \qquad r(t) \to r_0 \ .$$

No reference is made to the path: After a perturbation the vehicle cannot return to the previous path, and a correction by the driver or by an automatic control system is required in order to maintain the vehicle on the road.

25.14.1 Locked Controls

If the steering wheel is kept in a position that allows the vehicle to maintain the required path, the stability can be studied simply by using the homogeneous equation of motion

$$\dot{\mathbf{z}} = \mathbf{A}\mathbf{z} \ .$$

The eigenvalues of the dynamic matrix $\mathbf{A}$ are readily found and the stability is assessed from the sign of their real part, which must be negative. If the imaginary part is nonzero the behavior is oscillatory, which does not necessarily imply that the path is oscillatory but only that the time histories $\beta(t)$ and $r(t)$ are.

The analogy with the spring-mass-damper system allows a simpler approach to the study of the stability at constant speed.

Assuming a solution of the type

$$\beta(t) = \beta_0 e^{st} \ , \qquad r(t) = r_0 e^{st} \ ,$$

the characteristic equation yielding the poles of the system is

$$Ps^2 + Qs + U = 0 \ . \tag{25.141}$$

Since P, Q and U depend in general on the speed V, it is possible to compute the roots locus at various speed. By using the simplified expression for the derivatives of stability, the characteristic equation reduces to

$$J_z m V s^2 + \left[J_z (C_1 + C_2) + m(a^2 C_1 + b^2 C_2) \right] s +$$

$$+ mV(-aC_1 + bC_2) + C_1 C_2 \frac{l^2}{V} = 0 \ . \tag{25.142}$$

At any rate, the analogy allows us to state that

- to ensure static stability the stiffness U must be positive,
- to ensure dynamic stability the damping coefficient Q must be positive,
- if Q is lower than the critical damping $2\sqrt{PU}$ the system has an oscillatory behavior.

Using the simplified expression of the derivatives of stability, the following expression of the "stiffness" U can be readily obtained,

$$U = \frac{C_1 C_2 l^2}{V}(1 + KV^2) \,, \tag{25.143}$$

where K is the stability factor defined by Eq. (25.58).

U is thus always positive for understeer and neutral-steer vehicles, and in the latter case it tends to zero when the speed tends to infinity. In the case of oversteer vehicles, it is positive up to the critical speed, where it vanishes to become negative at higher speed. The critical speed is thus the threshold of instability for oversteer vehicles. Similar results are obtained if the complete expressions for the derivatives of stability are used.

It is also easy to verify that Q is always positive: If the vehicle is statically stable it is also dynamically stable. If the simplified expression for the derivatives of stability is accepted, the value of Q is independent of the speed

$$Q = J_z(C_1 + C_2) + m(a^2 C_1 + b^2 C_2) \,. \tag{25.144}$$

The *critical damping* of the equivalent system Q_{crit} is, under the same simplifying assumptions,

$$Q_{crit} = 2\sqrt{PU} = 2\sqrt{C_1 C_2 J_z m l^2 (1 + KV^2)} \,. \tag{25.145}$$

It is a constant in the case of neutral-steer vehicles, increases with speed for understeer vehicles, and decreases, vanishing at the critical speed, in case of oversteer ones.

By comparing the actual with the critical damping, it follows that understeer vehicles tend to develop an oscillatory behavior with a frequency which increases with the speed (similar to a spring-mass-damper system with constant damping and increasing stiffness). Oversteer vehicles, on the other hand, tend to return to the original state without oscillations, but in a way that slows with increasing speed, similar to a spring-mass-damper system with constant damping and decreasing stiffness.

In a neutral-steer vehicle, under the same assumptions seen above, when $K = 0$ and

$$C_1 a = C_2 b \,,$$

the values of Q_{crit} and Q are

$$Q_{crit} = 2\frac{C_1 l J_z}{b}\sqrt{\frac{mab}{J_z}}\ ,$$

$$Q = \frac{C_1 l J_z}{b}\left(1 + \frac{mab}{J_z}\right)\ . \tag{25.146}$$

In many cases ratio

$$\frac{mab}{J_z}$$

is not far from unity. By writing

$$\frac{mab}{J_z} = 1 + \epsilon,$$

and expanding the above expressions in a power series in ϵ it follows that

$$Q = \frac{C_1 l J_z}{b}(2 + \epsilon)\ . \tag{25.147}$$

$$Q_{crit} = 2\frac{C_1 l J_z}{b}\sqrt{1+\epsilon} = \frac{C_1 l J_z}{b}\left(2 + \epsilon - \frac{\epsilon^2}{4} + ...\right)\ .$$

Thus it is clear that the damping coefficient Q has its critical value with an error as small as a term in ϵ^2. A neutral-steer vehicle is then critically damped, at least in an approximate way, while understeer and oversteer vehicles are, respectively, underdamped and overdamped: The free behavior of the former can then be expected to be oscillatory. It must be noted, however, that the issue of whether a given vehicle has an oscillatory behavior or not cannot be satisfactorily resolved using the present rigid-body model since the presence of rolling motions, which are neglected here and are almost always underdamped and thus oscillatory, can also induce an oscillatory behavior for β and r. This is particularly true for vehicles whose suspensions exhibit roll steer.

Example 25.6 Study the stability with locked controls of the vehicle of Appendix E.2, taking into account the reduction of the cornering stiffness of the driving wheels caused by the longitudinal forces needed to move at constant speed.

The parameters of the equivalent spring-mass-damper system are evaluated first and then the poles of the system are computed. The values obtained at 100 km/h (27.78 m/s) are reported in Table 25.2.

It is clear that the effect of driving forces on stability at 100 km/h is not great, even if the available traction is quite low, and that the simplified formulae already yield satisfactory results.

Table 25.2 Example 25.6. Values of P, Q, U, Q_{crit} and of the real and imaginary parts of the roots at 100 km/h (27.78 m/s). Column 1: Simplified expression of the derivatives of stability; 2: Complete expressions, with no allowance for the effect of driving forces; 3: With driving forces with $\mu_p = 1$; 4: With driving forces with $\mu_p = 0.2$

	1	2	3	4
P [kg^{2}m^3/s]	2.790×10^7	2.790×10^7	2.790×10^7	2.790×10^7
Q [kg^{2}m^3/s^2]	2.876×10^8	2.899×10^8	2.897×10^8	2.829×10^8
U [kg^{2}m^3/s^3]	1.243×10^9	1.334×10^9	1.335×10^9	1.369×10^9
Q_{crit} [kg^{2}m^3/s^2]	3.725×10^8	3.858×10^8	3.860×10^8	3.908×10^8
$\Re(s)$ [1/s]	-5.155	-5.196	-5.192	-5.070
$\Im(s)$ [1/s]	± 4.242	± 4.562	± 4.573	± 4.834

The values of P, Q and U are reported, together with that of Q_{crit}, as functions of the speed in Fig. 25.26a. In the same figure, the real and imaginary parts of s and the roots locus are also shown. The figure has been obtained using the complete expressions of the derivatives of stability, but neglecting the effect of driving forces.

Note that the stiffness U reduces with speed without tending to zero as in the case of neutral vehicles, and that the vehicle is almost always underdamped, except for very low speed, when $Q > Q_{crit}$.

25.14.2 Free Controls

If the steering wheel is not controlled, motion of the vehicle with free controls occurs. The steering angle δ then becomes not an input to the system but one of its state variables, and a new equation stating the equilibrium of the steering system has to be included.

The same approach could be followed in the study of motion with locked controls, since what is locked is actually not the steering angle δ but the position of the steering wheel and, if the compliance of the steering system is accounted for, steering angle and position of the wheel do not coincide.

However, if the compliance of the steering system is considered, oscillatory motions with high frequency can usually be found, and it is unrealistic to consider the driver as a device that inputs a position signal δ to the vehicle. It is more correct to consider the driver as a device supplying a driving torque on the steering wheel. The motion thus occurs in conditions closer to a free than a locked control situation.

The actual situation is mixed: at low frequencies, such as those typical of the motion of the vehicle as a whole, the locked control model is adequate, while for high frequency modes the free control model is more suitable.

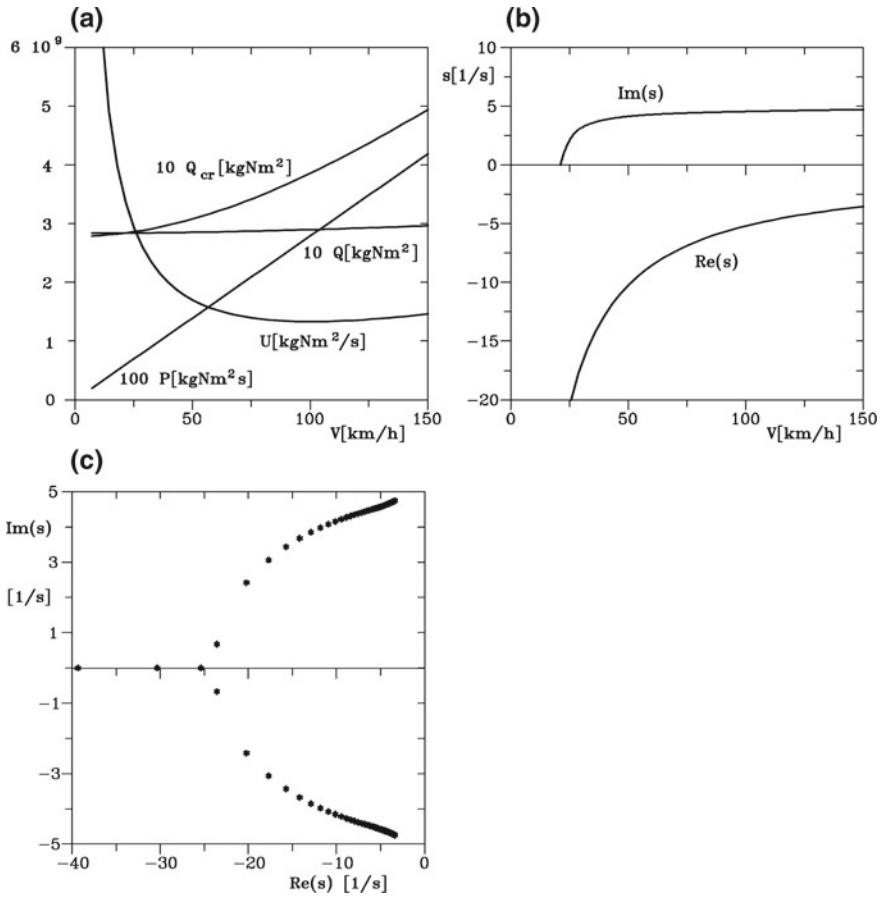

Fig. 25.26 Example 25.6: Study of the stability. **a** Parameters of the equivalent spring-mass-damper system as functions of the speed. **b** Real and imaginary parts of the eigenvalues as functions of the speed. **c** Roots locus at varying speed. Complete expressions of the derivatives of stability, with the effect of driving forces neglected

At any rate, since the motion of the vehicle includes high frequency components, the dynamic behavior of the tires cannot be neglected. The simplest way to include it into a linearized model is to use relationships of the type

$$\begin{aligned} F_y &= -C\left(\alpha - B\dot{\alpha}\right), \\ M_z &= \left(M_z\right)_{,\alpha}\left(\alpha - B'\dot{\alpha}\right), \end{aligned} \tag{25.148}$$

for the cornering force and the aligning torque.

The time derivatives of the sideslip angles are obviously

$$\dot{\alpha}_i = \dot{\beta} + \frac{x_i}{V}\dot{r} - \dot{\delta}_i \ . \tag{25.149}$$

The equations of motion (25.109) modify as

$$\begin{cases} mV\left(\dot{\beta} + r\right) + m\dot{V}\beta = Y_\beta \beta + Y_r r + Y_\delta \delta + Y_{\dot{\beta}}\dot{\beta} + Y_{\dot{r}}\dot{r} + Y_{\dot{\delta}}\dot{\delta} + F_{y_e} \\ J_z \dot{r} = N_\beta \beta + N_r r + N_\delta \delta + N_{\dot{\beta}}\dot{\beta} + N_{\dot{r}}\dot{r} + N_{\dot{\delta}}\dot{\delta} + M_{z_e} \end{cases} , \tag{25.150}$$

where the expressions of the derivatives of stability already seen still hold while those of the others are

$$\begin{cases} Y_{\dot{\beta}} = \sum_{\forall i} C_i B_i \\ Y_{\dot{r}} = \frac{1}{V} \sum_{\forall i} x_i C_i B_i \\ Y_{\dot{\delta}} = -\sum_{\forall i} K_i' C_i B_i \end{cases} , \tag{25.151}$$

$$\begin{cases} N_{\dot{\beta}} = \sum_{\forall i} \left[x_i C_i B_i - (M_{z_i})_{,\alpha} B_i' \right] \\ N_{\dot{r}} = \frac{1}{V} \sum_{\forall i} \left[x_i^2 C_i B_i - (M_{z_i})_{,\alpha} x_i B_i' \right] \\ N_{\dot{\delta}} = \sum_{\forall i} \left[-K_i' C_i x_i B_i + K_i' (M_{z_i})_{,\alpha} B_i' \right] \end{cases} .$$

The equation that must be added to Eqs. (25.150) states the equilibrium to rotation of the steering system, assumed to be a rigid system. The geometry of the steering system is sketched in Fig. 25.27. The wheel rotates about an axis, the kingpin axis, which is neither perpendicular to the ground nor passing through the centre of the contact area: The caster angle ν, the lateral inclination angle λ and the longitudinal and lateral offset at the ground d_l and d_t are reported in the figure. In the figure, the kingpin axis intersects with the rotation axis of the wheel, a very common situation. The case in which the two axes are skewed will not be dealt with here.

If the kingpin axis were perpendicular to the ground and no offset were present, the torque acting on the wheel as a consequence of the road-tire interaction forces would be the aligning torque alone. The actual situation is different, however, and the torque about the kingpin axis contains all forces and moments acting on the wheel.

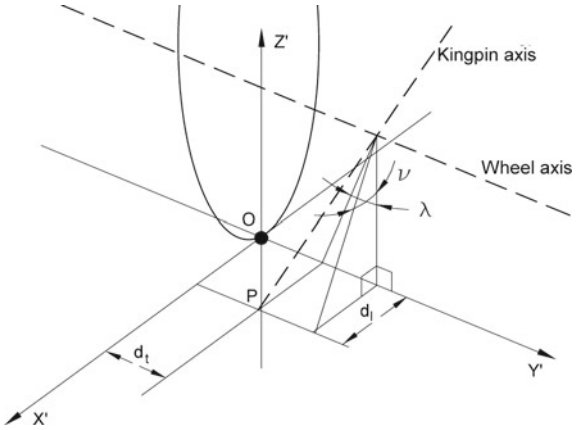

Fig. 25.27 Simplified geometry of the steering system and definition of the caster angle ν, the lateral inclination angle λ and the offset at the ground d_l and d_t. The right wheel is sketched and ν, λ and d_t are positive. The kingpin axis is assumed to intersect the rotation axis of the wheel

With geometrical reasoning, assuming that all angles are small, the total moment M_k about the kingpin axis of both wheels of a steering axle may be approximated as[10]

$$M_{sr} = -(F_{z_l} + F_{z_r})d_t \sin(\lambda)\sin(\delta) + (F_{z_l} - F_{z_r})d_t \sin(\nu)\cos(\delta) + \\ + (F_{y_l} + F_{y_r})r_s \tan(\nu) + (F_{x_l} - F_{x_r})d_t + (M_{z_l} + M_{z_r})\cos\left(\sqrt{\lambda^2 + \nu^2}\right) , \tag{25.152}$$

where r and l indicate the right and left wheels respectively.

In symmetrical conditions, the forces on the ground at the two wheels are equal. By assuming that the steering angle is small, Eq. (25.152) reduces to

$$M_{sr} = -F_z d_t \sin(\lambda)\delta + F_y r_s \tan(\nu) + M_z \cos\left(\sqrt{\lambda^2 + \nu^2}\right) , \tag{25.153}$$

where forces and moments refer to the whole axle.

By introducing expressions (25.148) into Eq. (25.153) the following linearized expression of the moment about the kingpin is obtained

$$M_{sr} = M_{\dot\beta}\dot\beta + M_{\dot r}\dot r + M_{\dot\delta}\dot\delta + M_\beta\beta + M_r r + M_\delta\delta , \tag{25.154}$$

where

$$\begin{aligned} M_{\dot\beta} &= C B r_s \tan(\nu) - (M_z)_{,\alpha} B' \cos\left(\sqrt{\lambda^2 + \nu^2}\right) , \\ M_{\dot r} &= M_{\dot\beta}\frac{a}{V} , \qquad M_{\dot\delta} = -M_{\dot\beta} , \\ M_\beta &= -C r_s \tan(\nu) + (M_z)_{,\alpha}\cos\left(\sqrt{\lambda^2 + \nu^2}\right) , \\ M_r &= M_\beta\frac{a}{V} , \qquad M_\delta = -M_\beta - F_z d_t \sin(\lambda) . \end{aligned} \tag{25.155}$$

[10]T. D. Gillespie, *Fundamentals of Vehicle Dynamics*, SAE, Warrendale, 1992.

The linearized equation of motion of the steering system is then

$$J_s\ddot{\delta} + c_s\dot{\delta} = M_{\dot{\beta}}\dot{\beta} + M_{\dot{r}}\dot{r} + M_{\dot{\delta}}\dot{\delta} + M_\beta\beta + M_r r + M_\delta\delta + M_s\tau_s, \qquad (25.156)$$

where M_s, τ_s, c_s and J_s are, respectively, the torque exerted by the driver on the steering wheel, the steering ratio (the ratio between the rotation angle of the wheel and that of the kingpin), the damping coefficient of the steering damper and the moment of inertia of the whole system, the latter two reduced to the kingpin. Note that the steering ratio is often not constant and that the compliance of the mechanism, here neglected, may have a large effect on it.

No gyroscopic effect of the wheels has been accounted for, which is consistent with the assumption of a rigid vehicle, even if a weak gyroscopic effect should be present if the kingpin axis is not perpendicular to the road.

Equation (25.156) holds also when more complicated geometries are accounted for, provided that a linearization about a reference position is performed. In this case, the expressions of the derivatives of stability M_β, M_r etc. also contain the longitudinal offset at the ground.

Since the second derivative of the state variable δ enters the equations of motion, a further state variable

$$v_\delta = \dot{\delta}$$

must be introduced and a further equation stating the mentioned identity must be added. The state equation is still Eq. (25.109)

$$\dot{\mathbf{z}} = \mathbf{A}\mathbf{z} + \mathbf{B}_c\mathbf{u}_c + \mathbf{B}_e\mathbf{u}_e \ ,$$

where the state and input vectors $\mathbf{z}$, $\mathbf{u}_c$ and $\mathbf{u}_e$ are

$$\mathbf{z} = \begin{Bmatrix} \beta \\ r \\ v_\delta \\ \delta \end{Bmatrix} \ , \qquad \mathbf{u}_c = M_s, \quad \mathbf{u}_e = \begin{Bmatrix} F_{y_e} \\ M_{z_e} \end{Bmatrix} \ ,$$

the dynamic matrix is

$$\mathbf{A} = \begin{bmatrix} mV - Y_{\dot{\beta}} & -Y_{\dot{r}} & -Y_{\dot{\delta}} & 0 \\ -N_{\dot{\beta}} & J_z - N_{\dot{r}} & -N_{\dot{\delta}} & 0 \\ -M_{\dot{\beta}} & -M_{\dot{r}} & J_s & 0 \\ 0 & 0 & 0 & 1 \end{bmatrix}^{-1}$$

$$\times \begin{bmatrix} Y_\beta & -mV + Y_r & 0 & Y_\delta \\ N_\beta & N_r & 0 & N_\delta \\ M_\beta & M_r & (M_{\dot{\delta}} - c_s) & M_\delta \\ 0 & 0 & 1 & 0 \end{bmatrix}$$

and the input gain matrices are

$$\mathbf{B}_c = \begin{bmatrix} mV - Y_{\dot\beta} & -Y_{\dot r} & -Y_{\dot\delta} & 0 \\ -N_{\dot\beta} & J_z - N_{\dot r} & -N_{\dot\delta} & 0 \\ -M_{\dot\beta} & -M_{\dot r} & J_s & 0 \\ 0 & 0 & 0 & 1 \end{bmatrix}^{-1} \begin{bmatrix} 0 \\ 0 \\ \tau_s \\ 0 \end{bmatrix},$$

$$\mathbf{B}_e = \begin{bmatrix} mV - Y_{\dot\beta} & -Y_{\dot r} & -Y_{\dot\delta} & 0 \\ -N_{\dot\beta} & J_z - N_{\dot r} & -N_{\dot\delta} & 0 \\ -M_{\dot\beta} & -M_{\dot r} & J_s & 0 \\ 0 & 0 & 0 & 1 \end{bmatrix}^{-1} \begin{bmatrix} 1 & 0 \\ 0 & 1 \\ 0 & 0 \\ 0 & 0 \end{bmatrix}.$$

The state equation can be used to study the stability of the vehicle and the response to any given law $M_s(t)$. In a similar way, it is possible to study the steady-state performance simply by assuming that all derivatives are vanishingly small (the last state equation may then be dropped, since it reduces to the identity $0 = 0$)

$$\begin{bmatrix} -Y_\beta & mV - Y_r & -Y_\delta \\ -N_\beta & -N_r & -N_\delta \\ -M_\beta & -M_r & -M_\delta \end{bmatrix} \begin{Bmatrix} \beta \\ r \\ \delta \end{Bmatrix} = \begin{Bmatrix} F_{y_e} \\ M_{z_e} \\ M_s \tau_s \end{Bmatrix}. \tag{25.157}$$

The *steering wheel torque gain* M_s/δ with reference to the steering angle and that referring to the curvature of the path $M_s R$, may be easily computed.

The eigenproblem

$$\det(\mathbf{A} - s\mathbf{I}) = 0 \tag{25.158}$$

allows one to study stability. Since the size of the dynamic matrix $\mathbf{A}$ is only 4, it is possible to write the characteristic equation and to solve it using the formula for 4-th degree algebraic equations. However, no closed form solution from which to draw general conclusions is available. The eigenvalues are either a pair of complex conjugate solutions—yielding damped oscillations (if both real parts are negative), one usually at low frequency and the other at high frequency—or two nonoscillatory solutions and one high frequency oscillation. The high frequency solution is usually linked with the dynamics of the steering device while the others are linked primarily to the behavior of the vehicle.

The vibrations of the steering system were of concern in the past, particularly in the 1930s, when they were referred to as *steering shimmy*. Such vibrations were also present in the tailwheel of aircraft undercarriages. The use of tires with lower pneumatic trail and, above all, the introduction of damping in the steering mechanism has completely rectified the problem. Both viscous damping and dry friction have been used with success, but the latter decreases the reversibility of the steering system and thus decreases its precision and its centering characteristics.

The, now common, use of servosystems in the steering control implies the presence of non-negligible damping with viscous characteristics in the steering device.

The present model is, however, too imprecise for a detailed study of this phenomenon, since the compliance of the steering system and the lateral compliance of the suspension are important causal factors in this type of vibration that may become self-excited.

If only the low-frequency overall behavior of the vehicle is studied, it is possible to neglect the dependence of the tire forces on the time derivative of the sideslip angle. In this case, the expressions of the dynamic matrix and of the input gain matrix simplify as follows:

$$\mathbf{A} = \begin{bmatrix} \frac{Y_\beta}{mV} & \frac{Y_r}{mV} - 1 & 0 & \frac{Y_\delta}{mV} \\ \frac{N_\beta}{J_z} & \frac{N_r}{J_z} & 0 & \frac{N_\delta}{J_z} \\ \frac{M_\beta}{J_s} & \frac{M_r}{J_s} & \frac{-c_s}{J_s} & \frac{-M_\delta}{J_s} \\ 0 & 0 & 1 & 0 \end{bmatrix},$$

$$\mathbf{B}_c = \begin{bmatrix} 0 \\ 0 \\ \frac{\tau_s}{J_s} \\ 0 \end{bmatrix}, \quad \mathbf{B}_e = \begin{bmatrix} \frac{1}{mV} & 0 \\ 0 & \frac{1}{J_z} \\ 0 & 0 \\ 0 & 0 \end{bmatrix}.$$

If the inertia and the damping of the steering system are likewise neglected, Eq. (25.156) can be solved in δ. By introducing this value into the equations of motion, an approximate model for the behavior of the vehicle with free controls is obtained.

By assuming that the speed V is constant, the homogeneous state equation for a vehicle with front axle steering only is then

$$\begin{Bmatrix} \dot{\beta} \\ \dot{r} \end{Bmatrix} = \begin{bmatrix} \frac{Y_\beta + Y_\delta}{mV} & \frac{Y_r + Y_\delta \frac{a}{V}}{mV} - 1 \\ \frac{N_\beta + N_\delta}{J_z} & \frac{N_r + N_\delta \frac{a}{V}}{J_z} \end{bmatrix} \begin{Bmatrix} \beta \\ r \end{Bmatrix}. \tag{25.159}$$

The equation is formally identical to the homogeneous Eq. (25.108) and in this case as well, it is possible to resort to a spring-mass-damper analogy and to study the constant speed stability in a simple way. It can be shown that both the stiffness and the damping coefficient are always positive, denoting both static and dynamic stability.

By introducing only the cornering forces due to the tires, the vehicle is overdamped at low speed, up to

$$V = \frac{1}{2}\left(b^2 + \frac{J_z}{m}\right)\sqrt{\frac{C_2}{J_z b}}\,.$$

Above that speed the behavior becomes more and more underdamped, with an increasingly oscillatory behavior.

Note, however, that the last simplification is usually too rough: In most cases, the high value of the steering ratio τ_s makes the inertia of the steering wheel when reduced to the kingpin axis non-negligible and the use of Eq. (25.159) can lead to non-negligible errors. Other errors may be introduced by neglecting steering damping since a certain amount of damping is present in the system, the neglect of which may cause dynamic instability.

Example 25.7 Compute the torque that must be exerted on the steering wheel necessary to maintain the vehicle of Appendix E.2 on a circular path with a radius of 100 m and to counteract a transversal slope of 1° at constant speed.

The additional data for the steering system are: $\lambda = 11°$, $\nu = 3°$, $d = 5$ mm and $\tau_s = 16$.

The steering wheel torque gain $M_s R$ can be computed from Eq. (25.157). By stating $F_{y_e} = 0$, $M_{z_e} = 0$ and $M_s = 1$, it is possible to obtain the yaw velocity r that follows the application of a unit torque to the steering wheel.

Since $R = V/r$, the gain $M_s R$ may be immediately computed and thus the value of the torque needed to maintain any given circular path. The results for $R = 100$ m are reported in Fig. 25.28a.

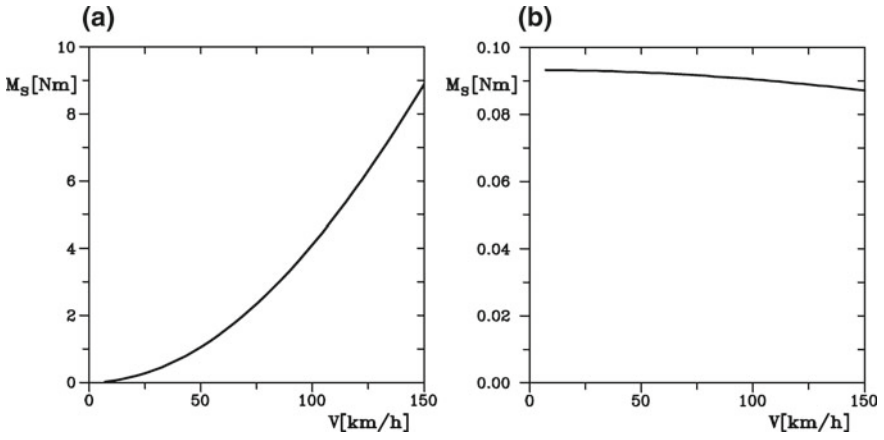

Fig. 25.28 Example 25.7: Steering wheel torque needed to maintain the vehicle on a circular path with a radius of 100 m (**a**) and to counteract a transversal slope of 1° at constant speed (**b**)

To obtain the steering torque needed to counteract a transversal road slope, Eq. (25.156) needs to be rearranged. The slope α_t is felt by the vehicle as a side force

$$F_{y_e} = mg\sin(\alpha_t);\,.$$

If the path is straight, $r = 0$ and also M_{z_e} is equal to zero, as no external moment acts on the vehicle. The unknowns are β, δ and M_s.

The equation is rearranged as

$$\begin{bmatrix} -Y_\beta & -Y_\delta & 0 \\ -N_\beta & -N_\delta & 0 \\ -M_\beta & -M_\delta & \tau_s \end{bmatrix} \begin{Bmatrix} \beta \\ \delta \\ M_s \end{Bmatrix} = \begin{Bmatrix} mg\sin(\alpha_t) \\ 0 \\ 0 \end{Bmatrix}.$$

The results obtained for a slope of 1° are reported in Fig. 25.28b.

25.15 Unstationary Motion

The response to a steering input in unstationary conditions may be computed using the constant-speed linearized model expressed by Eqs. (25.110) or (25.111), reported here without the terms due to external forces and moments,

$$\begin{aligned} P\ddot{\beta} + Q\dot{\beta} + U\beta &= S'\delta + T'\dot{\delta}, \\ P\ddot{r} + Q\dot{r} + Ur &= S''\delta + T''\dot{\delta}\,. \end{aligned} \tag{25.160}$$

If the variable for motion in the y direction is the lateral velocity v instead of the sideslip angle β, the first equation becomes

$$P\ddot{v} + Q\dot{v} + Uv = VS'\delta + VT'\dot{\delta}\,. \tag{25.161}$$

If an input of the type

$$\delta = \delta_0 e^{st}$$

is assumed, the solution takes the form

$$\beta = \beta_0 e^{st},\; r = r_0 e^{st},\; v = v_0 e^{st}.$$

The algebraic equations into which the differential equations transform are

$$\begin{aligned} \left(Ps^2 + Qs + U\right)\beta_0 &= \left(T's + S'\right)\delta_0, \\ \left(Ps^2 + Qs + U\right)r_0 &= \left(T''s + S''\right)\delta_0, \\ \left(Ps^2 + Qs + U\right)v_0 &= V\left(T's + S'\right)\delta_0. \end{aligned} \tag{25.162}$$

The transfer functions are then

$$\frac{\beta_0}{\delta_0} = \frac{T's + S'}{Ps^2 + Qs + U}, \tag{25.163}$$

$$\frac{r_0}{\delta_0} = \frac{T''s + S''}{Ps^2 + Qs + U}, \tag{25.164}$$

$$\frac{v_0}{\delta_0} = V\frac{\beta_0}{\delta_0} = V\frac{T's + S'}{Ps^2 + Qs + U}. \tag{25.165}$$

In non-stationary conditions, the lateral acceleration is

$$a_y = \dot{v} + rV \tag{25.166}$$

and thus the relevant transfer function is

$$\frac{a_{y_0}}{\delta_0} = V\frac{T's^2 + \left(T'' + S'\right)s + S''}{Ps^2 + Qs + U}. \tag{25.167}$$

By using the simplified expressions of the derivatives of stability, the denominator of all transfer functions is

$$\begin{aligned}\Delta = J_z mVs^2 + \left[J_z(C_1 + C_2) + m(a^2C_1 + b^2C_2)\right]s + \\ + mV(-aC_1 + bC_2) + C_1C_2\tfrac{l^2}{V}.\end{aligned} \tag{25.168}$$

The equation $\Delta = 0$ allows the poles of the system to be computed, as seen in Sect. 6.13.1.

Assuming only front axle steering, the transfer functions are

$$\frac{r_0}{\delta_0} = \frac{mVaC_1s + lC_1C_2}{\Delta}, \tag{25.169}$$

$$\frac{a_{y_0}}{\delta_0} = \frac{J_zVC_1s^2 + C_1C_2bls + lVC_1C_2}{\Delta}. \tag{25.170}$$

By equating the numerator of the transfer functions (25.169) and (25.170) to zero it is possible to find their zeros. For functions (25.169) the result is straightforward, and the only zero is real and negative

$$s = -\frac{lC_2}{mVa}. \tag{25.171}$$

The computation for function (25.170) is not as simple. The zeros are

$$s = \frac{-blC_2 \pm \sqrt{b^2l^2C_2^2 - 4V^2lJ_zC_2}}{2J_zV}. \tag{25.172}$$

At low speed, i.e. if

$$V \leq \sqrt{\frac{b^2lC_2}{4J_z}}, \tag{25.173}$$

the two solutions are both real and negative. They are distinct if Eq. (25.173) holds with (<), coincident if it holds with (=).

At higher speeds, the two solutions are complex conjugate

$$s = \frac{-blC_2}{2J_zV} \pm \sqrt{\frac{4V^2lJ_zC_2 - b^2l^2C_2^2}{4J_z^2V^2}}, \tag{25.174}$$

with a negative real part: the zeros lie in the left part of the Argand plane.

The situation may be different for the sideslip angle: S' may be either positive or negative depending on the values of the parameters. By using the simplified expressions of the derivatives of stability, the value of the relevant transfer function is

$$\frac{\beta_0}{\delta_0} = \frac{J_zVC_1s + C_1C_2bl - maV^2C_1}{V\Delta}. \tag{25.175}$$

The expression of the zero is obtained by equating to zero the numerator

$$s = \frac{maV^2C_1 - C_1C_2bl}{J_zVC_1}. \tag{25.176}$$

At low speed the zero is negative and real, but if

$$V > \sqrt{\frac{blC_2}{am}} \tag{25.177}$$

it moves to the positive part of the Argand plane and then the system is a non-minimum phase system.

From Eq. (25.110) and following it is clear that the response to steering is a linear combination of the laws $\delta(t)$ and $\dot{\delta}(t)$. If the numerator of the transfer function is linear in s, and if the zero of the transfer function (which is always real since the numerator is linear) is negative, the coefficients of the linear combination have the same sign and the sign of the response does not change in time.

Example 25.8 Plot the roots locus of the transfer function related to the lateral acceleration at varying speed for the vehicle in Appendix E.2, taking into account both the simplified and the complete expressions of the derivatives of stability used in Example 25.5. Compute the speed at which the transfer function β_0/δ_0 becomes a non-minimum phase function.

Then compute the response to a step steering input at a speed of 100 km/h.

The transfer function a_{y_0}/δ_0 has two real zeros up to a speed of 24.67 km/h; it then has two complex conjugate poles. The locus of the zeros is reported in Fig. 25.29a.

The two formulations yield practically the same results. Function β_0/δ_0 has a negative real zero up to a speed of 56.22 km/h; then it has a positive real zero.

If function $\delta(t)$ is a unit step function

$$\begin{cases} \delta = 0 & \text{for } t < 0 \\ \delta = 1 & \text{for } t \geq 0 \,, \end{cases}$$

its derivative $\dot{\delta}$ is an impulse function(Dirac's δ):

$$\begin{cases} \dot{\delta} = 0 & \text{for } t < 0 \\ \dot{\delta} = \infty & \text{for } t = 0 \\ \dot{\delta} = 0 & \text{for } t > 0 \end{cases}$$

$$\int_{-\infty}^{\infty} \dot{\delta} dt = 1 \ .$$

Since the vehicle is understeer, the step and impulse responses $g(t)$ and $h(t)$ are both oscillatory and are

$$h(t) = \frac{1}{m\omega_n\sqrt{1-\zeta^2}} e^{-\zeta\omega_n t} \sin\left(\sqrt{1-\zeta^2}\omega_n t\right) \,,$$
$$g(t) = \frac{1}{k} - \frac{e^{-\zeta\omega_n t}}{k}\left[\cos\left(\sqrt{1-\zeta^2}\omega_n t\right) + \frac{\zeta}{\sqrt{1-\zeta^2}} \sin\left(\sqrt{1-\zeta^2}\omega_n t\right)\right] \,,$$

where

$$m = P, \omega_n = \sqrt{\frac{U}{P}}, \zeta = \frac{Q}{2\sqrt{PU}} \,.$$

The total response is a linear combination of the step and impulse responses

$$\beta(t) = S' g(t) + T' h(t),$$
$$r(t) = S'' g(t) + T'' h(t) \,.$$

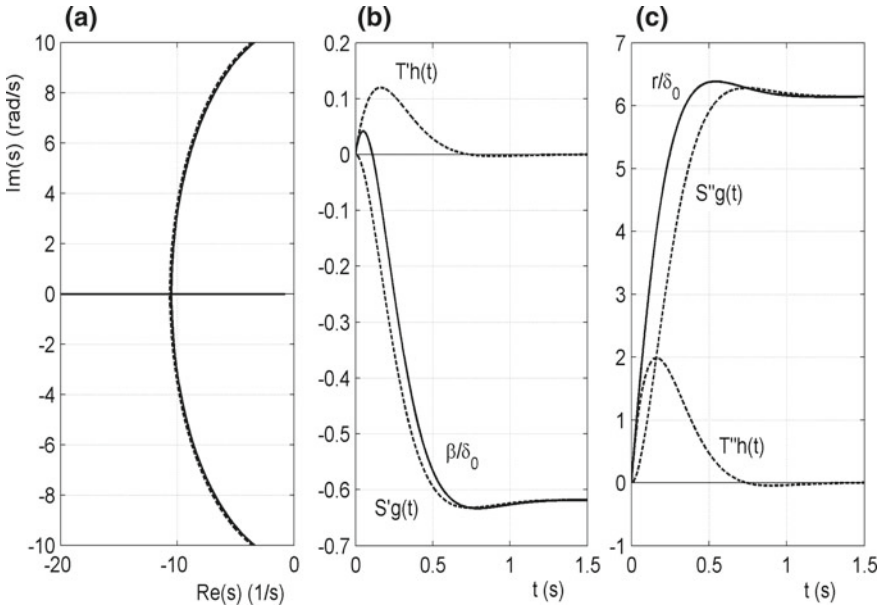

Fig. 25.29 **a** Locus of the zeros of the transfer function a_{y_0}/δ_0. Full line: complete expression of the derivatives of stability; dashed line: simplified expression. **b** and **c** response to a step steering input computed in closed form

At 100 km/h the mass-spring-damper system is underdamped, since the damping ratio has a value $\zeta = 0.77$. The natural frequency of the undamped system is $\omega_n = 6.67$ rad/s $= 1.06$ Hz, while the frequency of the free damped oscillations is $\omega_p = 4.24$ rad/s $= 0.68$ Hz.

The results are reported in Fig. 25.29b, c.

The step and impulse responses have the same sign for the yaw velocity, and they simply add in modulus. In the response for the sideslip angle they have opposite sign and initially the second one prevails. When, after some time, the first one begins to prevail, the sign of the response changes.

This is typical for non-minimum phase systems: the system initially reacts in a direction opposite to that of the steady state response, then goes to zero and changes its sign.

Once law $r(t)$ has been obtained, it is possible to integrate it to yield the yaw angle

$$\psi(t) = \int_0^t r(u)du \ . \tag{25.178}$$

The path can then be obtained directly in the inertial frame X, Y. The velocities $\dot{X}$ and $\dot{Y}$ can be expressed in terms of angles β and ψ,

$$\begin{Bmatrix} \dot{X} \\ \dot{Y} \end{Bmatrix} = V \begin{bmatrix} \cos(\psi) & -\sin(\psi) \\ \sin(\psi) & \cos(\psi) \end{bmatrix} \begin{Bmatrix} \cos(\beta) \\ \sin(\beta) \end{Bmatrix} . \tag{25.179}$$

By integrating Eqs. (25.179) the path is readily obtained,

$$\begin{cases} X = \int_0^t V\,[\cos(\beta)\cos(\psi) - \sin(\beta)\sin(\psi)]\,du \\ Y = \int_0^t V\,[\cos(\beta)\sin(\psi) + \sin(\beta)\cos(\psi)]\,du \end{cases} . \tag{25.180}$$

The integration to obtain the path must actually be performed numerically even in the simplest cases where laws $\beta(t)$ and $r\,(t)$ may be computed in closed form owing to the fact that angle ψ is usually too large to allow linearizing its trigonometric functions even when using the linearized model. In general, it is more convenient to integrate the equations of motion numerically, since there is no difficulty in doing so for Eq. (25.109) once laws $\delta(t)$, $F_{y_e}(t)$, $M_{z_e}(t)$ and $V(t)$ have been stated. Nowadays numerical integration is so straightforward that closed form solutions that are too complicated to allow a quick qualitative understanding of the phenomena to be obtained are considered of little use.

Example 25.9 Study the motion with locked controls of the vehicle of Appendix E.2 following a step steering input.

Assume that the value of the steering angle is that needed to obtain a circular path with a radius of 200 m at a speed of 100 km/h.

At 100 km/h the path curvature gain $1/R\delta$ is equal to 0.2472 1/m. To perform a curve with a radius of 200 m, a steering angle $\delta = 0.0202$ rad $= 1.159°$ is needed.

In kinematic conditions, the radius of the path corresponding to the same value of δ is 106.8 m. The fact that it is almost half the above was easily predictable, since 100 km/h is only slightly less than the characteristic speed.

The steady state values of r and β are respectively 0.1389 rad/s and -0.0131 rad $= -0.749°$.

The equation of motion of the vehicle was integrated numerically for a duration of 30 s. The results are plotted in Fig. 25.30. The time histories of the yaw velocity and sideslip angle are shown along with the path.

The steady-state conditions are reached after a few seconds, with a slightly underdamped behavior.

Example 25.10 Study the motion with locked controls of the vehicle of Appendix E.2 following a wind gust. Assume a step lateral gust, like the one encountered when exiting a tunnel. Assume an ambient wind velocity $v_a = 10$ m/s and a vehicle speed of 100 km/h.

The driver does not react to the gust and the steering angle is kept equal to zero.

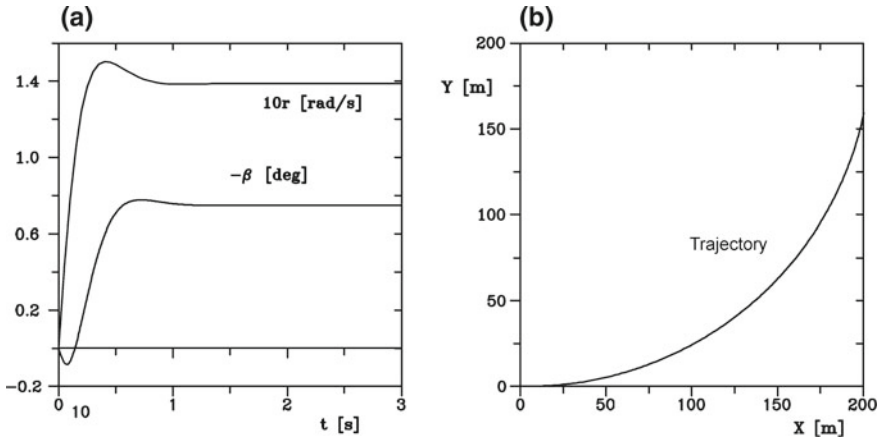

Fig. 25.30 Example 25.9: Response to a step steering input. **a** Time histories of the yaw velocity and sideslip angle and **b** path

The presence of a cross-wind is accounted for by adding a side force F_{y_e} and a yawing moment M_{z_e} equal to

$$\begin{cases} F_{y_e} = \dfrac{1}{2}\rho V^2 S (C_y)_{,\beta} \psi_w \\ \\ M_{y_e} = \dfrac{1}{2}\rho V^2 S l (C_{M_z})_{,\beta} \psi_w \end{cases},$$

where ψ_w is the angle between the direction of the relative velocity and the tangent to the path. This is clearly an approximation since it relies on the linearity of the aerodynamic forces and moments with the aerodynamic sideslip angle and holds only if angle $\beta + \psi_w$ remains small.

As the path of the vehicle curves after the manoeuvre, the components of the relative velocity along the path and in a direction perpendicular to it are

$$\begin{cases} V_{\parallel} = V - v_a \sin(\psi + \beta) \\ V_{\perp} = -v_a \cos(\psi + \beta) \end{cases},$$

yielding

$$\psi_w = \arctan\left(\frac{-v_a \cos(\psi + \beta)}{V - v_a \cos(\psi + \beta)}\right).$$

The above relationships may be approximated by neglecting angle β.

Another approximation is neglecting the contribution of the wind velocity to the airspeed, which is always considered at 100 km/h.

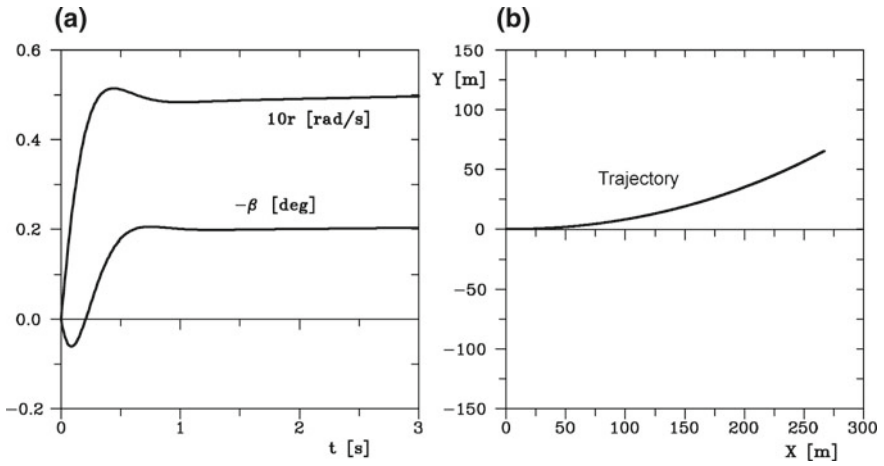

Fig. 25.31 Example 25.10: Response to a cross-wind gust. **a** Time histories of the yaw velocity and sideslip angle and **b** path

The equation of motion of the vehicle has been integrated numerically for a duration of 10 s. The results are plotted in Fig. 25.31. The time histories of the yaw velocity and sideslip angle are shown along with the path.

Quasi steady-state conditions are again reached after a few seconds, with a slightly underdamped behavior. The conditions are not actually steady-state since the direction of the wind is fixed, while the direction of the vehicle axes change. However, this effect is minimal for the duration of the manoeuvre, and a good approximation could have been obtained by assuming a constant value for angle ψ_w (ψ_w increases from 19.8° to 20.9° for $t = 0$ to $t = 10$ s).

At the end of the manoeuvre, the values of r and β are, respectively, 0.0505 rad/s and -0.0036 rad = $-0.2073°$. The errors linked to neglecting β in the above expression are thus negligible. The response in terms of β in this case is that typical of a non-minimum phase system.

Example 25.11 The following manoeuvre is often performed by test drivers to assess the handling and stability of a car: A step steering input is supplied and the steering wheel is kept in position for a short time. The driver then releases the wheel and the vehicle returns to a straight path. The whole manoeuvre is performed at constant speed.

Study the motion of the vehicle of Appendix E.2 following a manoeuvre of this kind with a 45° steering wheel input held for 1.5 s at 100 km/h.

The data for the steering system are J_s = 15 kg m^2, c_s = 150 Nms/rad, $\lambda = 11°$, $\nu = 3°$, $d = 5$ mm and $\tau_s = 16$.

The first part of the manoeuvre is the same as in Example 25.9, only with a greater value of δ: 2.81°.

The integration in time is performed in two parts: A locked controls model is used for the first 1.5 s; a free control model is used after the driver releases the wheel.

This second part of the simulation is performed using two alternative models: One in which the dependence of tire forces on the derivative $\dot{\alpha}$ is neglected, and a second in which the inertia and damping of the steering system are also not considered.

The time histories of the yaw velocity, sideslip angle and steering angle are reported together with the path in Fig. 25.32.

The inertia of the steering system plays an important role in the response, since it slows the recovery of the vehicle, thus affecting the path. It also increases the oscillatory behavior of the vehicle, and if no damping is considered, an unstable behavior emerges.

The effect of neglecting the inertia of the steering system can be verified by comparing the poles of the system: If neither inertia nor damping is accounted for, the two eigenvalues are $-3.011 \pm 7.709i$, while the more complete model yields four eigenvalues $-9.129 \pm 8.2921i$ and $-1.065 \pm 5.563i$. The first is quite damped and is not important in the motion, but the second is clearly different from that obtained

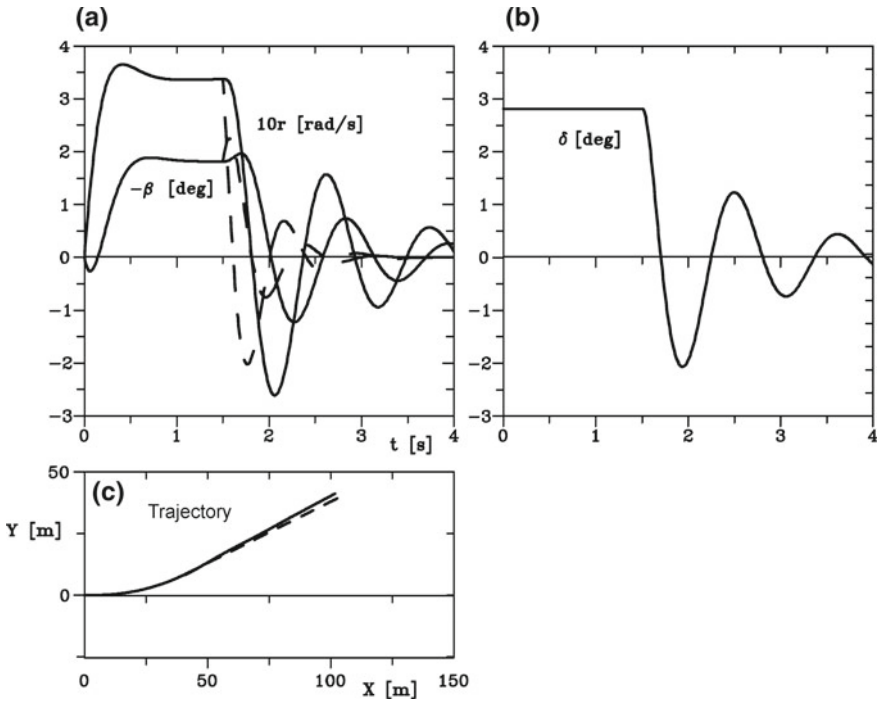

Fig. 25.32 Example 25.11: Response to a step steering input and a subsequent recovery of the straight path with free controls. **a** Time histories of the yaw velocity and sideslip angle and **b** of the steering angle; **c** path. The inertia and damping of the steering system are considered (full lines) and then neglected (dashed lines)

from the simpler model. The high value of the steering ratio, whose square enters the computation of the equivalent inertia of the steering wheel, is responsible for this effect.

25.16 Vehicles with Two Steering Axles (4WS)

In the majority of vehicles with two axles, only the front wheels are provided with a steering system. However, beginning in the 1980s, an increasing number of cars with steering on all four wheels (4WS) appeared on the market, in the beginning most of them Japanese. The primary goal was to improve manoeuvrability and handling characteristics both in low- and high-speed steering. 4WS system were dealt with in Part I, Chap. 6.

Simple four-wheel steering may be implemented by equipping the rear axle with a compliance purposely designed to provide the required steering action under the effect of road loads without adding an actual steering device. This approach is defined as passive steering. Active steering occurs when the rear axle is provided with a second steering device, operated by the driver along with that of the front axle through adequate actuators.

To reduce the radius of the path in low-speed (kinematic) conditions, the rear axle must steer in a direction opposite to the front; if the absolute values of the steering angles are equal, the radius is halved and the off-tracking of the rear axle is reduced to zero. Using the notation introduced in the preceding sections, this situation is characterized by

$$K_1' = 1 \ , \ K_2' = -1$$

(in the following it will always be assumed that $K_1' = 1$).

In practical terms, this value is too high since the rear axle would initially be displaced too far to the outside of the line connecting the centres of the wheels in the initial position, particularly when starting the motion with the wheels in a steered position. It would be difficult, for example, to move a vehicle parked near a curb or, worse, near a wall.

Assuming that $K_1' = 1$ and K_2' is constant, the path curvature gain and the off-tracking distance are

$$\frac{1}{R\delta} \approx \frac{1 + K_2'}{l} \ , \qquad R_a - R_1 \approx \frac{l^2(1 - K_2')}{2R(1 + K_2')} \ . \tag{25.181}$$

In high-speed cornering the situation is different. The equation of motion is still Eq. (25.108) and, if the speed V is constant, it is possible to use the spring-mass-damper analogy (either Eq. (25.110) or (25.111)).

To study the effect of rear steer, consider the simplified expression of the derivatives of stability. The expression of P, Q and U do not change, while

$$\begin{cases} S' = mV\left(-aC_1K_1' + bC_2K_2'\right) + C_1C_2\dfrac{l}{V}\left(K_1'b + K_2'a\right) \\ S'' = lC_1C_2\left(K_1' - K_2'\right) \\ T' = J_z\left(K_1'C_1 + K_2'C_2\right) \\ T'' = mV\left(aK_1'C_1 - bK_2'C_2\right) \ . \end{cases}$$

The expressions of the gains in steady state conditions become:

- path curvature gain

$$\frac{1}{R\delta} = \frac{1}{l}\frac{\left(K_1' - K_2'\right)}{1 + KV^2} \ , \tag{25.182}$$

- lateral acceleration gain

$$\frac{V^2}{R\delta} = \frac{V^2}{l}\frac{\left(K_1' - K_2'\right)}{1 + KV^2} \ , \tag{25.183}$$

- sideslip angle gain

$$\frac{\beta}{\delta} = \frac{b}{l}\left[K_1' + K_2'\frac{a}{b} - \frac{mV^2}{l}\left(\frac{aK_1'}{bC_2} - \frac{K_2'}{C_1}\right)\right]\frac{1}{1 + KV^2} \ , \tag{25.184}$$

- yaw velocity gain

$$\frac{r}{\delta} = \frac{V}{l}\frac{\left(K_1' - K_2'\right)}{1 + KV^2} \ . \tag{25.185}$$

From the equations above it is clear that opposite steering (K_1' and K_2' with opposite signs) produces an increase of the gains related to the curvature of the path, while steering with the same sign allows larger cornering forces to be produced for the same steering angle

However, the most important advantages of 4WS are felt in non-steady-state conditions, making it important to assess the transfer functions in these conditions. Equations from (25.162) to (25.167) still hold. If the simplified expressions of the derivatives of stability are used, it follows that

$$\frac{r_0}{\delta_0} = \frac{mV\left(aK_1'C_1 - bK_2'C_2\right)s + lC_1C_2\left(K_1' - K_2'\right)}{\Delta}, \tag{25.186}$$

$$\frac{a_{y_0}}{\delta_0} = \frac{J_zV\left(K_1'C_1 + K_2'C_2\right)s^2 + C_1C_2l\left(aK_1' + bK_2'\right)s + lVC_1C_2\left(K_1' - K_2'\right)}{\Delta}, \tag{25.187}$$

where Δ is still expressed by Eq. (25.168).

Opposite steering also makes the vehicle more responsive about the yaw axis in non-steady-state conditions. The second transfer function shows how steering in the same direction increases the response at the highest frequencies, in particular for lateral acceleration due to motion in the y direction, while opposite steering increases the contribution due to centrifugal acceleration, especially at low frequency.

Strong rear axle steering may cause some of the zeros of the transfer functions to lie in the positive half-plane of the complex plane, making the system a non-minimum phase system. This will be studied in greater detail in Chap. 27.

The limiting case of same sign steering is, for a vehicle with the center of mass at mid-wheelbase, that with equal steering angles

$$K_1' = K_2' = 1 \ .$$

Remark 25.17 This is, however, too theoretical, since the vehicle would be quick in a lane change, moving sideways, but would never be able to move on a curved path. Instead of turning, it would move sideways.

Thus it is clear that the steering mechanism must adapt the value of K_2' to the external conditions and to the requests of the driver. As seen in Part I, the simplest strategy is to use a device, possibly mechanical, to link the two steering boxes with a variable gear ratio: When angle δ is small, as typically occurs in high speed driving, K_2' is positive and the steering angles have the same direction while when δ is large, as occurs when manoeuvring at low speed, K_2' is negative. Obviously, K_2' must be much smaller than K_1'.

However, more complicated control laws for the steering of the rear axle must be implemented to fully exploit the potential advantages of 4WS. The parameters entering such laws are numerous, e.g., the speed V, the lateral acceleration, the sideslip angles α_i, etc. Such devices must be based on electronic controllers and actuators of different types, and their implementation enters into the important field of autronics (Chap. 27).

From the viewpoint of mathematical modelling, the situation is, at least in principle, simple. There is no difficulty in introducing a suitable function $K_2'(V, \delta, \dots)$ into the equations (actually it would appear only in the derivatives of stability Y_δ and N_δ) and in modifying the equations of the rigid-body model seen above accordingly. The more advanced models of the following sections can be modified along the same lines. If function K_2' includes some of the state variables, the modifications can be larger but no conceptual difficulty arises.

Except in the latter case, locked control stability is not affected by the introduction of 4WS, while stability with free controls can be affected by it.

Generally speaking, the advantages of 4WS are linked with an increase in the quickness of the response of the vehicle to a steering input, but this cannot be true for all types of manoeuvres: Steering all axles in the same direction may make the vehicle quick in lane change manoeuvres but slower in acquiring a given yaw velocity. The sensations of the driver may be strange and, at least at the beginning, unpleasant. A solution may be a device that initially steers the rear wheels in the opposite direction

for a short time, to initiate a yaw rotation, and then steers them in the same direction as the front wheels, to generate cornering forces. This requires a more complicated control logic, possibly based on microprocessors.

As a final consideration, most applications are based on vehicles already designed for conventional steering to which 4WS is then added, normally as an option. In this case, the steering of the rear wheel is limited to 1°–2° or even less since the rear wheel wells lack the space required for larger movement. Even if the car is designed from the beginning for 4WS, a trade-off between its advantages and the loss of available space in the trunk due to 4WS will take place.

25.17 Model with Four Degrees of Freedom for Articulated Vehicles

25.17.1 Equations of Motion

An articulated vehicle modelled as two rigid bodies hinged to each other has, in its motion on the road surface, four degrees of freedom (Fig. 25.33). The assumption of rigid bodies implies that the hinge is cylindrical and that its axis is perpendicular to the road: In practice different setups are used, but if rolling is neglected the present one is the only possible layout.

There is no difficulty in writing the six equations of motion of the two rigid bodies (each has three degrees of freedom in the planar motion on the road) and then in introducing the two equations for the constraints due to the hinge to eliminate two of the six. The forces exchanged between the two bodies are explicitly introduced.

Here a different approach is followed and the equations of motion are obtained through Lagrange equations. To this end, a set of four generalized coordinated is first stated: X and Y are the inertial coordinates of the centre of mass of the tractor and ψ is its yaw angle. They are the same coordinates used in the study of the insulated vehicle. The added coordinate is angle θ between the longitudinal axes x of the tractor and x_R of the trailer. Positive angles are shown in Fig. 25.33.

Instead of angle θ, it is possible to use the yaw angle of the trailer ψ_R, i.e. the angle between the inertial X-axis and the body-fixed axis x_R.

The model can be simplified and linearized, as seen for the model of the isolated vehicle, by assuming that the motion occurs in a condition not much different from the symmetrical, which implies that the trailer angle θ and the sideslip angles are small. Moreover, the vehicle will be assumed to be a monotrack vehicle, i.e. the sideslip angles of the wheels of each axle will be assumed to be equal. The model will be built in terms of axles rather than wheels.

As a damper with damping coefficient Γ may be attached to the hinge between tractor and trailer, a Raleigh dissipation function must be written along with the kinetic energy. No conservative forces act in the plane of the road, assuming the hinge has no elastic restoring force, and hence no potential energy need be computed.

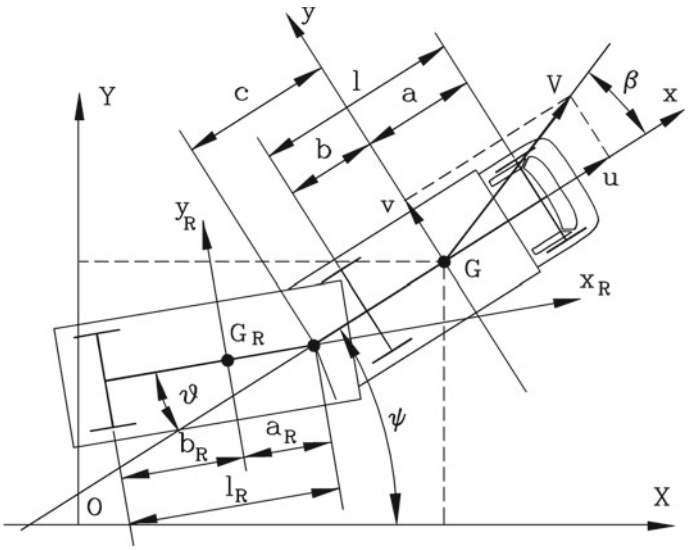

Fig. 25.33 Articulated vehicle. Reference frames and generalized coordinates

The position of the centre of mass of the trailer is

$$\left(\overline{\mathrm{G}_R - \mathrm{O}}\right) = \left\{ \begin{array}{l} X - c\cos(\psi) - a_R\cos(\psi - \theta) \\ Y - c\sin(\psi) - a_R\sin(\psi - \theta) \end{array} \right\} . \tag{25.188}$$

The velocity of the centre of mass of the tractor is simply

$$V_G = \left\{ \begin{array}{l} \dot{X} \\ \dot{Y} \end{array} \right\} , \tag{25.189}$$

while that of point G_R is

$$V_{\mathrm{G}_R} = \left\{ \begin{array}{l} \dot{X} + \dot{\psi}c\sin(\psi) + \left(\dot{\psi} - \dot{\theta}\right) a_R\sin(\psi - \theta) \\ \dot{Y} - \dot{\psi}c\cos(\psi) - \left(\dot{\psi} - \dot{\theta}\right) a_R\cos(\psi - \theta) \end{array} \right\} . \tag{25.190}$$

The kinetic energy of the system is then:

$$\mathcal{T} = \frac{1}{2}m_T V_G^2 + \frac{1}{2}m_R V_{G_R}^2 + \frac{1}{2}J_T\dot{\psi}^2 + \frac{1}{2}J_R\left(\dot{\psi} - \dot{\theta}\right)^2 , \tag{25.191}$$

where m_T, m_R, J_T and J_R are, respectively, the masses and the baricentric moments of inertia about an axis of the tractor and the trailer perpendicular to the road.

By introducing the expressions for the velocities into Eq. (25.191) and neglecting the terms containing squares and higher powers of small quantities, also in the series for trigonometric functions, it follows that

$$\begin{aligned}\mathcal{T} = &\tfrac{1}{2}m\left(\dot{X}^2+\dot{Y}^2\right)+\tfrac{1}{2}J_1\dot{\psi}^2+\tfrac{1}{2}J_3\dot{\theta}^2-J_2\dot{\psi}\dot{\theta}+\\ &+m_R\left[c\dot{\psi}+a_R\left(\dot{\psi}-\dot{\theta}\right)\right]\left[\dot{X}\sin(\psi)-\dot{Y}\cos(\psi)\right]+\\ &-m_R a_R\theta\left(\dot{\psi}-\dot{\theta}\right)\left[\dot{X}\cos(\psi)-\dot{Y}\sin(\psi)\right],\end{aligned} \tag{25.192}$$

where

$$\begin{cases} m = m_T + m_R\ , \\ J_1 = J_T + J_R + m_R\left[a_R^2 + c^2 + 2a_R c\right]\ , \\ J_2 = J_R + m_R\left[a_R^2 + a_R c\right]\ , \\ J_3 = J_R + m_R a_R^2\ . \end{cases}$$

The components of the velocity in the tractor reference frame may be used

$$\begin{Bmatrix} u \\ v \\ r \\ v_\theta \end{Bmatrix} = \begin{bmatrix} \cos(\psi) & \sin(\psi) & 0 & 0 \\ -\sin(\psi) & \cos(\psi) & 0 & 0 \\ 0 & 0 & 1 & 0 \\ 0 & 0 & 0 & 1 \end{bmatrix} \begin{Bmatrix} \dot{X} \\ \dot{Y} \\ \dot{\psi} \\ \dot{\theta} \end{Bmatrix}\ , \tag{25.193}$$

where r is the yaw angular velocity of the tractor and v_θ is the relative yaw angular velocity of the trailer with respect to the tractor. The relationship between angular velocities and derivatives of the generalized coordinates is

$$\mathbf{w} = \mathbf{A}^T\dot{\mathbf{q}}\ , \tag{25.194}$$

where the structure of $\mathbf{A}$ is that of a rotation matrix, and then

$$\mathbf{A}^T = \mathbf{A}^{-1}\ . \tag{25.195}$$

The final expression of the kinetic energy is then

$$\begin{aligned}\mathcal{T} = &\tfrac{1}{2}m\left(u^2+v^2\right)+\tfrac{1}{2}J_1 r^2+\tfrac{1}{2}J_3 v_\theta{}^2-J_2 r v_\theta+\\ &-m_R v\left[cr+a_R\left(r-v_\theta\right)\right]-m_R a_R\theta u\left(r-v_\theta\right)\ .\end{aligned} \tag{25.196}$$

The rotation kinetic energy of the wheels has been neglected: No gyroscopic effect of the wheels will be obtained in this way.

The Raleigh dissipation function due to the above mentioned viscous damper is simply

$$\mathcal{F} = \frac{1}{2}\Gamma\dot{\theta}^2 \ . \tag{25.197}$$

The equations of motion obtained in the form of Lagrange equations are

$$\frac{d}{dt}\left(\frac{\partial \mathcal{T}}{\partial \dot{q}_i}\right) - \frac{\partial \mathcal{T}}{\partial q_i} + \frac{\partial \mathcal{F}}{\partial \dot{q}_i} = Q_i \ , \tag{25.198}$$

where the coordinates q_i are X, Y, ψ and θ and Q_i are the corresponding generalized forces F_X, F_Y and the moments related to rotations ψ and θ.

The velocities in the reference frame fixed to the tractor can be considered as derivatives of pseudo-coordinates. Operating in the same way as for the isolated vehicle, and remembering that the kinetic energy does not depend on coordinates X and Y:

$$\left(\frac{\partial \mathcal{T}}{\partial X} = \frac{\partial \mathcal{T}}{\partial Y} = 0\right) \ ,$$

that the dissipation function does not depend on the linear velocities

$$\left(\frac{\partial \mathcal{F}}{\partial \dot{X}} = \frac{\partial \mathcal{F}}{\partial \dot{Y}} = 0\right)$$

and that angular velocities r and v_θ coincide with $\dot{\psi}$ and $\dot{\theta}$, the equation of motion can be written in the form (25.85), with the derivatives of the dissipation function added[11]

$$\begin{aligned} &\frac{\partial}{\partial t}\left(\left\{\frac{\partial \mathcal{T}}{\partial w}\right\}\right) + \mathbf{A^T}\left(\dot{\mathbf{A}} - \left[\mathbf{w}^T\mathbf{A}^T\frac{\partial \mathbf{A}}{\partial q_k}\right]\right)\left\{\frac{\partial \mathcal{T}}{\partial w}\right\} + \\ &-\mathbf{A}^T\left\{\frac{\partial \mathcal{T}}{\partial q_k}\right\} + \left\{\frac{\partial \mathcal{F}}{\partial w}\right\} = \mathbf{A}^T\begin{Bmatrix} F_X \\ F_Y \\ Q_\psi \\ Q_\theta \end{Bmatrix} \ . \end{aligned} \tag{25.199}$$

The terms included in the equation of motion are

[11] In this case, the equation of motion is not written in its general form, but only for the case with $\mathbf{A}^T = \mathbf{A}^{-1}$.

$$\left\{\frac{\partial \mathcal{T}}{\partial w}\right\} = \left\{\begin{array}{c} mu - m_R a_R \theta \left(r - v_\theta\right) \\ mv - m_R \left[\left(c + a_R\right) r - a_R v_\theta\right] \\ J_1 r - J_2 v_\theta - m_R a_R \theta u - m_R v \left(c + a_R\right) \\ J_3 v_\theta - J_2 r + m_R v a_R + m_R a_R \theta u \end{array}\right\}, \tag{25.200}$$

$$\frac{d}{dt}\left(\left\{\frac{\partial \mathcal{T}}{\partial w}\right\}\right) = \left\{\begin{array}{c} m\dot{u} - m_R a_R v_\theta \left(r - v_\theta\right) - m_R a_R \theta \left(\dot{r} - \dot{v}_\theta\right) \\ m\dot{v} - m_R \left[\left(c + a_R\right) \dot{r} - a_R \dot{v}_\theta\right] \\ J_1 \dot{r} - J_2 \dot{v}_\theta - m_R a_R \theta \dot{u} - m_R a_R u v_\theta - m_R \dot{v} \left(c + a_R\right) \\ J_3 \dot{v}_\theta - J_2 \dot{r} + m_R \dot{v} a_R + m_R a_R \theta \dot{u} + m_R a_R u v_\theta \end{array}\right\}, \tag{25.201}$$

$$\mathbf{A^T}\left(\dot{\mathbf{A}} - \left[\mathbf{w}^T \mathbf{A}^T \frac{\partial \mathbf{A}}{\partial q_k}\right]\right)\left\{\frac{\partial \mathcal{T}}{\partial w}\right\} =$$

$$= \left\{\begin{array}{c} -r \left\{mv - m_R \left[\left(c + a_R\right) r - a_R v_\theta\right]\right\} \\ r \left[mu - m_R a_R \theta \left(r - v_\theta\right)\right] \\ -v \left[mu - m_R a_R \theta \left(r - v_\theta\right)\right] + u \left\{mv - m_R \left[\left(c + a_R\right) r - a_R v_\theta\right]\right\} \\ 0 \end{array}\right\}, \tag{25.202}$$

$$\mathbf{A}^T \left\{\frac{\partial \mathcal{T}}{\partial q_k}\right\} = \left\{\begin{array}{c} 0 \\ 0 \\ 0 \\ -m_R a_R u \left(r - v_\theta\right) \end{array}\right\}, \tag{25.203}$$

$$\left\{\frac{\partial \mathcal{F}}{\partial w}\right\} = \left\{\begin{array}{c} 0 \\ 0 \\ 0 \\ \Gamma \dot{\theta} \end{array}\right\}, \quad \mathbf{A}^T \left\{\begin{array}{c} F_X \\ F_Y \\ Q_\psi \\ Q_\theta \end{array}\right\} = \left\{\begin{array}{c} Q_x \\ Q_y \\ Q_\psi \\ Q_\theta \end{array}\right\}. \tag{25.204}$$

The first two equations are then

$$\left\{\begin{array}{l} m\left(\dot{u} - vr\right) - m_R a_R \theta \left(\dot{r} - \dot{v}_\theta\right) - 2 m_R a_R r v_\theta + m_R a_R {v_\theta}^2 + \\ \qquad + m_R \left(c + a_R\right) r^2 = Q_x \\ \\ m\left(\dot{v} + ur\right) - m_R \left[c + a_R\right] \dot{r} + m_R a_R r \dot{v}_\theta - m_R a_R \theta r \left(r - v_\theta\right) = Q_y \,. \end{array}\right. \tag{25.205}$$

Remembering that, owing to the assumption of small angles, $V \approx u$ and also that v is small, Eqs. (25.205) may be linearized as

$$\left\{\begin{array}{l} m\dot{V} = Q_x \\ m\left(\dot{v} + Vr\right) - m_R \left(c + a_R\right) \dot{r} + m_R a_R r \ddot{\theta} = Q_y \,. \end{array}\right. \tag{25.206}$$

The third and forth equations, those for generalized coordinates ψ and θ, once linearized, are

$$\begin{cases} J_1\dot{r} - J_2\dot{v}_\theta - m_R\,(c + a_R)\,(\dot{v} + Vr) - m_R a_R \dot{V}\theta = Q_\psi \\ J_3\dot{v}_\theta - J_2\dot{r} + m_R a_R\,(\dot{v} + Vr) + m_R a_R \theta \dot{V} = Q_\theta \end{cases} \tag{25.207}$$

where the damping term $\Gamma\dot{\theta}$ is included in term Q_θ.

25.17.2 Sideslip Angles of the Wheels

The sideslip angles of the wheels of the tractor are the same as for the insulated vehicle. In a similar way, it is possible to write the sideslip angles of the wheels of the trailer.

With reference to Fig. 25.34, the coordinates of point P_i, the centre of the contact zone of the ith wheel of the trailer, are

$$\begin{cases} X_{P_i} = X - c\cos(\psi) - l_i\cos\,(\psi - \theta) - y_{R_i}\sin\,(\psi - \theta) \\ Y_{P_i} = Y - c\sin(\psi) - l_i\sin\,(\psi - \theta) + y_{R_i}\cos\,(\psi - \theta)\ . \end{cases} \tag{25.208}$$

The velocity of the same point may be obtained by differentiating the expressions of the coordinates. For the computation of the sideslip angle the velocity of point P_i must be expressed in the reference frame $G_R x_R y_R$ of the trailer

$$\begin{Bmatrix} \dot{X}_{P_i} \\ \dot{Y}_{P_i} \end{Bmatrix}_R = \begin{bmatrix} \cos\,(\psi - \theta) & \sin\,(\psi - \theta) \\ -\sin\,(\psi - \theta) & \cos\,(\psi - \theta) \end{bmatrix} \begin{Bmatrix} \dot{X}_{P_i} \\ \dot{Y}_{P_i} \end{Bmatrix}\ . \tag{25.209}$$

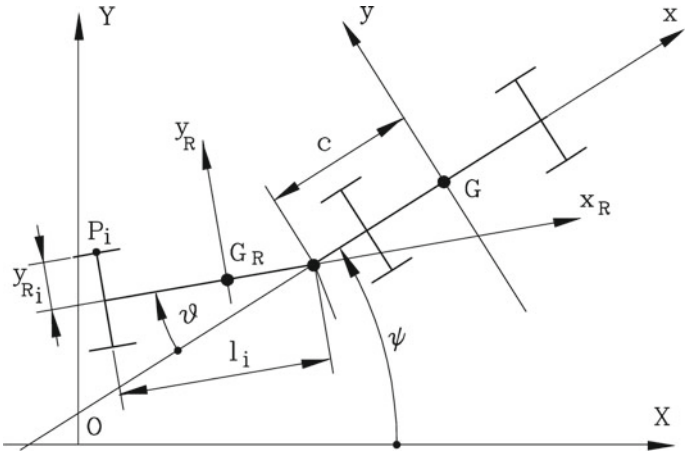

Fig. 25.34 Position of the centre P_i of the contact area of the i-th wheel of the trailer

The velocity of the centre of the contact area can thus be expressed in the reference frame of the trailer as

$$\begin{cases} \dot{V}_{x_R}(P_i) = u\cos(\theta) - v\sin(\theta) + c\dot{\psi}\sin(\theta) - y_{R_i}\left(\dot{\psi} - \dot{\theta}\right) \\ \dot{V}_{y_R}(P_i) = u\sin(\theta) + v\cos(\theta) - c\dot{\psi}\cos(\theta) - l_i\left(\dot{\psi} - \dot{\theta}\right) \end{cases}, \tag{25.210}$$

or, remembering that some of the quantities are small,

$$\begin{cases} \dot{V}_{x_R}(P_i) = V - y_{R_i}\left(\dot{\psi} - \dot{\theta}\right) \\ \dot{V}_{y_R}(P_i) = V\theta + v - c\dot{\psi} - l_i\left(\dot{\psi} - \dot{\theta}\right) \end{cases}. \tag{25.211}$$

Since the sideslip angle of a steering wheel can be obtained as the arctangent of the ratio of the y and x components of the velocity minus the steering angle δ, it follows that

$$\alpha_i = \arctan\left[\frac{V\theta + v - c\dot{\psi} - l_i\left(\dot{\psi} - \dot{\theta}\right)}{V - y_{R_i}\left(\dot{\psi} - \dot{\theta}\right)}\right] - \delta_i \ . \tag{25.212}$$

Using the monotrack vehicle model ($y_{R_i} = 0$) and remembering that the sideslip angle is small, it follows that

$$\alpha_i = \theta + \beta - \frac{r}{V}(c + l_i) + \frac{\dot{\theta}}{V}l_i - \delta_i \ . \tag{25.213}$$

The term in y_{R_i} does not enter the expression of the sideslip angle: The wheels of the same axle have the same sideslip angle, and it is also possible to work in terms of axles instead of single wheels for the trailer.

The steering angle δ_i is either 0 or, if the axle can steer, is usually not directly controlled by the driver but is linked with the variables of the motion, e.g. with angle θ. If law $\delta_i(\theta)$ is simply

$$\delta_i = -K_i'\theta \ ,$$

the expression for the sideslip angle is

$$\alpha_i = \theta(1 + K_i') + \beta - \frac{r}{V}(c + l_i) + \frac{\dot{\theta}}{V}l_i \ . \tag{25.214}$$

If some of the wheels of the trailer are free to pivot about their kingpin, an equilibrium equation for the relevant parts of the steering system of those axles must be written, similar to the procedure for the study of motion with free controls.

25.17.3 Generalized Forces

The contributions to the generalized forces Q_x, Q_y and Q_ψ due to the tractor are the same as those of the insulated vehicle. The tractor does not give any contribution to force Q_θ. To compute the contributions due to the ith wheel of the trailer and the aerodynamic forces of the latter, the easiest method is to write their virtual work $\delta\mathcal{L}$ due to a virtual displacement

$$\{\delta s\} = [\delta x, \delta y, \delta\psi, \delta\theta]^T \ .$$

Using the assumption of small angles, it follows that

$$\begin{cases} \delta x_R(P_i) = \delta x - \theta\delta y + c\theta\delta\psi - y_{R_i}\,(\delta\psi - \delta\theta) \\ \delta y_R(P_i) = \theta\delta x + \delta y - c\delta\psi - l_i\,(\delta\psi - \delta\theta) \ . \end{cases} \tag{25.215}$$

If the ith wheel has a steering angle δ_i, the forces it exerts in the reference frame $G_R x_R y_R z_R$, the same in which the virtual displacement has been written, are simply

$$\begin{aligned} F_{x_{i_R}} &= F_{x_{i_p}}\cos(\delta_i) - F_{y_{i_p}}\sin(\delta_i) \approx F_{x_{i_p}} - F_{y_{i_p}}\delta_i, \\ F_{y_{i_R}} &= F_{x_{i_p}}\sin(\delta_i) + F_{y_{i_p}}\cos(\delta_i) \approx F_{x_{i_p}}\delta_i + F_{y_{i_p}}, \end{aligned} \tag{25.216}$$

where $F_{x_{i_p}}$ and $F_{y_{i_p}}$ are the forces in the reference frame of the tire.

The virtual work can be computed by multiplying the forces and moments (the aligning torque M_{z_i}) by the corresponding virtual displacement (for the moment, rotation $\delta\psi - \delta\theta$)

$$\begin{aligned} \delta\mathcal{L} = &\left[F_{x_{i_p}} + F_{y_{i_p}}(\theta - \delta_i)\right]\delta x + \left[-F_{x_{i_p}}(\theta - \delta_i) + F_{y_{i_p}}\right]\delta y + \\ &+ \left\{F_{x_{i_p}}\left[c(\theta - \delta_i) - y_{R_i} - l_i\delta_i\right] + F_{y_{i_p}}\left(-c + y_{R_i}\delta_i - l_i\right) + M_{z_i}\right\}\delta\psi + \\ &+ \left\{F_{x_{i_p}}\left(y_{R_i} + l_i\delta_i\right) + F_{y_{i_p}}\left(-y_{R_i}\delta_i + l_i\right) - M_{z_i}\right\}\delta\theta. \end{aligned} \tag{25.217}$$

The generalized forces due to the ith wheel of the trailer can be obtained by differentiating the virtual work $\delta\mathcal{L}$ with respect to the virtual displacements δx, δy, $\delta\psi$ and $\delta\theta$:

$$\begin{cases} Q_{x_i} = \dfrac{\partial\delta\mathcal{L}}{\partial\delta x} = F_{x_{i_p}} + F_{y_{i_p}}(\theta - \delta_i) \\ Q_{y_i} = \dfrac{\partial\delta\mathcal{L}}{\partial\delta y} = -F_{x_{i_p}}(\theta - \delta_i) + F_{y_{i_p}} \\ Q_{\psi_i} = \dfrac{\partial\delta\mathcal{L}}{\partial\delta\psi} = F_{x_{i_p}}\left[c(\theta - \delta_i) - y_{R_i} - l_i\delta_i\right] + F_{y_{i_p}}\left(-c + y_{R_i}\delta_i - l_i\right) + M_{z_i} \\ Q_{\theta_i} = \dfrac{\partial\delta\mathcal{L}}{\partial\delta\theta} = F_{x_{i_p}}\left(y_{R_i} + l_i\delta_i\right) + F_{y_{i_p}}\left(-y_{R_i}\delta_i + l_i\right) - M_{z_i} \ . \end{cases} \tag{25.218}$$

In a similar way, the generalized forces resulting from the aerodynamic forces and moments acting on the trailer can be accounted for. It is usually difficult to distinguish between the forces acting on the tractor and those acting on the trailer, as what is measured in the wind tunnel are the forces acting on the whole vehicle. In the following equations, it will be assumed that the forces acting on the tractor are measured separately from those acting on the trailer, and that they are applied at the centre of mass of the relevant rigid body and decomposed along the axes fixed to it. The forces acting on the trailer are so decomposed along axes $x_R y_R z_R$.

The generalized forces due to aerodynamic forces acting on the tractor contribute to Q_x, Q_y and Q_ψ just as they do for the insulated vehicle, while the expression of the generalized aerodynamic forces applied on the trailer can be obtained from Eqs. (25.218), by substituting $F_{x_{R_{aer}}}$, $F_{y_{R_{aer}}}$, $M_{z_{R_{aer}}}$ and a_R to $F_{x_{i_p}}$, $F_{y_{i_p}}$, M_{z_i} and l_i and by setting both y_{R_i} and δ_i to zero.

The external force $F_{y_{e_R}}$ acting on the centre of mass or the trailer and the component of the weight $m_R g \sin(\alpha)$ due to a longitudinal grade α of the road will be assumed to act in the directions of axes x and y of the tractor; consequently the relevant equations must be modified accordingly.

25.17.4 Linearized Expressions of the Forces

The linearized expressions of the generalized forces Q_x, Q_y, Q_ψ and Q_θ can be obtained with the methods used for the isolated vehicle. Linearization can be performed by introducing the cornering and aligning stiffnesses C_i and $(M_{z_i})_{,\alpha}$ of the axles (subscript i refers now to the ith axle and not to the ith wheel). In the same way, the derivatives of the aerodynamic coefficients $(C_y)_{,\beta}$, etc. can also be introduced.

A simple expression for Q_x is thus obtained:

$$\begin{aligned} Q_x = X_m - \left(f_0 + K V^2\right)\left[mg\cos(\alpha) - \tfrac{1}{2}\rho V^2\left(SC_z + S_R C_{z_R}\right)\right] + \\ -\tfrac{1}{2}\rho V^2\left(SC_x + S_R C_{x_R}\right) - mg\sin(\alpha), \end{aligned} \tag{25.219}$$

where, as usual, X_m is the driving force of the driving axle, but may also be the total braking force.

By substituting the sideslip angle β of the vehicle for ratio v/V, the expressions of the forces appearing in the handling equations are

$$\begin{cases} Q_y = (Q_y)_{,\beta}\beta + (Q_y)_{,r} r + (Q_y)_{,\dot\theta}\dot\theta + (Q_y)_{,\theta}\theta + (Q_y)_{,\delta}\delta + F_{y_e} + F_{y_{e_R}} \\ Q_\psi = (Q_\psi)_{,\beta}\beta + (Q_\psi)_{,r} r + (Q_\psi)_{,\dot\theta}\dot\theta + (Q_\psi)_{,\theta}\theta + (Q_\psi)_{,\delta}\delta + M_{z_e} + \\ \quad + M_{z_{e_R}} - (c + a_R) F_{y_{e_R}} \\ Q_\theta = (Q_\theta)_{,\beta}\beta + (Q_\theta)_{,r} r + (Q_\theta)_{,\dot\theta}\dot\theta + (Q_\theta)_{,\theta}\theta - M_{z_{e_R}} + a_R F_{y_{e_R}} \end{cases}. \tag{25.220}$$

The derivatives of stability entering the expression for Q_y are

$$\begin{cases} (Q_y)_{,\beta} = Y_\beta - \sum_{\forall i_R} C_i + \frac{1}{2}\rho V_r^2 S_R (C_{Y_R})_{,\beta} \\ (Q_y)_{,r} = Y_r + \frac{1}{V}\left[\sum_{\forall i_R}(c+l_i)C_i + \frac{1}{2}\rho V_r^2 S_R (c+a_R)(C_{Y_R})_{,\beta}\right] \\ (Q_y)_{,\dot\theta} = -\frac{1}{V}\left[\sum_{\forall i_R} l_i C_i - \frac{1}{2}\rho V_r^2 S_R a_R (C_{Y_R})_{,\beta}\right] \\ (Q_y)_{,\theta} = -\sum_{\forall i_R} C_i + \frac{1}{2}\rho V_r^2 S_R (C_{Y_R})_{,\beta} \\ (Q_y)_{,\delta} = Y_\delta \,, \end{cases} \tag{25.221}$$

where Y_β, Y_r and Y_δ are the derivatives of stability of the tractor expressed by Eqs. (25.103).

The derivatives of stability entering the expression for Q_ψ and Q_θ are respectively

$$\begin{cases} (Q_\psi)_{,\beta} = N_\beta + \sum_{\forall i_R} C_1 + (c+l_i)C_i + (M_{z_i})_{,\alpha} \\ (Q_\psi)_{,r} = N_r - \frac{1}{V}\left[\sum_{\forall i_R}(c+l_i)^2 C_i + (c+l_i)(M_{z_i})_{,\alpha} + (c+a_R)C_{a1}\right] \\ (Q_\psi)_{,\dot\theta} = \frac{1}{V}\left[\sum_{\forall i_R} l_i(c+l_i)C_i + l_i(M_{z_i})_{,\alpha} + a_R C_{a1}\right] \\ (Q_\psi)_{,\theta} = \sum_{\forall i_R}(c+l_i)C_i + (M_{z_i})_{,\alpha} + C_{a1} \\ (Q_\psi)_{,\delta} = N_\delta \,, \end{cases} \tag{25.222}$$

$$\begin{cases} (Q_\theta)_{,\beta} = \sum_{\forall i_R} C_2 - l_i C_i - (M_{z_i})_{,\alpha} \\ (Q_\theta)_{,r} = \frac{1}{V}\left[\sum_{\forall i_R}(c+l_i)l_i C_i + (c+l_i)(M_{z_i})_{,\alpha} + (c+a_R)C_{a2}\right] \\ (Q_\theta)_{,\dot\theta} = -\frac{1}{V}\left[\sum_{\forall i_R} l_i^2 C_i + l_i(M_{z_i})_{,\alpha} + a_R C_{a2}\right] - \Gamma \\ (Q_\theta)_{,\theta} = (Q_\theta)_{,\beta} \\ (Q_\theta)_{,\delta} = 0 \,, \end{cases} \tag{25.223}$$

where aerodynamic terms C_{a1} and C_{a2} are:

$$C_{a1} = \frac{1}{2}\rho V_r^2 S_R \left[l_R (C_{N_R})_{,\beta} - (c + a_R)(C_{Y_R})_{,\beta} \right] ,$$

$$C_{a2} = \frac{1}{2}\rho V_r^2 S_R \left[l_R (C_{N_R})_{,\beta} - a_R (C_{Y_R})_{,\beta} \right] .$$

N_β, N_r and N_δ are the derivatives of stability of the tractor expressed by Eqs. (25.107). All axles of the trailer have been assumed as non-steering.

If the axles of the trailer can steer and their steering angles δ_i are linked with angle θ by the law

$$\delta_i = -K_i' \theta ,$$

the expressions of the derivatives of stability reported above still hold, except for $(Q_y)_{,\theta}$, $(Q_\psi)_{,\theta}$ and $(Q_\theta)_{,\theta}$ in which all terms in C_i and $(M_{z_i})_{,\alpha}$ must be multiplied by $(1 + K_i')$.

25.17.5 Final Expression of the Equations of Motion

As with the equations of the insulated vehicle, the linearization of the equations allows the longitudinal behavior (first equation of motion) to be uncoupled from the lateral, or handling behavior, which can be studied using only the three remaining equations. This occurs if the law $u(t)$, which can be confused with $V(t)$, is considered as a stated law, while the unknowns are the driving or braking forces F_x for the longitudinal behavior and β, r and θ for handling.

The linearized equation for the longitudinal behavior

$$m\dot{V} = Q_x \tag{25.224}$$

can thus be studied separately.

The linearized equations for the lateral behavior of the articulated vehicle can be expressed in the space of the configurations as

$$\mathbf{M}\ddot{\mathbf{x}} + \mathbf{C}\dot{\mathbf{x}} + \mathbf{K}\mathbf{x} = \mathbf{F} , \tag{25.225}$$

where the vectors of the generalized coordinates and of the forces are

$$\mathbf{x} = \begin{Bmatrix} y \\ \psi \\ \theta \end{Bmatrix} , \qquad \mathbf{F} = \begin{Bmatrix} (Q_y)_{,\delta}\delta + F_{y_e} + F_{y_{e_R}} \\ (Q_\psi)_{,\delta}\delta + M_{z_e} + M_{z_{e_R}} - (c + a_R) F_{y_{e_R}} \\ -M_{z_{e_R}} + a_R F_{y_{e_R}} \end{Bmatrix} \tag{25.226}$$

and the matrices are

$$\mathbf{M} = \begin{bmatrix} m & -m_R(c+a_R) & m_R a_R \\ -m_R(c+a_R) & J_1 & -J_2 \\ m_R a_R & -J_2 & J_3 \end{bmatrix},$$

$$\mathbf{C} = \begin{bmatrix} -\dfrac{(Q_y)_{,\beta}}{V} & mV - (Q_y)_{,r} & -(Q_y)_{,\dot{\theta}} \\ -\dfrac{(Q_\psi)_{,\beta}}{V} & -m_R V(c+a_R) - (Q_\psi)_{,r} & -(Q_\psi)_{,\dot{\theta}} \\ -\dfrac{(Q_\theta)_{,\beta}}{V} & m_R V a_R - (Q_\theta)_{,r} & -(Q_\theta)_{,\dot{\theta}} \end{bmatrix}, \tag{25.227}$$

$$\mathbf{K} = \begin{bmatrix} 0 & 0 & -(Q_y)_{,\theta} \\ 0 & 0 & -(Q_\psi)_{,\theta} \\ 0 & 0 & -(Q_\theta)_{,\theta} \end{bmatrix}.$$

The set of differential equations (25.225) is actually of the fourth order and not of the sixth, since variables y[12] and ψ appear in the equation only as first and second derivatives (the first two columns of matrix $\mathbf{K}$ vanish). The equation can thus be written in the state space in the form of a set of four first-order differential equations by introducing a fourth state variable $v_\theta = \dot{\theta}$,

$$\dot{\mathbf{z}} = \mathbf{A}\mathbf{z} + \mathbf{B}_c\mathbf{u}_c + \mathbf{B}_e\mathbf{u}_e \,.$$

The state vector $\mathbf{z}$ is simply

$$\mathbf{z} = \begin{bmatrix} \beta & r & v_\theta & \theta \end{bmatrix}^T \,,$$

the dynamic matrix is

$$\mathbf{A} = \begin{bmatrix} -\mathbf{M}^{-1}\mathbf{C} & \mathbf{M}^{-1} \begin{Bmatrix} (Q_y)_{,\theta} \\ (Q_\psi)_{,\theta} \\ (Q_\theta)_{,\theta} \end{Bmatrix} \\ \begin{bmatrix} 0 & 0 & 1 \end{bmatrix} & 0 \end{bmatrix},$$

the input gain matrices are

[12] Actually, as already stated, v is the derivative of a pseudo-coordinate and thus y has no physical meaning. It has been introduced into the equations only for completeness and, since it is always multiplied by 0, its presence can be accepted.

$$\mathbf{B}_c = \begin{bmatrix} \mathbf{M}^{-1} \begin{bmatrix} (Q_y)_{,\delta} \\ (Q_\psi)_{,\delta} \\ 0 \end{bmatrix} \\ 0 \end{bmatrix} ,$$

$$\mathbf{B}_e = \begin{bmatrix} \mathbf{M}^{-1} \begin{bmatrix} 1 & 1 & 0 & 0 \\ 0 & -(c+a_R) & 1 & 1 \\ 0 & a_R & 0 & -1 \end{bmatrix} \\ \begin{bmatrix} 0\,0\,0\,0 \end{bmatrix} \end{bmatrix} ,$$

and the input vector is

$$\mathbf{u}_c = \delta \, . \quad \mathbf{u}_e = \begin{bmatrix} F_{y_e} & F_{y_{e_R}} & M_{z_e} & M_{z_{e_R}} \end{bmatrix}^T \, .$$

25.17.6 Steady-State Motion

To study the steady-state behavior of the vehicle, Eq. (25.225) can be used, along with the assumption that $\dot{v} = \dot{r} = \dot{\theta} = \ddot{\theta} = 0$. The following equation is thus obtained:

$$\begin{bmatrix} -(Q_y)_{,\beta} & mV - (Q_y)_{,r} & -(Q_y)_{,\theta} \\ -(Q_\psi)_{,\beta} & -m_R V(c+a_R) - (Q_\psi)_{,r} & -(Q_\psi)_{,\theta} \\ -(Q_\theta)_{,\beta} & m_R V a_R - (Q_\theta)_{,r} & -(Q_\theta)_{,\theta} \end{bmatrix} \begin{Bmatrix} \beta \\ r \\ \theta \end{Bmatrix} = \\ = \begin{Bmatrix} (Q_y)_{,\delta}\delta + F_{y_e} + F_{y_{e_R}} \\ (Q_\psi)_{,\delta}\delta + M_{z_e} + M_{z_{e_R}} - (c+a_R)F_{y_{e_R}} \\ -M_{z_{e_R}} + a_R F_{y_{e_R}} \end{Bmatrix} . \tag{25.228}$$

There is no difficulty in solving such a set of equations. For instance, after stating that $\delta = 1$ and setting all other inputs to zero, the gains $1/R\delta$, β/δ etc. can be computed.

A particularly simple solution is obtained for a two-axle vehicle with a one-axle trailer if only the cornering forces of the wheels are accounted for

$$\begin{cases} \dfrac{1}{R\delta} = \dfrac{1}{l} \dfrac{1}{1+KV^2} \\ \dfrac{\theta}{\delta} = \dfrac{a+c+K'V^2}{l(1+KV^2)} \end{cases} , \tag{25.229}$$

where the stability factor K and K' are

$$\begin{cases} K = \dfrac{1}{l^2}\left[\left(m_T + m_R\dfrac{l_R - a_R}{l_R}\right)\left(\dfrac{b}{C_1} - \dfrac{a}{C_2}\right) + \right. \\ \qquad \left. - m_R\dfrac{c(l_R - a_R)}{l_R}\left(\dfrac{1}{C_1} + \dfrac{1}{C_2}\right)\right] \\ K' = \dfrac{1}{l}\left\{m\dfrac{a}{C_2} + \dfrac{m_R}{l_R}\left[\dfrac{(a+c)(l_R - a_R)}{C_2} - \dfrac{l_R a_R}{C_1}\right]\right\} . \end{cases} \tag{25.230}$$

The same definitions used for the insulated vehicle also hold in this case and, if the derivatives of stability are constant or proportional to $1/V$, the sign of the stability factor allows one to state immediately whether the vehicle is oversteer, neutral-steer or understeer.

The simplified expression of the stability factor (25.230) is composed of two terms: The first usually has the same sign of $bC_1 - aC_2$, i.e. of the factor that decides the behavior of the tractor alone. The second term is negative, unless the product $c(l_R - a_R)$ is negative, i.e. the centre of mass of the trailer is behind its axle.

If

$$c(l_R - a_R) > 0 ,$$

the trailer increases the understeering character of the vehicle, more so if the hinge is far from the centre of mass of the tractor and the centre of mass of the trailer is close to the hinge. In the case of trailers with a single axle, like caravans, this effect can be reduced by reducing the distance between its centre of mass and the axle.

If the centre of mass is exactly on the axle, that is, if

$$l_R - a_R = 0 ,$$

the trailer has no effect on the steady state behavior of the tractor; it does, however, affect its dynamic behavior and stability.

If the centre of mass of the trailer is behind its axle,

$$l_R - a_R < 0 ,$$

the trailer increases the oversteer behavior of the tractor. If the vehicle is oversteer, the presence of a critical speed can be expected.

Remark 25.18 This way of comparing the behavior of the tractor alone with that of the complete vehicle is not correct however: The presence of the trailer can change the loads on the wheels of the former, thus affecting their cornering stiffness.

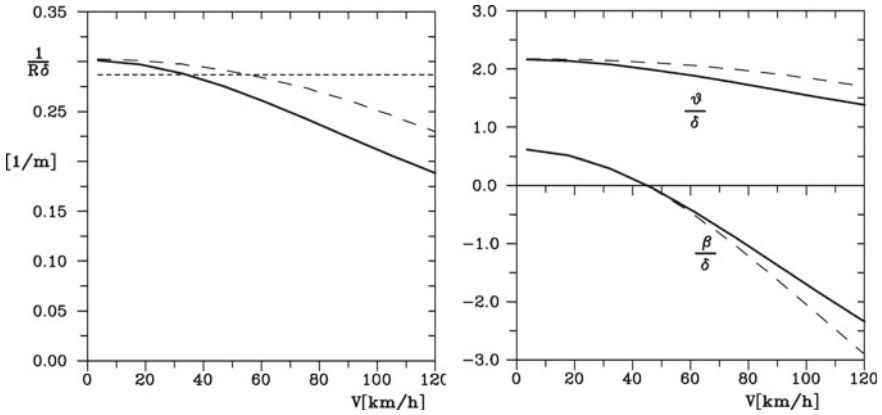

Fig. 25.35 Example 25.12: Path curvature gain, sideslip angle gain and trailer angle gain as functions of the speed. Full lines: Values obtained from the complete expressions of the derivatives of stability; dashed lines: Simplified approach obtained considering only the cornering forces

Example 25.12 Study the steady state directional behavior of the articulated truck of Appendix E.10. Compare the results obtained using the complete expressions of the derivatives of stability with those computed considering only the cornering forces of the tires.

The computation is straightforward. At each value of the speed the normal forces on the ground must be computed, although they change little with the speed. The cornering stiffness and the aligning stiffness of the axles are readily obtained from the normal forces.

At 100 km/h, for instance, the normal forces on the axles are 57.25, 107.28, 79.83, 83.56 and 56.14 kN, yielding the following values for the cornering stiffness and the aligning stiffness: 422.05, 806.64, 641.34, 665.89, 416.42 kN/rad and 22.724, 41.472, 26.102, 28.175, 22.116 kNm/rad.

The path curvature gain, the sideslip angle gain and the trailer angle gain θ/δ are plotted as functions of the speed in Fig. 25.35. The values obtained from the complete expressions of the derivatives of stability are shown as full lines while the dashed lines refer to the simplified expressions for the derivatives of stability obtained by considering only the cornering forces.

When the speed tends to zero, the path curvature gain does not tend to the kinematic value $1/l$ of the tractor: The trailer has a number of axles greater than 1 and correct kinematic steering is impossible. The vehicle is understeer, even if weakly.

The simplified approach allows one to obtain a fair approximation of the directional behavior of the vehicle, the differences between the two results being due mostly to the aligning torques of the tires and only marginally to aerodynamic forces and moments.

25.17.7 Stability and Nonstationary Motion

The study of the stability in the small, i.e., for small changes of the state of the system around the equilibrium conditions, may be performed by computing the eigenvalues of the dynamic matrix. The plot of the eigenvalues (their real and imaginary parts) as functions of the speed and the plot of the roots locus give a picture of the stability of the system that can be easily interpreted.

The eigenvalues of the system are four; two of these are usually complex conjugate showing an oscillatory behavior; the corresponding eigenvector shows that the motion of the trailer is primarily involved. These oscillations are usually lightly damped, and can become, mainly at high speed, self excited leading to a global instability of the vehicle.

Remark 25.19 The presence of an eigenvalue with positive real part, and hence of an instability in the mathematical sense, is felt by the driver as a source of discomfort rather than an actual instability. If the values of both the imaginary and the real parts of the eigenvalue are small enough, i.e., if the frequency is low and the amplitude grows slowly, the driver is forced to introduce continuous steering corrections without actually recognizing the instability of the vehicle.

The introduction of a damper at the trailer-tractor connection can solve this problem, while the use of steering axles on the trailer makes things worse. A steering axle, controlled so that the wheels steer in the direction opposite to those of the tractor with a magnitude proportional to angle θ, provides a restoring force to keep the trailer aligned with the tractor. The effect is similar to that of increasing the stiffness of a system: If the damping is not increased the underdamped character is magnified, while the natural frequency is also increased.

For the study of motion in nonstationary conditions, the considerations already seen for the insulated vehicle still hold. The more complicated nature of the equations of motion, however, compels us to resort to numerical integration in a larger number of cases.

Example 25.13 Study the stability with locked controls of the articulated truck of Appendix E.10.

The plot of the real and imaginary parts of s and the roots locus are shown in Fig. 25.36.

The figure has been obtained using the complete expressions of the derivatives of stability, but neglecting the effect of driving forces. At 100 km/h the eigenvalues are

$$-2.3364 \pm 1.5896i \ , \ -2.2698 \pm 3.4037i;$$

the corresponding eigenvectors are

$$\begin{Bmatrix} -0.8723 \pm 0.4849i \\ 0.0305 \pm 0.0424i \\ -0.0037 \mp 0.0346i \\ 0.0058 \pm 0.0109i \end{Bmatrix}, \quad \begin{Bmatrix} -0.6448 \mp 0.6533i \\ -0.0521 \pm 0.0862i \\ -0.1322 \pm 0.3429i \\ 0.0518 \mp 0.0734i \end{Bmatrix}.$$

The vehicle has a strong oscillatory behavior, even if both modes are well damped and no dynamic instability occurs; both modes involve the tractor as well as the trailer.

Example 25.14 Study the directional response and the stability with locked controls of the car of Appendix E.5 with a caravan with a single axle. Assume the following data for the caravan: Mass $m_R = 600$ kg, moment of inertia $J_R = 800$ kg m^2, $c = 2.87$ m, $a_R = l_3 = 2.5$ m, $h_R = 1$ m, $S_R = 2.5$ m^2; $(C_{Y_R})_{,\beta} = -1.5$, $(C_{N_R})_{,\beta} = -0.6$. Assume that the trailer has the same tires as used on the tractor.

The path curvature gain, sideslip angle gain and trailer angle gain are plotted against the speed in Fig. 25.37. Both the complete and simplified expressions of the derivatives of stability have been used, while the effect of driving forces has been neglected.

Note that the curve obtained from the simplified expressions of the derivatives of stability is completely superimposed on that describing the behavior of the insulated vehicle, as was predictable since $a_R = l_3$. Note also that the path curvature gain tends to the kinematic value for a speed tending to zero, since the trailer has a single axle and correct kinematic steering is possible.

The plot of the real and imaginary parts of s and the roots locus are reported in Fig. 25.38a, b. Here only the complete expressions of the derivatives of stability have been used. The vehicle is stable, but the absolute value of the real part of the Laplace

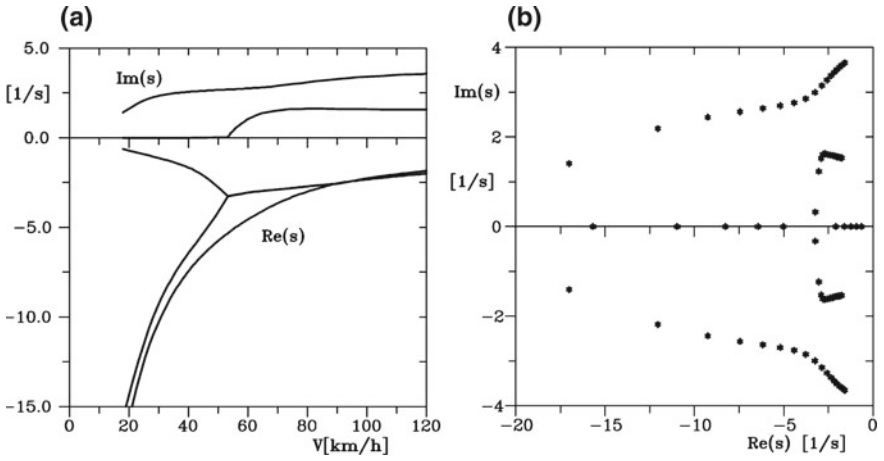

Fig. 25.36 Example 25.13: Study of the stability. **a** Real and imaginary parts of s as functions of the speed. **b** Roots locus at varying speed. Complete expressions of the derivatives of stability, with the effect of driving forces neglected

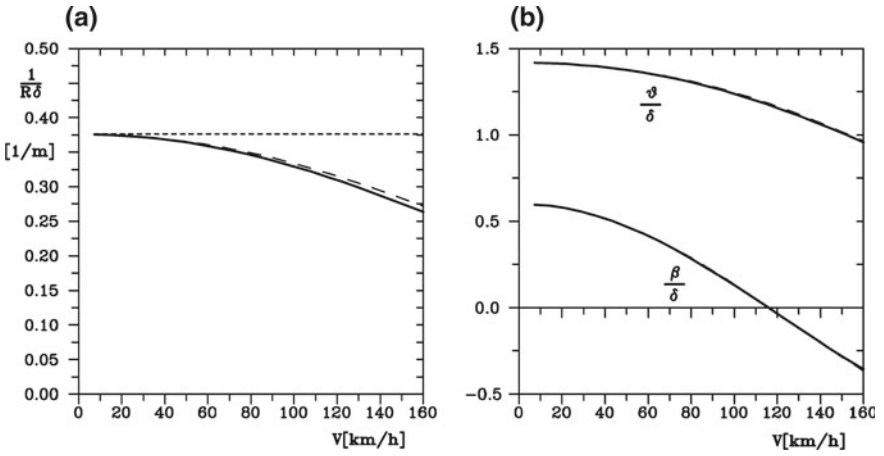

Fig. 25.37 Example 25.14: Path curvature gain, sideslip angle gain and trailer angle gain as functions of speed. Full lines: Values obtained from the complete expressions of the derivatives of stability; dashed lines: Simplified approach obtained considering only the cornering forces

variable s is quite low at high speed, denoting a strong and little damped oscillatory motion, which occurs at low frequency.

To compare the behavior of the vehicle with and without trailer the computation has been repeated without the latter and the results are shown in Fig. 25.38c, d.

The comparison shows that the modes affecting primarily the vehicle are fairly uncoupled from those primarily affecting the trailer, although a correct analysis of such coupling demands a through analysis of the eigenvectors.

The trailer mode with low frequency and low dynamic stability is superimposed on the more stable tractor mode, which is not strongly affected by the presence of the trailer. The motion of the tractor in the trailer mode can also be quite large, as this mode affects the whole system.

Example 25.15 Study the stability with locked controls of the car of Appendix E.2 with the caravan of Example 25.14. Assume that the tires of the caravan are the same as those used on the tractor. Then study the motion with locked controls of the same vehicle following a step steering input at 80 and 140 km/h. Assume that the value of the steering angle is that needed to obtain a circular path with a radius of 200 m, computed neglecting the presence of the trailer.

The plot of the real and imaginary parts of s and the roots locus computed using the complete expressions of the derivatives of stability are shown in Fig. 25.40a, b. The vehicle is stable only up to a speed of about 120 km/h, where the real part of the Laplace variable s related to one of the two modes vanishes, to become positive at higher speed.

The absolute value of the real part of s is always quite low, denoting a marginal dynamic stability at low speed and a marginal instability at higher speed.

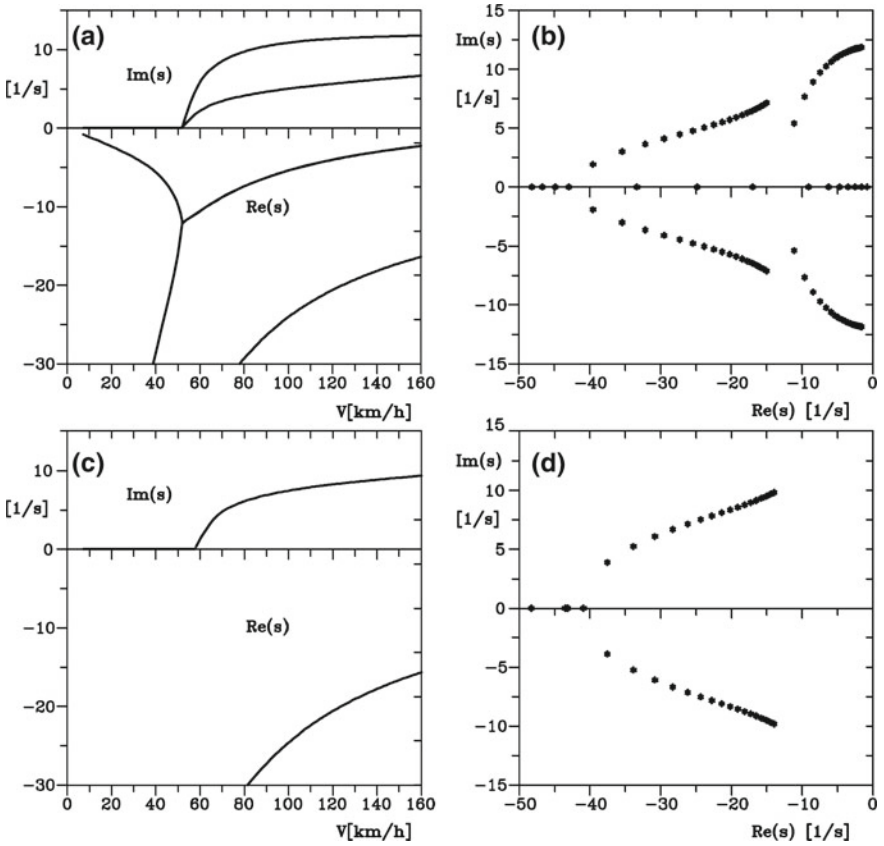

Fig. 25.38 Example 25.14: Study of the stability. **a** Real and imaginary parts of s as functions of the speed. **b** Roots locus at varying speed. **c**, **d** Same as (**a**), (**b**) but for the vehicle without trailer. Complete expressions of the derivatives of stability, with the effect of driving forces neglected

This type of behavior is quite evident in the response to a step steering input. The steering angle needed to obtain a radius of the path of 200 m is 0.9659° at 80 km/h and 1.7271° at 140 km/h. The integration of the equation of motion was performed numerically. At 80 km/h the response is stable but the step input excites a strong, slowly damped, oscillatory behavior (Fig. 25.40a).

The strong oscillatory behavior is primarily due to the trailer, and the time history showing more pronounced oscillations is that of the trailer angle θ. After 6 s the values of $r/V\delta$, $\beta\delta$ and $\theta\delta$ are almost stabilized at the values of 0.3018, −0.4056 and 0.3098 that characterize the steady state behavior (the former two are almost the same as those obtained for the vehicle without trailer, except for a small difference due to the difference in aerodynamic drag, which influences the loads on the road and hence the cornering stiffness). The path is, however, not oscillatory.

At 140 km/h the vehicle is unstable and the oscillations of r, β and θ quickly diverge. The path reported in Fig. 25.39b, however, is not strongly oscillatory.

This example is a limiting case since the trailer is not correctly matched to the vehicle, nor are the tires correct for the trailer; it has been shown as an example of unstable behavior occurring in an incorrectly designed vehicle with trailer.

Note that a step input is prone to excite strongly an unstable behavior and is the worst thing to do with a marginally stable vehicle. The oscillations have a low frequency, and it is possible that the driver may be able to stabilize the vehicle even

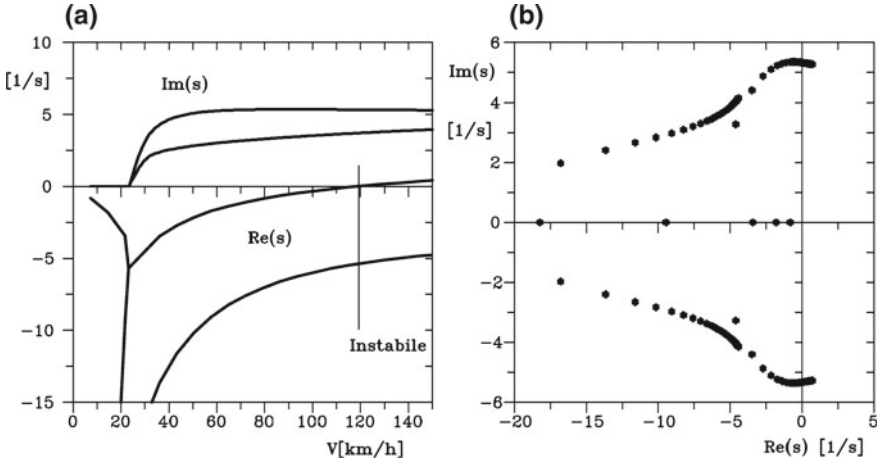

Fig. 25.39 Example 25.15: Response to a step steering input. **a** Time histories of the yaw velocity, sideslip angle β and trailer angle θ at 80 km/h and **b** path at 80 and 140 km/h

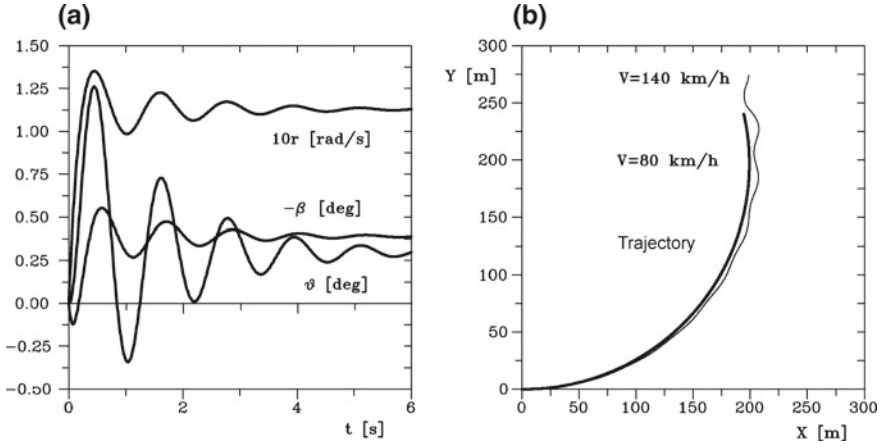

Fig. 25.40 Example 25.15: Study of the stability. **a** Real and imaginary parts of s as functions of speed. **b** Roots locus at varying speed. Note the instability threshold at about 120 km/h. Complete expressions of the derivatives of stability, with the effect of driving forces neglected

at speeds at which the real part of s is positive: A test driver would probably find the handling and comfort of the vehicle poor rather than seeing the vehicle as unstable, owing to the need for continuous steering corrections.

On the other hand, it is possible that a vehicle with a low negative real part of s becomes unstable because of the action of the driver. Ultimately, the stability of the vehicle-driver system is what counts, but intrinsic stability of the vehicle is necessary, so that the driver is not forced to stabilize a system that is itself unstable.

25.18 Multibody Articulated Vehicles

25.18.1 Equations of Motion

Consider a vehicle with a trailer with two axles, one connected to its body, the other connected to the draw bar (Fig. 25.41a). Its dynamic behavior may be studied using the same kind of model seen in the previous section, where the trailer is modelled as two simple trailers connected in sequence. The model has five degrees of freedom, and the five generalized coordinates may be X Y, ψ, θ_1 and θ_2. The first two coordinates can be substituted by displacements x and y referred to the frame of the tractor and the first equation for longitudinal motion may be decoupled from the others, if the equations of motion are linearized. The transversal behavior can be studied using a set of four differential equations that can be linearized under the usual conditions, yielding a set of linear differential equations whose order is 6.

This procedure can be generalized to a generic multibody vehicle made of a tractor and a set of n trailers (Fig. 25.41b). Note that while in Europe no vehicle with multiple trailers is legal for road use, in America and Australia such vehicles are legal but subject to restrictions. The model here described, leading to a set of $n + 3$ differential equations ($n + 2$ for the lateral behavior if the first equation is uncoupled), allows one to study the behavior of any vehicle of this type.

With reference to Fig. 25.41b, the position of the centre of mass of the ith trailer is

$$\left(\overline{\mathrm{G}_i - \mathrm{O}}\right) = \left\{ \begin{array}{l} X - c\cos(\psi) - \displaystyle\sum_{k=1}^{i-1} l_k \cos(\psi - \theta_k) - a_i \cos(\psi - \theta_i) \\ Y - c\sin(\psi) - \displaystyle\sum_{k=1}^{i-1} l_k \sin(\psi - \theta_k) - a_i \sin(\psi - \theta_i) \end{array} \right\} . \quad (25.231)$$

The velocity of point G_i is

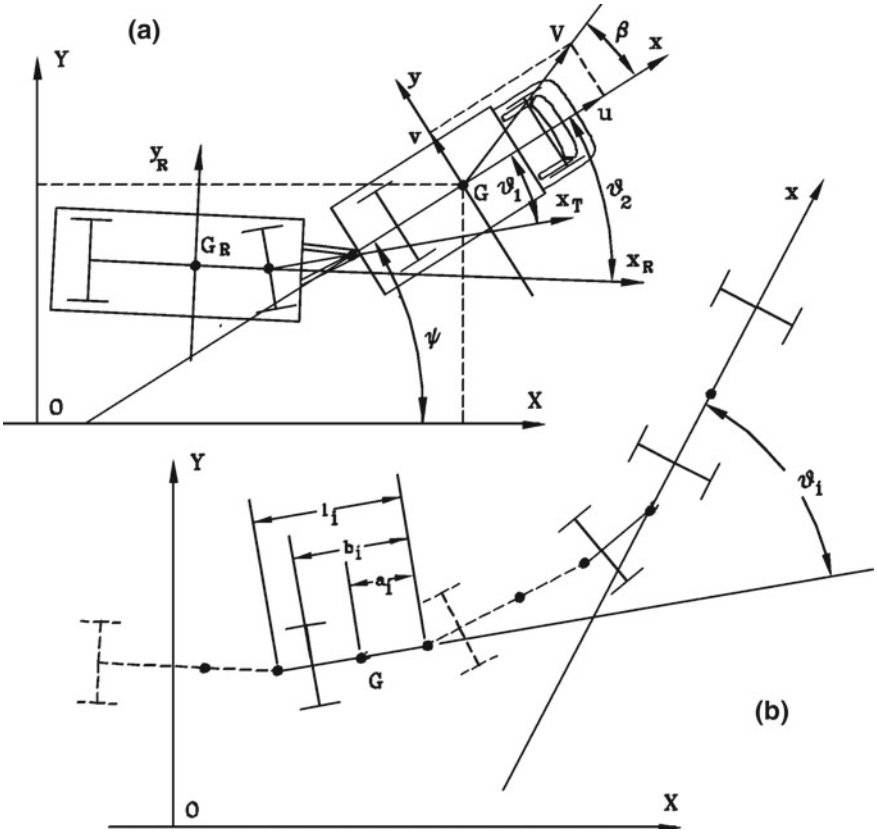

Fig. 25.41 **a** Vehicle with a trailer with two axles. **b** model of a multibody articulated vehicle; parameters for the i-th trailer

$$V_{G_i} = \left\{ \begin{array}{l} \dot{X} + \dot{\psi} c \sin(\psi) + \sum_{k=1}^{i-1} \left(\dot{\psi} - \dot{\theta}_k\right) l_k \sin(\psi - \theta_k) + \left(\dot{\psi} - \dot{\theta}_i\right) a_i \sin(\psi - \theta_i) \\ \dot{Y} - \dot{\psi} c \cos(\psi) - \sum_{k=1}^{i-1} \left(\dot{\psi} - \dot{\theta}_k\right) l_k \cos(\psi - \theta_k) - \left(\dot{\psi} - \dot{\theta}_i\right) a_i \cos(\psi - \theta_i) \end{array} \right\} . \tag{25.232}$$

The contribution to the kinetic energy due to the ith trailer with mass m_i and moment of inertia J_i about a baricentric axis parallel to the z-axis is then

$$\mathcal{T}_i = \frac{1}{2} m_i V_i^2 + \frac{1}{2} J_i \left(\dot{\psi} - \dot{\theta}_i\right)^2 , \tag{25.233}$$

i.e.,

$$\begin{aligned}\mathcal{T}_i = \tfrac{1}{2}m\Big[\dot{x}'^2 + \dot{y}'^2 - 2\left(\dot{X}\alpha_i + \dot{Y}\beta_i\right)\cos(\psi) + \\ +2\left(\dot{X}\beta_i - \dot{Y}\alpha_i\right)\sin(\psi)\Big] + \tfrac{1}{2}J_i\left(\dot{\psi} - \dot{\theta}_i\right)^2 ,\end{aligned} \tag{25.234}$$

where

$$\alpha_i = \sum_{j=1}^{i} l_{ij}\left(\dot{\psi} - \dot{\theta}_j\right)\sin(\theta_j) ,$$

$$\beta_i = c\dot{\psi} + \sum_{j=1}^{i} l_{ij}\left(\dot{\psi} - \dot{\theta}_j\right)\cos(\theta_j),$$

and constants l_{ij} are the elements of the matrix

$$\mathbf{l} = \begin{bmatrix} a_1 & 0 & 0 & 0 \\ l_1 & a_2 & 0 & 0 \\ l_1 & l_2 & a_3 & 0 \\ \cdots & \cdots & \cdots & \cdots \\ l_1 & l_2 & l_3 & a_n \end{bmatrix} .$$

Here again the rotation kinetic energy of the wheels has been neglected and no gyroscopic effect of the wheels can be obtained.

The Raleigh dissipation function due to a generic viscous damper located between the $(i-1)$-th and the ith trailer is simply

$$\mathcal{F} = \frac{1}{2}\Gamma\left(\dot{\theta}_i - \dot{\theta}_{i-1}\right)^2 . \tag{25.235}$$

Operating in the manner used for the insulated vehicle and linearizing the result, the first equation of motion, related to the displacement in x direction, is

$$m\dot{V} = Q_x , \tag{25.236}$$

where

$$m = m_T + \sum_{i=1}^{n} m_i$$

is the total mass of the vehicle.

The second equation of motion, related to the displacement in the y direction, is

$$m\left(\dot{v} + V\dot{\psi}\right) + \sum_{i=1}^{n}\left[-\ddot{\psi}\left(c + \sum_{j=1}^{i} l_{ij}\right) + \sum_{j=1}^{i} l_{ij}\ddot{\theta}_j\right] = Q_y . \tag{25.237}$$

The third equation refers to the degree of freedom ψ

$$\begin{aligned}\left\{J_T+\sum_{i=1}^{n}\left[m_i\left(S_i^2+C_i^2\right)+J_i\right]\right\}\ddot{\psi}+\sum_{i=1}^{n}m_i\Bigg\{\left(-\dot{u}+v\dot{\psi}\right)S_i+\\ -\left(\dot{v}+u\dot{\psi}\right)C_i-S_i\sum_{j=1}^{i}l_{ij}\left[\ddot{\theta}_j\sin(\theta_j)-\dot{\theta}_j\left(\dot{\psi}-\dot{\theta}_j\right)^2\cos(\theta_j)\right]+\\ -C_i\sum_{j=1}^{i}l_{ij}\left[\ddot{\theta}_j\cos(\theta_j)+\dot{\theta}_j\left(\dot{\psi}-\dot{\theta}_j\right)^2\sin(\theta_j)\right]+\\ +\dot{\psi}S_i\sum_{j=1}^{i}l_{ij}\dot{\theta}_j\cos(\theta_j)-\left(\dot{\psi}C_i+v\right)\sum_{j=1}^{i}l_{ij}\dot{\theta}_j\sin(\theta_j)\Bigg\}=Q_\psi\ ,\end{aligned} \tag{25.238}$$

where

$$\begin{aligned}S_i&=\sum_{j=1}^{i}l_{ij}\sin(\theta_j)\ ,\\ C_i&=c+\sum_{j=1}^{i}l_{ij}\cos(\theta_j)\ .\end{aligned}$$

The third equation can also be linearized, yielding

$$\begin{aligned}\left\{J_T+\sum_{i=1}^{n}\left[m_iC_i^2+J_i\right]\right\}\ddot{\psi}+\\ +\sum_{i=1}^{n}m_i\left[\dot{V}S_i-\left(\dot{v}+V\dot{\psi}\right)C_i-C_i\sum_{j=1}^{i}l_{ij}\ddot{\theta}_j\right]=Q_\psi\ ,\end{aligned} \tag{25.239}$$

where

$$S_i=\sum_{j=1}^{i}l_{ij}\theta_j\ ,\quad C_i=c+\sum_{j=1}^{i}l_{ij}\ .$$

The following n equations refer to the rotational generalized coordinates θ_j (for $j=1,2,\ldots,n$). The generic equation for θ_k, i.e., the $(3+k)$-th equation, is

$$\sum_{i=k}^{n} m_i l_{ik} \left\{ \sin(\theta_k) \left[\dot{u} - v\dot{\psi} + \dot{\psi}^2 C_i - \ddot{\psi} S_i - \sum_{j=1}^{i} l_{ij} \ddot{\theta}_j \sin(\theta_j) + \right. \right.$$
$$\left. - 2\dot{\psi} \sum_{j=1}^{i} l_{ij} \dot{\theta}_j \cos(\theta_j) + \sum_{j=1}^{i} l_{ij} \dot{\theta}_j^2 \cos(\theta_j) \right] +$$
$$+ \cos(\theta_k) \left[\dot{v} + u\dot{\psi} - \ddot{\psi} C_i + - \dot{\psi}^2 S_i + \sum_{j=1}^{i} l_{ij} \ddot{\theta}_j \cos(\theta_j) + 2\dot{\psi} \sum_{j=1}^{i} l_{ij} \dot{\theta}_j \sin(\theta_j) + \right.$$
$$\left. \left. - \sum_{j=1}^{i} l_{ij} \dot{\theta}_j^2 \sin(\theta_j) \right] \right\} + J_k \left(\ddot{\theta}_k - \ddot{\psi} \right) = Q_{\theta_k} \ . \tag{25.240}$$

By linearizing also these equations, it follows that

$$J_k \left(\ddot{\theta}_k - \ddot{\psi} \right) + \sum_{i=k}^{n} m_i l_{ik} \left(\theta_k \dot{V} + \dot{v} + V\dot{\psi} - \ddot{\psi} C_i + \sum_{j=1}^{i} l_{ij} \ddot{\theta}_j \right) = Q_{\theta_k} \ . \tag{25.241}$$

The derivatives of the Raleigh dissipation function have not been included in the equations: The generalized forces due to the dampers, if they exist at all, will be included in the forces Q_{θ_k}.

25.18.2 Sideslip Angles of the Wheels and Generalized Forces

The sideslip angles of the wheels of the trailer can be computed as they were for the articulated vehicle. If the rth wheel of the ith trailer has a steering angle δ_{i_r}, using the monotrack vehicle model, the sideslip angle is

$$\alpha_{i_r} = \theta_i + \beta - \frac{\dot{\psi}}{V} \left(c + \sum_{j=1}^{i} l_{ij}^* \right) + \sum_{j=1}^{i} l_{ij}^* \frac{\dot{\theta}_i}{V} - \delta_{i_r} \ , \tag{25.242}$$

where l_{ij}^* are equal to l_{ij}, but defined using distance b_{i_r} of the axle instead of a_i.

The contributions to the generalized forces Q_x, Q_y and Q_ψ due to the tractor are the same as for the insulated vehicle. As usual, the tractor does not give any contribution to the forces Q_{θ_k}. To compute the contributions due to the rth wheel of the ith trailer and to the aerodynamic forces of the latter, it is possible to proceed as for the previous models, by writing their virtual work and then differentiating with respect to the virtual displacements.

The results obtained for the wheels are

$$\begin{cases} Q_{x_{i_r}} = F_{x_{i_{rt}}} + F_{y_{i_{rt}}}(\theta_i - \delta_{i_r}) \\ Q_{y_{i_r}} = -F_{x_{i_{rt}}}(\theta_i - \delta_{i_r}) + F_{y_{i_{rt}}} \\ Q_{\psi_{i_r}} = F_{x_{i_{rt}}}\left[c(\theta_i - \delta_{r_i}) + \sum_{j=1}^{i} l_{ij}^*(\theta_i - \theta_j - \delta_{r_i}) - y_{i_r}\right] + \\ \qquad\qquad + F_{y_{i_{rt}}}\left[-c - \sum_{j=1}^{i} l_{ij}^* + y_{i_r}(\delta_{r_i})\right] + M_{z_{r_i}} \\ Q_{\theta_{k_{i_r}}} = F_{x_{i_{rt}}} l_{ik}^*(\theta_i - \theta_k - \delta_{r_i}) + F_{y_{i_{rt}}} l_{ik}^* \qquad \text{if } k < i \\ Q_{\theta_{k_{i_r}}} = F_{x_{i_{rt}}}\left[y_{i_r} + l_{ik}^*\delta_{r_i}\right] + F_{y_{i_{rt}}}\left[-y_{i_r}\delta_{r_i} + l_{ik}^*\right] - M_{z_{r_i}} \qquad \text{if } k = i \\ Q_{\theta_{k_{i_r}}} = 0\,. \qquad \text{if } k > i \end{cases} \tag{25.243}$$

The generalized forces due to the aerodynamic forces and moments acting on the trailers can be accounted for in a similar way. Assuming that it is possible to distinguish between the forces acting on the various rigid bodies, the generalized forces can be computed immediately from Eqs. (25.243), using l_{ij} instead of l_{ij}^*, setting δ_{i_r} to zero and using the aerodynamic forces and moments instead of the forces acting between road and wheels.

The generalized forces due to dampers located between the various bodies are

$$\begin{cases} Q_x = Q_y = 0 \\ Q_\psi = -\Gamma_1\dot{\psi} + \Gamma_1\dot{\theta}_1 \\ Q_{\theta_1} = \Gamma_1\dot{\psi} - (\Gamma_1 + \Gamma_2)\,\dot{\theta}_1 + \Gamma_2\dot{\theta}_2 \\ Q_{\theta_k} = \Gamma_k\dot{\theta}_{k-1} - (\Gamma_k + \Gamma_{k+1})\,\dot{\theta}_k + \Gamma_{k+1}\dot{\theta}_{k+1} \qquad k = 2, ..., n\,. \end{cases} \tag{25.244}$$

The external forces $F_{y_{e_i}}$ acting in the centres of mass of the trailers and the components of the weight $m_i g \sin(\alpha)$ are assumed to act in the directions of axes x and y of the tractor; the expressions of the generalized forces must therefore be modified accordingly.

The equations of motion are $n + 3$; together with the equations yielding the sideslip angles of the wheels, those expressing the forces and moments of the tires as functions of the sideslip angles, the load, and the other relevant parameters, they allow one to study the handling of the vehicle.

As was the case for all the previous models, the linearization of the equations allows one to uncouple the longitudinal behavior (first equation of motion) from the lateral behavior, which can be studied using the remaining $n + 2$ equations:

$$
\begin{cases}
m\left(\dot{v}+u\dot{\psi}\right)-\ddot{\psi}\sum_{i=1}^{n}m_i d_i+\sum_{i=1}^{n}\ddot{\theta}_i\left(\sum_{j=i}^{i}m_j l_{ji}\right)= \\
\quad=(Q_y)_\beta\beta+(Q_y)_\psi\psi+\sum_{i=1}^{n}\left[(Q_y)_{\theta_i}\theta_i\right]+(Q_y)_{\dot{\theta}_i}\dot{\theta}_i+(Q_y)_\delta\delta+F_{y_e}+\sum_{i=1}^{n}F_{y_{e_i}} \\
J'\ddot{\psi}-\sum_{i=1}^{n}J'_i\ddot{\theta}_i+\sum_{i=1}^{n}m_i\left\{-\dot{V}\sum_{j=1}^{i}l_{ij}\theta_j-\left(\dot{v}+V\dot{\psi}\right)d_i\right\}= \\
\quad=(Q_\psi)_\beta\beta+(Q_\psi)_\psi\psi+\sum_{i=1}^{n}\left[(Q_\psi)_{\theta_i}\theta_i+(Q_\psi)_{\dot{\theta}_i}\dot{\theta}_i\right]+(Q_\psi)_\delta\delta+ \\
\quad+M_{z_e}+\sum_{i=1}^{n}M_{z_{e_i}}-\sum_{i=1}^{n}F_{y_{e_i}}d_j \\
\sum_{i=k}^{n}m_i l_{ik}\left(\theta_k\dot{V}+\dot{v}+V\dot{\psi}-d_i\ddot{\psi}+\sum_{j=1}^{i}l_{ij}\ddot{\theta}_j\right)=(Q_{\theta_k})_\beta\beta+(Q_{\theta_k})_\psi\psi+ \\
\quad+\sum_{i=1}^{n}\left[(Q_{\theta_k})_{\theta_i}\theta_i+(Q_{\theta_k})_{\dot{\theta}_i}\dot{\theta}_i\right]+(Q_{\theta_k})_\delta\delta-M_{z_{e_i}}+\sum_{i=1}^{k}F_{y_{e_i}}l_{ik}\ ,
\end{cases}
\tag{25.245}
$$

where

$$
d_i=\sum_{j=1}^{i}l_{ij},\ J'=J_T+\sum_{i=1}^{n}(J_i+m_i d_i^2)
$$

and

$$
J'_i=\sum_{j=1}^{i}(J_i+m_i d_j l_{ji})\ .
$$

By linearizing the generalized forces Q_x, Q_y, Q_ψ and Q_{θ_k} as for the previous models, the derivatives of stability entering Eq. (25.245) are readily computed.

The set of $(n+2)$ differential equations (25.245) is of the $(2n+2)$-th order, since variables y and ψ appear in the equation only as first and second derivatives. The equation can thus be written in the state space in the form of a set of $2n+2$ first-order differential equations by introducing the state variables $v_{\theta_i}=\dot{\theta}_i$.

25.19 Limits of Linearized Models

Linearized models have some features that make them particularly useful. These are namely:

- They allow us to simplify the equations of motion to obtain closed form solutions which, when simple enough, provide a general insight into the dynamic behavior of the vehicle, particularly in terms of the effect of changes to its parameters.
- The possibility of studying the stability with the usual methods of linear dynamics.

The disadvantages are also clear: Linearized models can be applied only within a limited range of sideslip angles and lateral acceleration, and used for trajectories whose radius is large with respect to the size of the vehicle. They can thus be applied with confidence to the conditions corresponding to normal vehicle use, while they fail for sport driving and above all for the motions involved in road accidents.

Another consideration for the models seen in the present chapter is that they are based on rigid body dynamics, with the presence of the suspensions neglected. This assumption is well suited to describe the behavior of a vehicle driven in a relaxed way: Although dependent on the stiffness of the suspensions, the roll and pitch angles under these conditions are very small and may be assumed to have little effect on the dynamic behavior.

It must, however, be stated that a linearization carried too far will lead to results contradicting experimental evidence.

If the cornering stiffness is assumed to be proportional to the load F_z acting on the wheel not only for the small load variations acting on each wheel but also for the differences of load between front and rear axle, in the case of a vehicle with two axles with equivalent tires it follows that

$$\frac{C_1}{C_2} = \frac{F_{z_1}}{F_{z_2}} = \frac{b}{a} \, . \tag{25.246}$$

If only the cornering forces of the tires are included in the formula for the neutral-steer point, it follows that this point always coincides with the centre of mass, leading to the conclusion, clearly incorrect, that all vehicles with four equivalent wheels are neutral-steer.